Natural fractures and *in situ* stresses in the Bowen-Surat Basins, Australia: implications for structural permeability and fluid flow

Thomas Lynch

November 2016

THE UNIVERSITY

STRESS AND FRACTURES: BOWEN-SURAT BASINS

ABSTRACT

In situ stress orientations and natural fractures have been observed on image logs from ten wells in the Bowen-Surat Basins in Queensland and New South wales, Australia. The in-situ orientation of the maximum horizontal stress (σ_{Hmax}) at the location of each well was inferred from Drilling Induced Tensile Fractures (DITFs) and Borehole Breakouts (BOs) indicating variable orientations throughout the basins, however overall trends show a rotation of the σ_{Hmax} from NW-SE in the northern regions to NE-SW in the southern regions. 1708 fractures were identified and divided into twelve fracture sets based on their electrical characteristics, orientations, and degree of dip. Resistive and Conductive Set A exhibited a WNW-ESE orientation, Set B was oriented NW-SE, Set C was oriented N-S, Set D was oriented NW-SE and Set E was oriented ENE-WSW. Conductive and Resistive Set F contained approximately horizontal fractures of any orientation. The variability in the orientations of fractures and in-situ σ_{Hmax} orientations were likely due to influences from regional scale structures in the basins. Fractures that were electrically resistive on image logs were assumed to be closed to fluid flow, while electrically conductive fractures were taken to be hydraulically conductive, i.e able to serve as pathways for fluid flow. In order to test this, daily drilling reports for each well were analysed to identify depths at which significant loss of drilling fluid were observed. These fluid loss zones corresponded with an abundance of electrically conductive fractures, suggesting that those fractures were open and acting as pathways for fluid flow. These fractures also tended to belong to a set which was aligned with the in situ σ_{Hmax}, further suggesting that electrically conductive fractures that are optimally aligned with the in situ σ_{Hmax} are likely to be open and hydraulically conductive.

KEYWORDS

in situ stress, natural fracture, Bowen-Surat basins, stress, structural permeability, hydraulic conductivity

TABLE OF CONTENTS

LIST OF FIGURES AND TABLES

1 INTRODUCTION

An understanding of structural permeability has become increasingly important for the exploration and production of unconventional resources, such as coal seam gas and geothermal energy (Bailey et al., 2012). When targeting unconventional resources in sedimentary basins, the primary permeability of formations at great depths is often low

due to compaction and diagenesis over time (Gray, 1987), and so, focus has been shifted towards energy rich basins with high structural permeability (Brook-Barnett et al., 2015). The structural permeability of a basin relies on the presence of natural fracture networks that serve as pathways for fluid flow (Barton, et al., 1995). However, natural fractures are not always able to serve as pathways for fluid flow as they can be closed over time (Nelson, 2001);(Laubach, 1998). It is only factures that are optimally aligned such that they strike within 26° of the in-situ maximum horizontal stress (σ_{Hmax}) that will be hydraulically conductive, i.e. able to provide a pathway for fluid flow (Zoback, 2007);(Healy et al, 2006). The present-day stress regime is defined by the orientation and relative magnitudes of the three principal stresses acting on a region (Anderson, 1951). Therefore, in order to understand fractures and their role in structural permeability, it is also important to understand in-situ stress orientations in sedimentary basins.

The energy-rich, vertically stacked Bowen-Surat basins in eastern Australia (Figure 1) provide the perfect natural laboratory to investigate natural fractures, in-situ stresses and structural permeability. Previous studies such as Brook-Barnett, 2015, Schadler, 2013 and King et al., 2012 have investigated natural fractures and in-situ stress magnitudes, orientations and variability in sedimentary basins. In the Bowen Basin, Brook Barnett, 2015 attributed variations in the σ_{Hmax} to influences from both complex interactions at the Indo-Australian Plate Boundary as well as regional scale structures within the Basin. This is supported by King et al., 2012, which suggests that the in-situ σ_{Hmax} can be rotated by regional scale structures to become approximate parallel as well as stating that fractures optimally aligned with the in-situ σ_{Hmax} are more likely to serve as pathways for fluid flow (Brook-Barnett et al., 2015);(Schadler, 2013).

4

In this paper, Formation Micro Imager (FMI) and Compact Micro Imager (CMI) logs have been used from ten wells across the Bowen-Surat basins to identify natural fractures and stress indicators such as Borehole Breakouts (BOs) and Drilling Induced Tensile Fractures (DITFs) (Figure 7). Natural Fracture orientations were measured from 1708 fractures which were then divided into twelve fracture sets based on their orientations, dip angles, and electrical characteristics (Table 2). In-situ σ_{Hmax} orientations were also determined from BOs and DITFs, and demonstrated a range of σ_{Hmax} orientations across the basins from NNE-SSW in the southern and northern regions of the basins, to NW-SE in the central northern region, and ENE-WSW in the southern central region (Figures 2 and 9). Relative stress magnitudes in the Bowen-Surat basins were obtained from Schadler, 2013, and used to assess the likelihood for fractures that are optimally aligned with the in-situ σ_{Hmax} a strike slip faulting stress regime which had previously been determined across the basin (Figure 10). These critically stressed fractures were then compared with fluid loss and gain observations from drilling reports to determine whether they were hydraulically conductive, thus, assessing the structural permeability (Figure 11).

2 GEOLOGICAL SETTING/BACKGROUND

2.1 Bowen-Surat Basins

The Bowen and Surat basins are two energy rich basins in southern Queensland and northern New South Wales hosting some of the largest coal and gas reserves in Australia (Figure 1). The Bowen Basin is an early Permian to middle Triassic foreland basin in Queensland, Australia which covers an area of approximately 160,000km^2 and contains two north trending depocentres, the Denison trough and the Taroom trough

(Figure 1) (Cadman et al., 1997). Deposition of sediments in the basin began during an early Permian magmatic rift phase during which volcanics, and fluvial and lacustrine sediments accumulated in the east of the basin in a series of half graben (Figure 2) (Dickins & Malone, 1973). At this time in the west of the basin deposition of non-marine clastic sediments was occurring and the development of a thick succession of coals (Figure 2) (Dickins & Malone, 1973). Following the cessation of rifting the basin underwent a period of thermal sag in the mid to late Permian, during which there was a marine transgression across the entire basin resulting in the deposition of clastic, shallow marine, and deltaic sediments, as well as, extensive coal measures (Figure 2) (Totterdell et al., 2009).

From the late Permian to early Triassic the basin underwent foreland loading which resulted in rapid subsidence (Cadman et al., 1997). This allowed for the relatively rapid deposition of fluvial and marine clastic sediments and coal in the late Permian and fluvial and lacustrine sediments in the early to middle Triassic and finally contraction of the basin in the late Triassic resulted in the cessation of sedimentation and further deformation of pre-existing formations (Figure 2) (Dickins & Malone, 1973).

The younger Surat Basin is an early Jurassic to early Cretaceous intracratonic Basin which covers around 300,000km^2 of northern New South Wales and southern Queensland and unconformably overlies the Bowen Basin (Figure 1) (Cadman et al., 1997). Sediment deposition in the Surat Basin began during a period of thermal sag which effected a large area of Eastern Australia (Exon, 1976). Sediments were mostly fluvial and lacustrine in the early Jurassic however most of the basin exhibited a peat/coal swamp environment during the middle Jurassic (Figure 2) (Cadman et al., 1997).
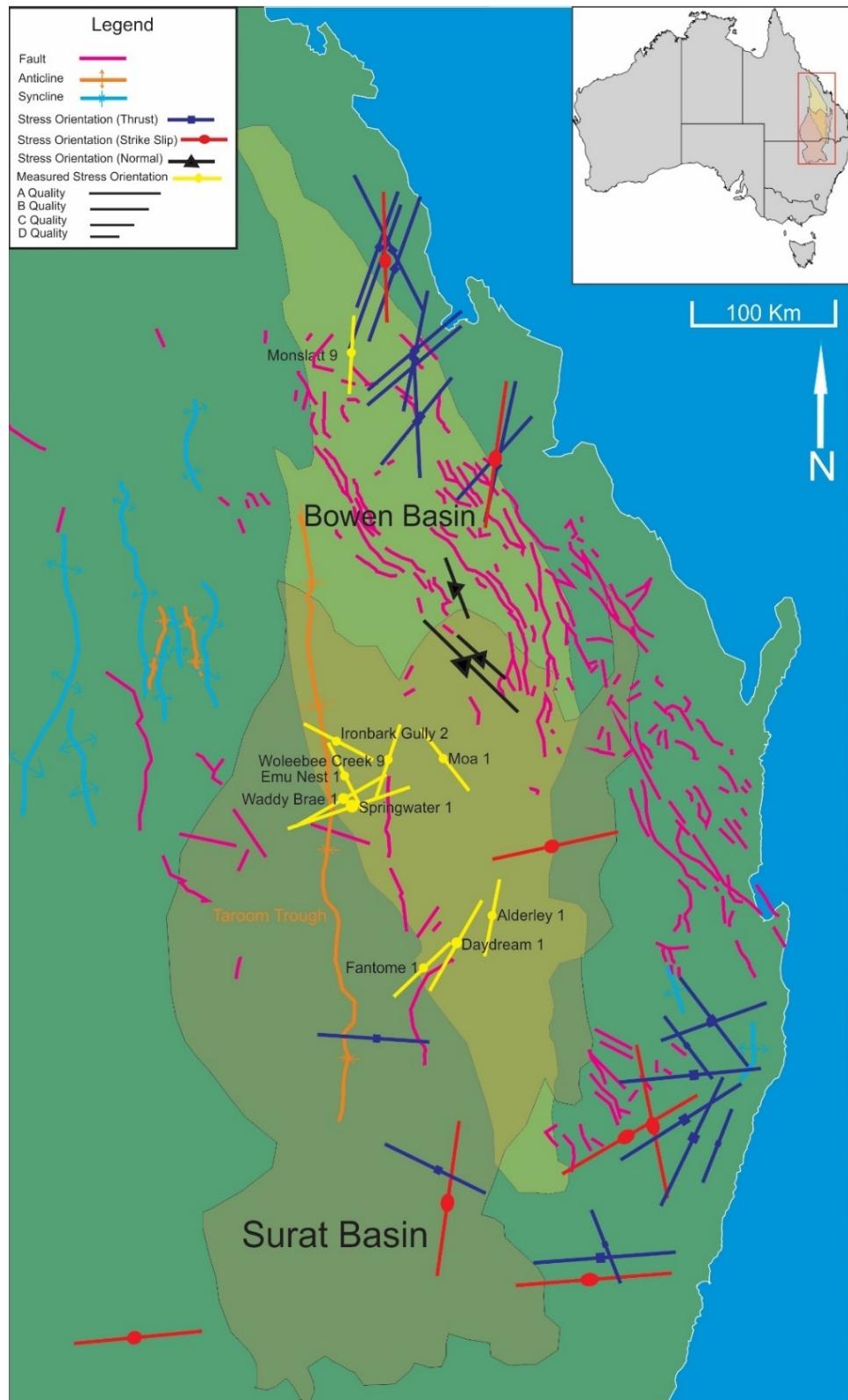
Figure 1: Map of Eastern Australia showing the study area, the Bowen and Surat Basins, and locations and in-situ σ_{Hmax} of the ten wells studied as well as regional structures such as faults and folds and maximum horizontal stress orientations obtained from the World Stress Map Project (Zoback, 1992)

The middle to late Jurrasic saw continued deposition of fluvio-lacustrine sediments up until the early Cretaceous at which point transgression resulted in the deposition of marine and clastic sediments through to the middle Cretaceous (Figure 2) (Cadman et al., 1997). The following marine regression brought more fluvio-lacustrine sediments to the basin and deposition ceased in the middle Cretaceous (Figure 2) (Exon, 1976). Tectonically, the Surat basin has been relatively inactive throughout its history and many of its structures tend to be influenced by structures in the underlying basement such as the Taroom Trough of the Bowen Basin (Figure 1) (Brooke-Barnett et al., 2015). As the Surat Basin partially overlies the Bowen Basin, their stratigraphic records are often considered together, with a major unconformity separating them possibly due to slowing or cessation of sediment deposition, and erosion (Figure 2) (Cadman et al., 1997).

Figure 2: Stratigraphic record of the Bowen-Surat Basins showing an unconformity separating them. (Buck et al,. 2009)

2.2 Natural Fractures

Nelson (2001) defines natural fractures as planar discontinuities in rocks that have resulted from physical diagenesis or brittle deformation. In general, the term fracture encompasses all forms of brittle failure within a rock, such as faults and joints, which occur when the crustal stress of the area exceeds the crustal rock strength (Zang and Stephansson 2008). Natural fractures can be formed by a number of different processes resulting in extension and shear stresses, and are divided into three categories based on the relative motion of the fracture plane (Peacock et al., 2016);(Lacazette, 2001). Mode I fractures are formed purely by extensional stresses whereby the relative motion propagates perpendicular to the fracture plane (Figure 3) (Peacock et al., 2016);(Lacazette, 2001). Mode II fractures are formed by shear stresses resulting in a relative motion that is parallel to the fracture plane (Figure 3) (Peacock et al., 2016);(Lacazette, 2001). Mode III fractures are also formed by shear stresses, however, they exhibit a relative motion that is perpendicular to the fracture plane (Figure 3) (Twiss and Moores 2007). Fractures which exhibit both extensional and shear displacement are referred to as being mixed mode, or oblique extension fractures (Twiss and Moores 2007).
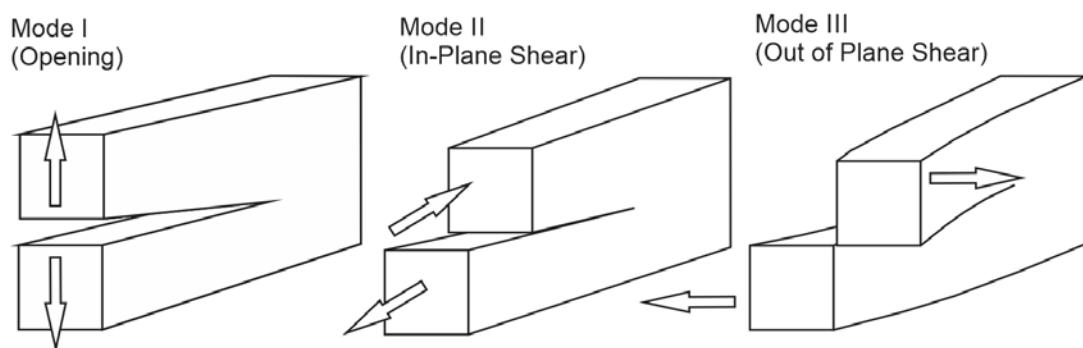
Figure 3: Block diagram illustrating the three modes of fractures (Twiss and Moores, 2007)

2.2.1 FRACTURE FORMATION

Natural fractures can be formed or initiated by a variety of processes that cause stresses to act on and exceed the strength of rocks resulting in brittle failure (Zang and Stephannsson, 2008). Common sources of stress great enough to cause brittle failure in rocks include:

- Fluid overpressure at large depths causing hydraulic fractures (Laubach, 1988). Hydraulic fractures are very common and are directly influenced by pore pressures within the rock which is simply the pressure of fluids within the pores of a rock (Cosgrove and Engelder, 2004). This pressure is usually hydrostatic, however, when this pressure approaches the lithostatic pressure of the surrounding rock it overcomes the yield strength of the rock and hydraulic fractures are formed; which are primarily tensile or Mode I fractures (Figures 3 and 4) (Corcoran and Dore, 2002).

- Tectonic unloading is a common driver for fracture formation (Cosgrove and Engelder 2004). During uplift significant changes to temperature and stress within the crustal column may occur when material is removed or eroded in significant quantities. This can alter the stress regime so that even minor increases in pore pressures are significant enough to result in tensile or extensional fractures (Figure 4) (Laubach, 1988) (Cosgrove and Engelder, 2004). Fractures formed by unloading tend to be aligned with the in-situ stress regime (Cosgrove and Engelder, 2004).

- Human activity such as mining and drilling can result in Drilling Induced Tensile Fractures (DITFs) and Borehole Breakouts (BOs) (Tingay et al., 2008). The removal of material from the borehole during drilling allows for the

10

concentration of stresses around the borehole to result in tensile failure in the

case of DITFs and compressive failure in the case of BOs.

During diagenesis, previously open and hydraulically conductive fractures can be

closed, usually by compaction or the precipitation of a fracture filling cement (Peacock

et al., 2016);(Barton and Zoback, 2000). Closed pre-existing fractures can also be

reactivated if they become aligned optimally with the in-situ stress orientation and "the

rock strength, stress magnitudes and pore-fluid pressure satisfy the failure criteria"

(King et al., 2008);(Clausing, 1959). Fractures which are oriented approximately

parallel to one another are grouped into 'sets,' which are thought to be of similar mode

and age having formed under the same stress regime (Peacock et al,. 2016).

2.2.2 FAILURE CRITERIA

Rock failure and thus natural fracture formation occur in response to in-situ stresses,

pore pressure and rock strength, these are referred to as Mohr-Coulomb failure criteria

(Terzaghi and Peck, 1948);(Sibson, 1977). Mohr circles can be used to show failure will

occur under particular stress conditions (Figure 4) (Terzaghi and Peck, 1948);(Sibson,

1977). They show a failure envelope based on the rock strength and the shear and

normal stress acting on the rock, and a circle representing a rock under stable

conditions, its size and position defined by the three principal stresses (Figure 4)

(Terzaghi and Peck, 1948);(Sibson, 1977). Increasing the pore pressure of the system

decreases the effective stress, shifting this circle closer to the failure envelope resulting

in failure or fracturing (Figure 4) (Terzaghi and Peck, 1948);(Sibson, 1977). Increasing

the differential stress will increase the radius of the mohr circle, and thus bring it closer

to failure (Figure 4) (Terzaghi and Peck, 1948);(Sibson, 1977).

11
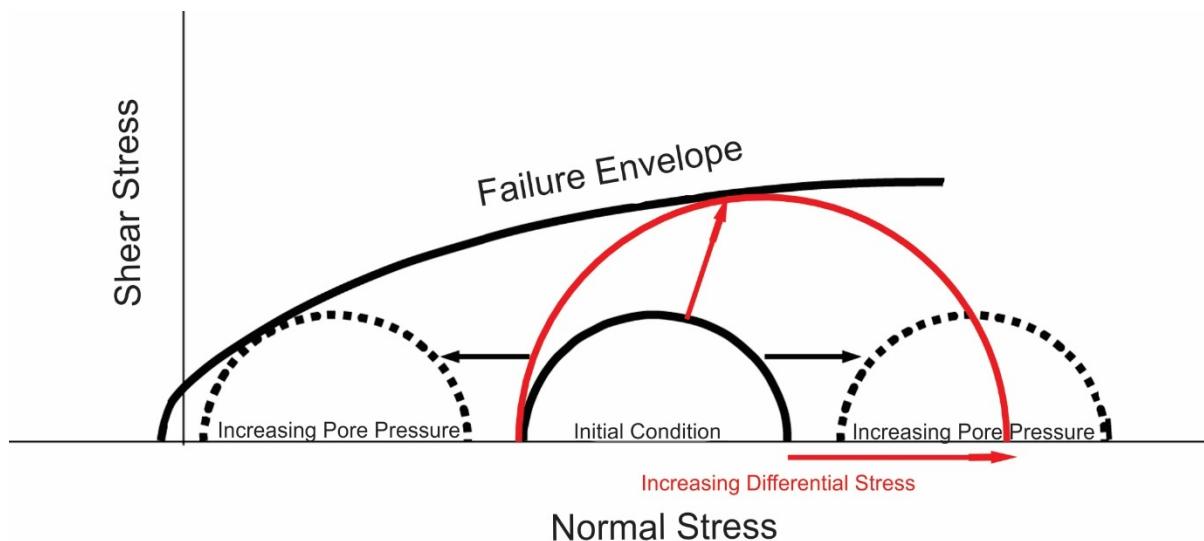
Figure 4: Mohr Circle failure diagram showing the effects of changes to pore pressure and differential stress on the likelihood of rock failure and fracture formation (Terzaghi and Peck, 1948);(Sibson, 1977).

2.3 Stress

Stress (σ) on a body is usually defined as acting in three principal directions that are mutually perpendicular and acting normal to the body meaning they possess no component of shear (Lacazette, 2001);(Anderson, 1951). The three principal stresses are considered such that $\sigma_1 > \sigma_2 > \sigma_3$, and fractures form at specific orientations to these stresses i.e. shear fractures form approximately 26° to σ_1 and tensile fractures forming parallel to σ_1 (Figure 5) (Healy et al,. 2006);(Lacazette, 2001). Anderson 1951, defined the three principal stresses in the Earth's crust as being vertical (gravity)(σ_v), and two horizontal stress, a maximum (σ_{Hmax}), and a minimum (σ_{hmin}). The relative magnitudes of these stresses determine the faulting regime (Figure 5) (Anderson, 1951).
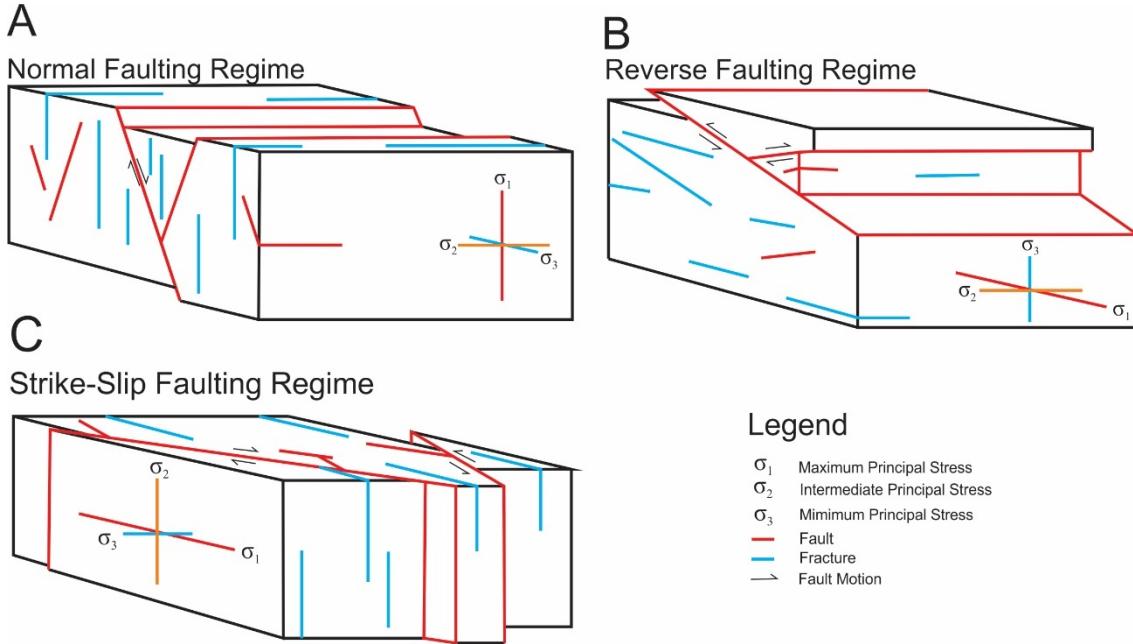
Figure 5: Orientations of faults and fractures under Andersonian stress regimes. A) Normal faulting regime showing fractures forming parallel to the maximum principal stress on the vertical axis. B) Reverse faulting regime showing fractures forming parallel to the maximum principal stress on the horizontal axis. C) Strike-slip faulting regime showing fractures forming in the vertical axis parallel to the maximum principal stress (Anderson, 1951);(Lacazette, 2001).

2.3.1 STRESS ORIENTATIONS

Fractures generally form in accordance with Andersonian faulting theory (Anderson, 1951). An extensional or normal faulting stress regime occurs when the maximum principal stress is vertical and both the intermediate and minimum principal stresses are horizontal such that $\sigma_v > \sigma_{Hmax} > \sigma_{hmin}$ (Figure 5) (Anderson, 1951);(Lacazette, 2001). Under this stress regime tensile fractures will form more or less vertical, perpendicular to the minimum horizontal stress, and faults and shear fractures will form at acute angles to the vertical axis striking parallel to σ_2 (Figure 5) (Anderson, 1951);(Lacazette, 2001). A compressional or reverse faulting stress regime occurs when σ_3 is vertical and results in tensile fractures that are horizontal and faults and shear fractures that form at acute angles to σ_1 (Figure 5) (Anderson, 1951);(Lacazette, 2001). A reverse regime can also be described by $\sigma_{Hmax} > \sigma_{hmin} > \sigma_v$ (Anderson, 1951). Strike-Slip faulting regimes

13

occur when both the maximum and minimum principal stresses are horizontal and the intermediate principal stress is oriented vertically such that $\sigma_{Hmax} > \sigma_v > \sigma_{hmin}$ (Figure 5) (Anderson, 1951);(Lacazette, 2001). This regime results in tensile fractures that are formed vertically and strike in the same orientation as the maximum principal stress, and faults and shear fractures that form at acute angles to the maximum principal stress (Figure 5) (Anderson, 1951);(Lacazette, 2001). Finally, when the magnitudes of the principal stresses are equal to one another ($\sigma_1 = \sigma_2 = \sigma_3$), it is referred to as an isotropic stress regime, under which no fracturing or deformation occurs (Anderson, 1951).

2.3.2 STRESS AND BOREHOLE FAILURE

The process of drilling a well can result in BOs and DITFs which are both useful indicators of the maximum horizontal stress (σ_{Hmax}) of the region (Bell and Gough, 1979). As a well bore is drilled, material is removed from the subsurface and consequently no longer supports what is now the well bore wall and when the stresses around the borehole are large enough a borehole breakout occurs which is seen as compressive failure of the borehole wall (Figure 6) (Bell and Gough, 1979);(Kirsch, 1898). This failure results from the formation of shear fractures, causing the borehole to break away leaving a section of the borehole "ovalised" or "elliptical" (Figure 6) (Bell, 1996a). Borehole Breakouts form perpendicular to the regional maximum horizontal stress and therefore can be used to constrain the orientation of one another (Figure 6) (Bell and Gough, 1979);(Kirsch, 1898). When the stress concentrated around a borehole become large enough to result in tensile failure of the borehole wall DITFs are formed (Brudy and Zoback, 1999);(Peska and Zoback, 1995). These fractures form parallel to the maximum horizontal stress and therefore can also be used to constrain the orientation of the stress (Figure 6) (Bell, 1996). Drilling Induced Tensile Fractures are

14

generally seen as pairs of approximately vertical dipping fractures separated by 180° in the wall of a vertical borehole (Aadnoy and Bell, 1998);(Brudy and Zoback, 1999).
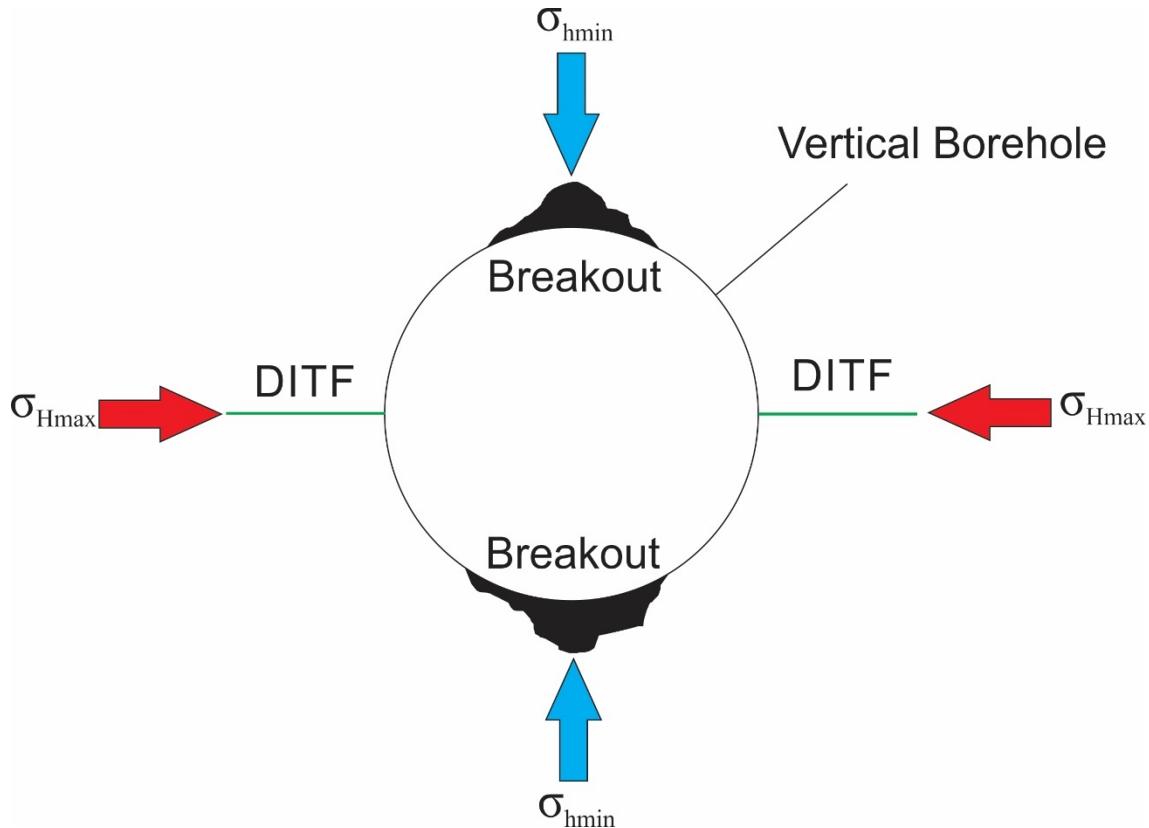
Figure 6: Diagram showing a borehole with breakouts and drilling induced tensile fractures and their orientations relative to the maximum and minimum principal stresses. (Lacazette, 2001);(Bell, 1996a)

2.4 Structural Permeability

Permeability is the measure of the ability for a fluid to move through a rock, i.e fluids will more readily flow through a highly permeable rock than they would through a rock of low permeability (Sibson, 1996). Primary permeability is the flow of fluid through interconnected pore spaces in the rock, which is generally dependant on the sorting and sizes of grains within the rock (Sibson, 1996). Sandstones tend to have larger grains with larger spaces between them and so have a greater number of interconnected pores and are therefore highly permeable whereas siltstones and shales have much smaller, well sorted grains and are therefore much less permeable (Fossen, 2010);(Sibson, 1996).

15

The secondary permeability of a rock is the ability for fluids to flow through cavities and fractures within a rock, therefore highly fractured rocks can act as exceptional reservoirs for hydrocarbons or other fluids (Bailey et al., 2012). When specifically looking at fractures and how fluids flow through them, hydraulic conductivity is a measure of the proportion of fluid fractures can transmit (Bailey et al., 2012).

On an image log fractures appear as either electrically conductive (dark), or electrically resistive (light)(Figure 8)(Barton et al., 1995). It is generally assumed that electrically conductive fractures will be open and hydraulically conductive as they have allowed the conductive drilling mud to fill them, and that electrically resistive fractures are closed and will not act as a fluid pathway (King et al., 2008);(Barton et al., 1995).

As fluids pass through open fractures minerals precipitate to form a fracture filling cement and in some cases, this can serve to completely close the fracture and prevent any further fluid flow (Laubach, 2003). An open, hydraulically conductive fracture will appear as electrically conductive on an image log as the conductive drilling mud passes into the free space, however in some cases the fracture has been filled previously by a cement that contains conductive minerals such as siderite (Bailey et al., 2012). This can be a problem as the fracture will appear to be open and hydraulically conductive however in reality is closed by a cement (Laubach, 2003). Conversely, in some cases fluids can precipitate a cement which partially fills a fracture and acts to 'bridge' open a fracture but not completely seal it, thus, allowing it to remain open to fluid flow (Laubach, 2003).

3 METHODOLOGY

Ikon Science's 'RokDoc' software was used to load and analyse image logs from ten wells in the Bowen-Surat Basins (Figure 1)(Table 1). All files required for the analysis

of image logs were obtained from the Queensland Government's Department of Natural

Resources and Mines online database. Primarily, six CMI and four FMI image logs

where used to identify and measure natural fractures, BOs, and DITFs. These logs

provide a pseudo-image of the borehole walls based on resistivity of the rock forming

the walls (King et al., 2008). Each image is oriented 360° from left (000°) to right

(360°)(Figure 7).

Well Name	Location (Latitude)	Location (Longitude)	Image Log Tool	Image Log Interval (m)
Monslatt 9	-21.858369	148.522706	CMI	226-1000
Ironbark Gully 2	-25.529056	148.933194	CMI	500-765
Moa 1	-25.3151	149.830326	FMI	875-2265
Woleebee Creek 9	-26.31378	149.744782	CMI	410-920
Emu Nest 1	-25.489583	148.9205	CMI	50-650
Waddy Brae 1	-25.682194	148.919556	CMI	1330-1610
Springwater 1	-25.734333	149.004639	CMI	1296-1670
Alderley 1	-26.657308	150.295306	CMI	126-530
Daydream 1	-27.148917	149.643451	FMI	2850-4150
Fantome 1	-26.898177	149.889689	FMI	2810-4700

Table 1: Table showing the wells used in this study, their coordinates, the image log tool used during drilling, and the top and bottom depths of the image log section.

3.1 FRACTURE IDENTIFICATION USING IMAGE LOGS

Formation Micro-Imager and CMI logs were used to identify fractures and to determine

whether they were hydraulically open or closed and measure their orientation. Both

hydraulically open and closed fractures can be identified by the sinusoid shape they

form on an image log, and are distinguished from bedding by their anomalous dip and

dip direction when compared to that of the surrounding bedding (Figures 7a and 7b)

(Rider and Kennedy, 2011);(Barton and Zoback, 2000). The peak and the trough of the

sinusoid show the dip direction with trough showing down dip direction (Figure 7a and

7b). The amplitude or 'steepness' of the sinusoid depends on the dip of the fracture,

such that fractures with high dip angles will produce a sinusoid of greater amplitude.

(Rider and Kennedy, 2011). Fractures that are electrically conductive are dark on an

image log and are assumed to be open as they have been filled by the conductive

drilling mud (Figure 7a) (Rider and Kennedy, 2011);(King et al., 2008). Conversely,

fractures that appeared light and electrically resistive on image logs are thought to be

closed and/or cemented by the precipitation of minerals from fluids (Figure 7b) (Rider

and Kennedy, 2011);(King et al., 2008).
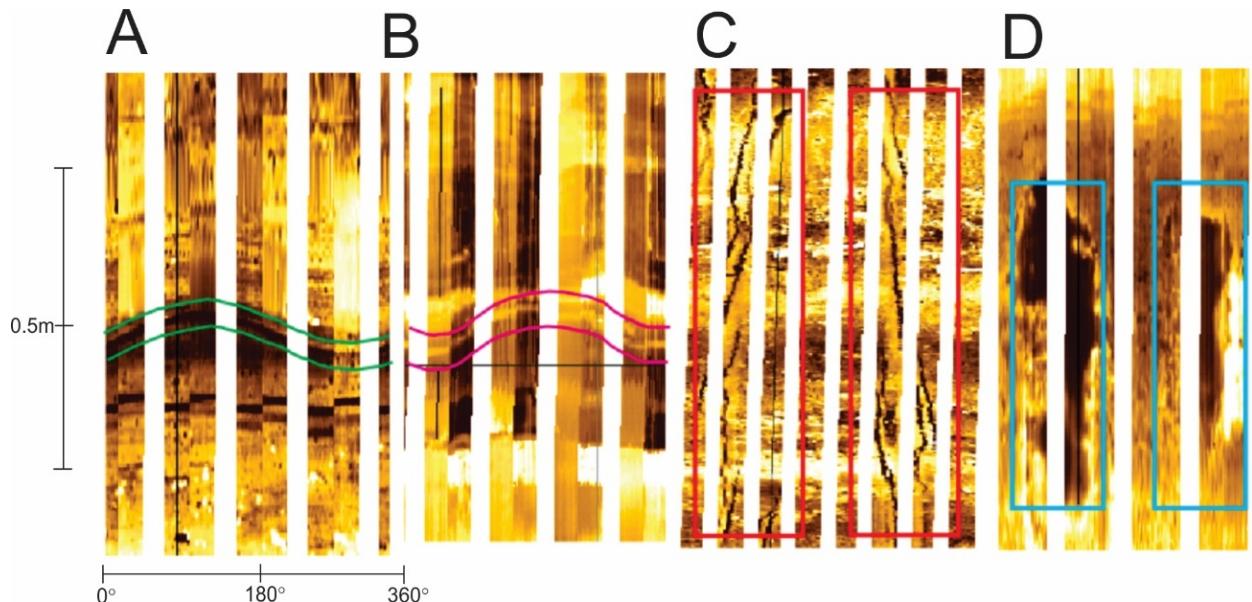
Figure 7: A series of image logs showing examples of identified features A) Shows an example of an electrically conductive fracture outlined by green lines. B) shows an example of an electrically resistive fracture outlined by pink lines. C) Shows an example of DITFS outlined by red rectangles. D) Shows an example of BOs outlined by blue rectangles.

Identified fractures were separated into fracture sets based on their dip and dip direction.

The depths at which each well penetrated different formations and lithologies were

obtained from well completion reports in order to determine a stratigraphy for each

image log. The stratigraphy of each image log and the formations in which the defined fracture sets occurred, was analysed to determine whether stratigraphy was exerting a control on fracture distribution.

3.2 IN SITU STRESS MEASUREMENT

In order to constrain the orientation of the maximum horizontal stress (σ_{Hmax}), image logs were used to identify and measure the orientations of DITFs and BOs, as DITFs form parallel to σ_{Hmax} and BOs form perpendicular to σ_{Hmax} (Figure 4) (Bell and Gough, 1979);(Bell, 1996a). Drilling Induced Tensile Fractures generally appear as a pair of narrow, conductive (dark), well defined lines separated by 180° (Figure 7c) (Rider and Kennedy, 2011). They are conductive on an image log as they are filled by the conductive drilling mud as they are formed (Figure 7c) (Rider and Kennedy, 2011);(Barton and Zoback, 2000). Borehole Breakouts are shown as large, "poorly resolved" conductive zones due to loss of contact between the logging tool and the bore wall as the wall experiences breakout (Figure 7d) (Bell, 1996a);(Zoback et al., 1985);(Rider and Kennedy, 2011). In some instances, when there was uncertainty in identifying BOs, caliper logs were used as a supplementary, qualitative identification method (Hillis and Williams, 1993). As the pads of the image logging tool move over a borehole breakout zone the calipers lose contact with the wall due to the elliptical shape of the borehole and this will show on the caliper log allowing to further identify zones of wall collapse (Rider and Kennedy, 2011);(Bell, 1996a). RokDoc was used to identify and measure the orientations of BOs and DITFs based on these descriptions. They were then plotted on rose diagrams and their averages taken using circular statistics in order to determine the orientation of σ_{Hmax} adjusting 90° for BOs. The wells were then ranked for the quality of the stress indicator data based on the World Stress Map quality

ranking system to determine the level of uncertainty in the orientation of σ_{Hmax}

measured from each well based on the number, length, and standard deviation of stress

indicator measurements (Figure 9) (Table 3) (Zoback, 1992). A well ranked A quality

will have a σ_{Hmax} uncertainty of $\pm$ 15°, a B quality well will have an uncertainty of $\pm$

20°, a C quality well will have an uncertainty of $\pm$ 25° and a D quality well will have an

uncertainty of $\pm$ 40° (Figure 9) (Table 3) (Zoback, 1992).

The measured σ_{Hmax} orientations were then used along with relative stress magnitudes

taken from Brook-Barnett et al., 2015 and Schadler, 2013, to create fracture

susceptibility diagrams in RokDoc (Figure 10). These diagrams are a combination of

Mohr-Coulomb Failure and stereonets which demonstrate the ability or likelihood for a

fracture to allow or enhance fluid flow (King et al., 2008). Diagrams were produced for

regimes with specific σ_{Hmax} orientations based on stress indicator measurements in an

Andersonian strike-slip regime as suggested by Schadler, 2013 and also an isotropic

stress regime as suggested by Brook-Barnett et al., 2015 (Figure 10).

4 OBSERVATIONS AND RESULTS

4.1 FRACTURE SETS IN THE BOWEN-SURAT BASINS

From ten wells in the Bowen-Surat basins a total of 1708 fractures were identified, of

which there were 1113 electrically conductive (Figure 8a-c) and 595 electrically

resistive (Table 2)(Figure 8d-f).
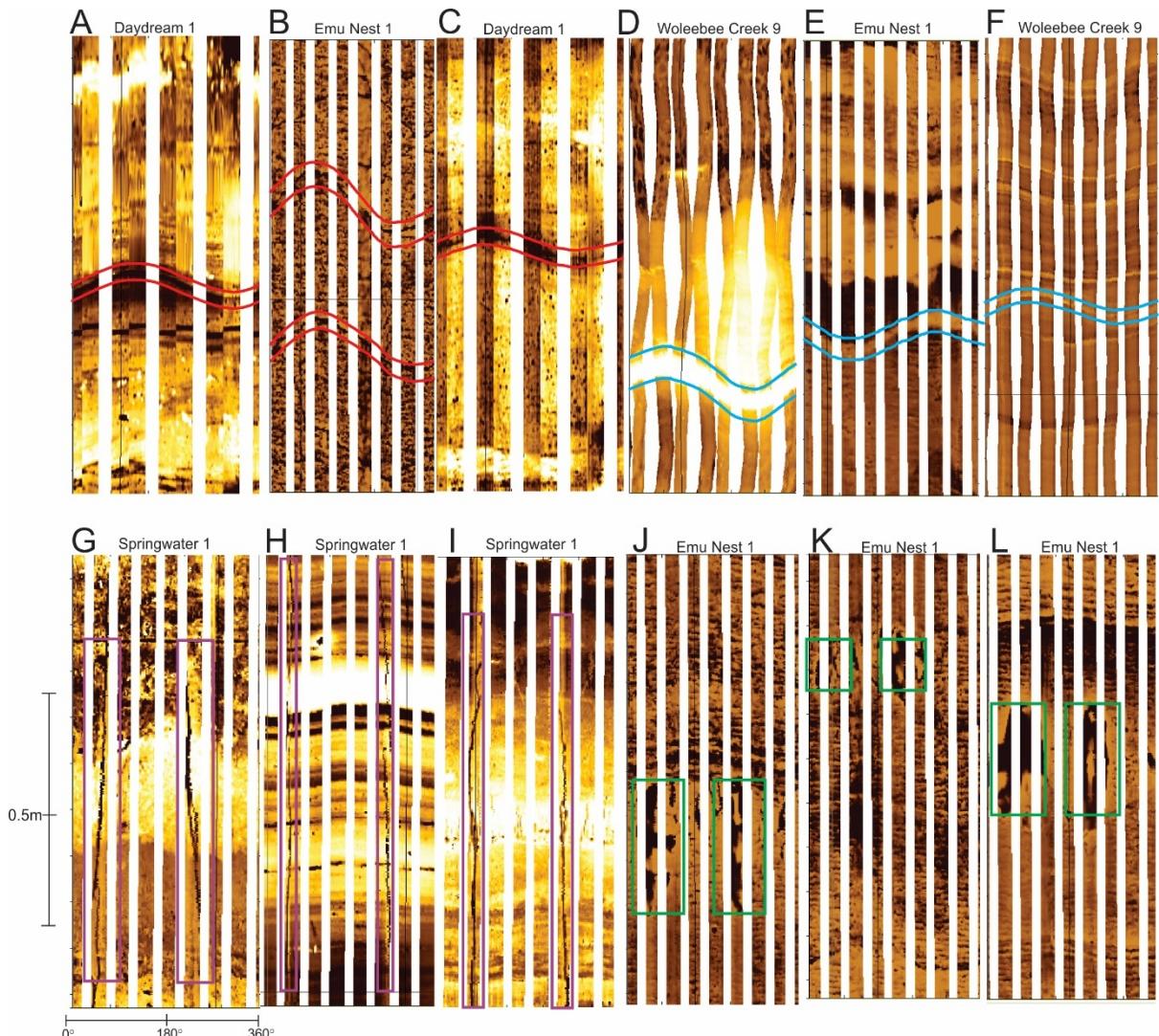
Figure 8: Examples of features identified on image logs from various wells. A-C shows electrically conductive fractures. D-F shows electrically resistive fractures. G-I shows Drilling Induced Tensile Fractures. J-L shows Borehole Breakouts.

The fractures showed a range of orientations in each well however some wells such as

Emu Nest 1 and Springwater 1 showed clear trends (Figure 9). The fractures were

divided into twelve sets based on their electrical characteristics, as well as their

orientations and degree of dip (Table 2).

Fractures belonging to Conductive Set A exhibited dip angles greater than 15°, and had

strikes between 270 and 300° giving the set an approximate WNW-ESE orientation.

Throughout the basins 65 fractures were identified belonging to this set, in seven of the

ten wells (Table 2).

Conductive Set B contained 241 fractures striking between 300 and 345° with dip angles greater than 15°, giving the set an approximate NW-SE orientation. Fractures belonging to this set were identified in nine of the ten wells (Table 2).

Conductive Set C contained 43 fractures striking between 350 and 15°, with dip angles greater than 15° giving the set an approximate N-S orientation. This set was seen in seven of the ten wells (Table 2).

Conductive Set D contained 111 fractures striking between 15 and 45°, with dip angles greater than 15° giving the set an approximate NE-SW orientation. This set was seen in all ten wells (Table 2).

Conductive Set E contained 158 fractures striking between 50 and 90°, with dip angles greater than 15°, giving the set an approximate ENE-WSW orientation. This set was seen in all ten wells (Table 2).

Fractures with dip angles shallower than 15° where placed in Conductive Set F regardless of their dip direction. Across all of the wells there were 493 electrically conductive fractures which were approximately horizontal. Well Springwater 1 was the only well to contain no conductive fractures with dips shallow enough to be considered horizontal (Table 2).

Electrically resistive fractures were considered to be part of different fracture sets, regardless of whether they had similar orientations and dips to electrically conductive fractures as resistive fractures are assumed to be closed or inactive. Resistive Set A had an approximate WNW-ESE orientation being comprised of 41 fractures striking between 270 and 300°, and dip angles greater than 15°. This set was seen in nine of the ten wells (Table 2).

Resistive Set B had an approximate NW-SE orientation, containing 86 fractures striking between 300 and 45°, with dip angles greater than 15°. This set was seen in all ten wells (Table 2).

Resistive Set C had an approximate N-S orientation, containing 10 fractures striking between 350 and 15°, with dip angles greater than 15°. This set was seen in six of the ten wells (Table 2).

Resistive Set D had an approximate NE-SW orientation, being comprised of 81 fractures striking between 15 and 45°, with dip angles greater than 15°. This set was seen in all ten wells (Table 2).

Resistive Set E had an approximate ENE-WSW orientation, containing 55 fractures striking between 50 and 90°, with dip angles greater than 15°. This set was seen in nine of the ten wells (Table 2).

There were also a large number of electrically resistive fractures which were close to horizontal and these were placed in Resistive Set F, containing 322 fractures of dips less than 15° at any orientation (Table 2). This set was seen in all ten wells.

4.2 FRACTURE DISTRIBUTION

Overall, the orientations of fractures in the wells were highly variable, particularly in wells Moa 1, Waddy Brae 1, Alderley 1, Daydream 1, and Fantome 1 (Figure 9). However, dividing the fractures into sets made it easier to analyse for any pattern in the distribution of the fractures.

Well	Monslatt 9	Ironbark Gully 2	Moa 1	Woleebee Creek 9	Emu Nest 1	Waddy Brae 1	Springwater 1	Alderley 1	Daydream 1	Fantome 1	Total In Set
Conductive Set A	7	0	4	0	21	1	0	6	8	18	65
Conductive Set B	73	9	13	8	25	18	0	6	18	71	241
Conductive Set C	7	0	0	0	6	0	2	4	6	18	43
Conductive Set D	29	8	12	1	9	5	6	7	7	27	111
Conductive Set E	5	2	13	2	51	9	46	4	7	19	158
Conductive Set F	3	5	7	12	3	2	0	11	136	314	493
Total Conductive	**125**	**24**	**49**	**23**	**116**	**35**	**54**	**38**	**182**	**467**	**1113**
Resistive Set A	6	1	2	2	1	2	0	15	7	5	41
Resistive Set B	19	3	7	4	2	11	5	5	11	19	86
Resistive Set C	2	0	1	2	0	0	2	2	1	0	10
Resistive Set D	3	6	13	1	3	2	6	14	13	20	81
Resistive Set E	2	3	5	1	7	3	0	15	9	10	55
Resistive Set F	1	15	16	34	8	6	10	35	84	113	322
Total Resistive	**33**	**28**	**44**	**44**	**21**	**24**	**23**	**86**	**125**	**167**	**595**
Total In Well	**158**	**52**	**93**	**67**	**137**	**59**	**77**	**124**	**307**	**634**	**1708**

Table 2: Table of values showing the number of fractures belonging to particular sets found in each well. Also shown are the total number of fractures in each well, each set, and the basin as a whole.

For example, well Monslatt 9 is situated in the northern region of the Bowen Basin and

exhibited 73 fractures belonging to Conductive Set B, however 71 fractures belonging

to the same set were also seen in well Fantome 1, which is situated in the southern

region of the Bowen basin. (Table 2)(Figure 1). This was the case for every fracture set,

such that fractures belonging to every set were geographically spread across both basins without any obvious pattern for occurring in a particular region or location.

On the other hand, fracture sets appeared to be more predominant in some wells than others. Wells Emu Nest 1 and Springwater 1 are relatively proximal to one another in the central region of the study area, and exhibited 51 and 46 fractures belonging to Conductive Set E, respectively (Table 2) (Monslatt 9). Few fractures belonging to this set were seen in other wells.

The fracture sets were also considered in terms of the depths at which they were seen to occur in particular wells, in particular which sections of the stratigraphy. Conductive Set B was seen to occur across almost the entire stratigraphy at depths as great as 4000m and as shallow as 50m. There did not appear to be any pattern in the occurrence of fracture sets in different stratigraphic sections as fracture sets were seen in different formations across a wide range of depths in each well. As well as being geographically and stratigraphically widespread, the fracture sets were not seen cross-cutting one another.

4.3 STRESS ORIENTATIONS

Throughout the two basins 134 BOs and 314 DITFs were identified from ten image logs in order to determine the orientation of σ_{Hmax} (Table 3)(Figure 8 g-l). Some features were more predominant in certain wells than others, for example well Daydream 1 showed 26 BOs but no DITFs whereas well Springwater 1 showed 86 DITFs and no BOs. Stress indicators were not seen to be occurring in any particular lithologies and were seen across a wide range of depths.
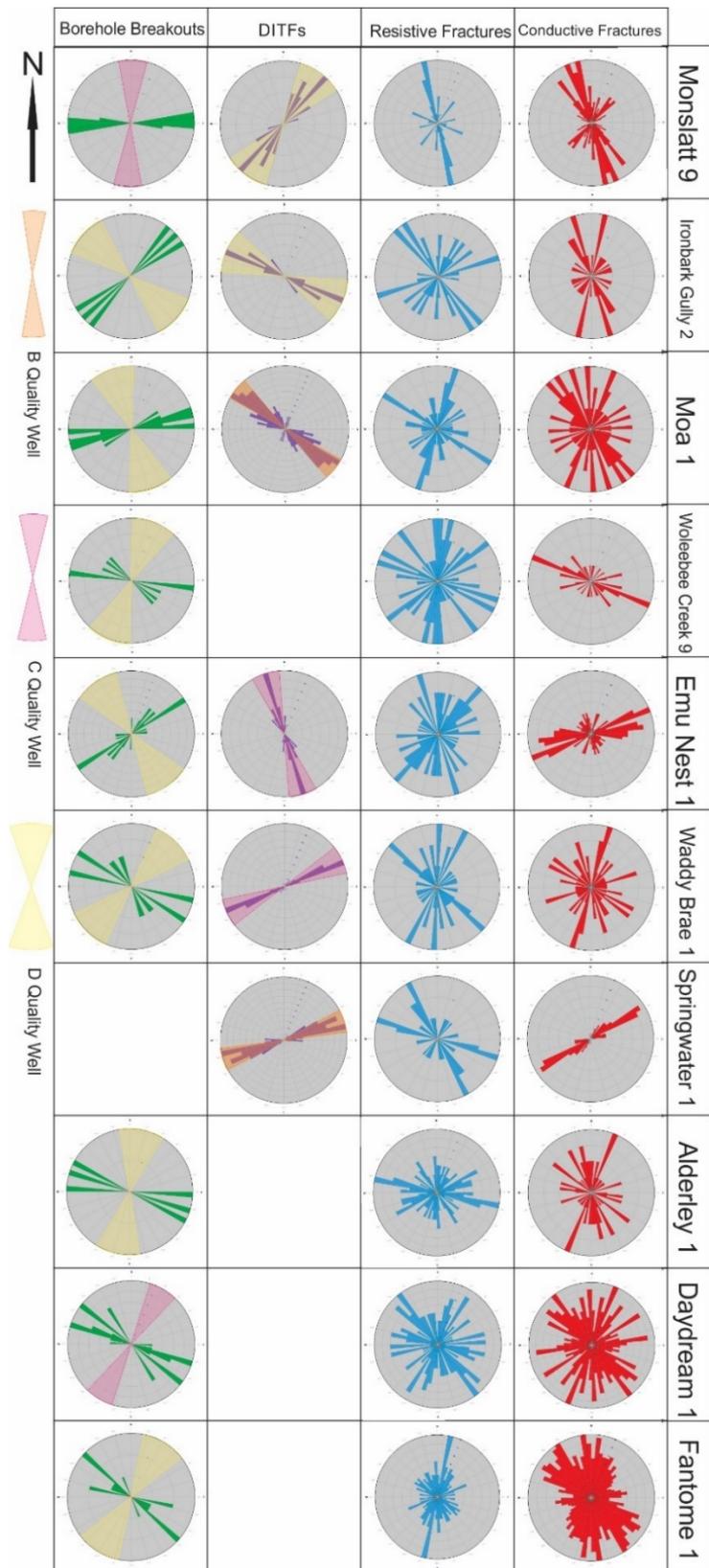
Figure 9: Rose diagrams for each well arranged by their location from North to South, showing the orientations of resistive and conductive fractures along with DITF and BO orientations. Also shown are the measured σ_{Hmax} orientations with error cones signifying their well quality ranking.

The World Stress Map's quality ranking system was used to evaluate σ_{Hmax} orientations derived from BOs and DITFs. This ranking system takes into account the standard deviation of stress indicator orientations, the number identified, and their combined length. All of the wells had a C or D quality, apart from Springwater 1 which exhibited 86 DITFs spread across a large range of depths making it B quality (Table 3). Although many of the wells exhibited a reasonable number of DITFs and/or BOs they were typically short in length, and had a relatively large standard deviation (Table 3). Circular statistics were then used to obtain a mean orientation of σ_{Hmax} from the BOs and DITFs identified in each well (Table 3).

There was a large variation in the σ_{Hmax} of each well, however there appears to be an overall rotation of σ_{Hmax} from NW-SE in the northern regions to NE-SW in the southern regions (Figure 9). It also appears that there are three trends to the present day σ_{Hmax} stress orientations or regimes affecting the wells studied.

All wells exhibited conductive fractures with the same approximate orientation as the measured in-situ σ_{Hmax} however Springwater 1 in particular showed a very strong correlation between the orientation of the in-situ σ_{Hmax} and the orientation of the conductive fractures (Figure 9). Figure 9 also shows a large number of conductive fractures which are not oriented parallel to the σ_{Hmax} and a large number of resistive fractures which are oriented parallel to σ_{Hmax}.

	No. of indicators	Total Length (m)	Standard Deviation	Mean σ_{Hmax} Orientation (°)	Quality Ranking
BOs					
Monslatt 9	14	3	8	356	D
Ironbark Gully 2	6	2	13	317	D
Moa 1	18	4	26	343	D
Woleebee Creek 9	10	2	32	24	D
Emu Nest 1	28	6	18	322	D
Waddy Brae 1	16	5	38	50	D
Springwater 1	0	-	-	-	-
Alderley 1	6	2	17	17	D
Daydream 1	26	7	23	25	D
Fantome 1	10	2	24	32	D
DITFs					
Monslatt 9	14	7	27	27	D
Ironbark Gully 2	32	12	18	296	D
Moa 1	103	37	23	299	C
Woleebee Creek 9	0	-	-	-	-
Emu Nest 1	46	33	12	338	C
Waddy Brae 1	33	31	9	70	C
Springwater 1	86	134	16	74	B
Alderley 1	0	-	-	-	-
Daydream 1	0	-	-	-	-
Fantome 1	0	-	-	-	-

Table 3: Table shows the number of Borehole Breakouts and Drilling Induced Tensile Fractures identified in each well, and the criteria for the quality ranking of each well.

4.4 FRACTURE SUSCEPTIBILITY

Based on the σ_{Hmax} in figure 9, it appears that there are three trends to present day σ_{Hmax} stress orientations or regimes affecting the wells studied:

- A NNE-SSW oriented σ_{Hmax} is observed in Alderley 1, Daydream 1 and Fantome 1 in the southern region of the basins, and Monslatt 9 in the far northern region of the basins (Figure 9).

- A NW-SE oriented σ_{Hmax} is observed in Springwater 1 and Waddy Brae 1 in the south central region of the basins (Figure 9).

- A ENE-WSW σ_{Hmax} is observed in Emu Nest 1, Moa 1, and Ironbark Gully 2 in the north central region of the basin. Despite being proximal to these wells the σ_{Hmax} measured in Woleebee Creek 9 was oriented NNE-SSW regime (Figure 9).

Schadler, (2013), provides stress magnitudes in the Bowen Basin showing $\sigma_{Hmax} > \sigma_v > \sigma_{hmin}$ which is indicative of a strike-slip faulting stress regime.

Figure 10 presents fracture susceptibility diagrams based on a strike slip faulting stress regime with three σ_{Hmax} orientations: NNE-SSW, NW-SE, and ENE-WSW. These diagrams show the probability of resistive fractures to be critically stressed such that they may be reactivated and the probability of conductive fractures to be open and oriented optimally with the maximum horizontal stress such that they may serve as fluid flow pathways (King et al., 2008).

These diagrams are a combination of stereonets and Mohr-Circles, and are constructed

based on the stress conditions acting on the fractures. This means using the relative stress magnitudes to define the regime, in this case being strike-slip faulting, as well as the orientation of the σ_{Hmax} orientation of the regime. The poles to the planes of measured fractures are then plotted on the stereonet and their position indicates their likelihood to be critically stress or reactivated (King et al, 2008).

Under a NNE-SSW regime conductive fracture sets B, D and E all expressed a substantial number of fractures that were likely to be critically stressed or aligned optimally with σ_{Hmax} (Figure 10a) whereas most resistive fracture sets were unlikely to be open or reactivated with the exception of a small number of fractures from Resistive Set B (Figure 10d).

Under a NW-SE regime conductive fracture sets B and D expressed a substantial number of fractures which are likely to be critically stressed, and a small number of fractures belonging to Conductive Set A (Figure 10b). There were very few resistive fractures that were likely to be reactivated by this stress regime apart from a few fractures from Resistive Set B (Figure 10e).

Under a NE-SW regime conductive fracture sets D and E exhibited a significant number of fractures that were likely to be critically stressed (Figure 10c), while there were no resistive sets with a significant number of fractures likely to be reactivated (Figure 10f).

Under all three stress regimes the horizontal conductive and the horizontal resistive fracture sets showed a very low likelihood to be critically stressed (Figure 10 a-f) and under an isotropic stress regime there was low likelihood for any fractures to be critically stressed for failure (Figure 10g).
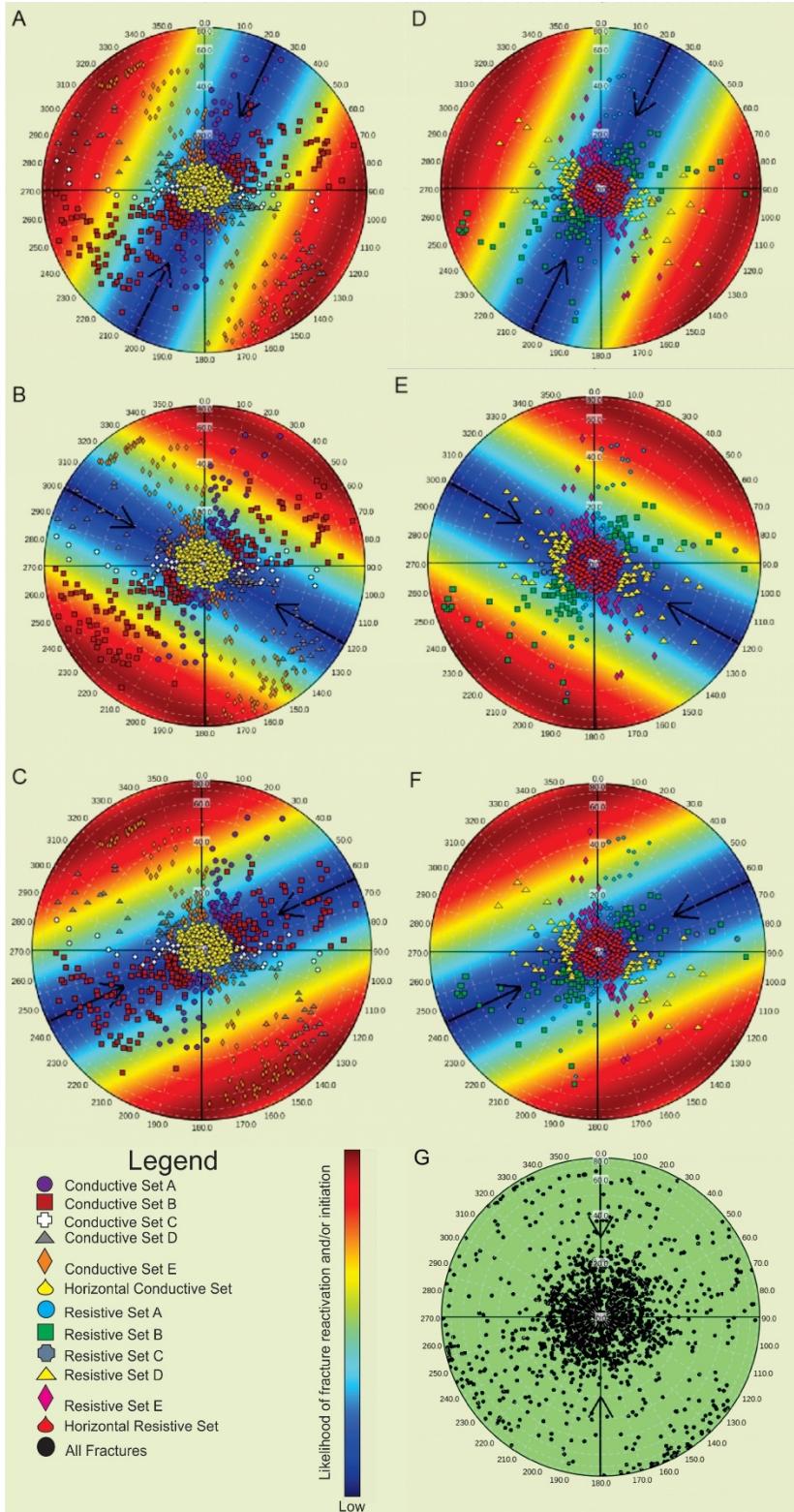
Figure 10: Fracture susceptibility diagrams showing the poles to plane for both conductive and resistive fracture sets under strike-slip faulting stress regimes of varying maximum horizontal stress orientation. A) shows conductive sets under a NNE-SSW regime. B) shows conductive sets under a NW-SE regime. C) shows conductive sets under a NE-SW regime. D) shows resistive sets under a NNE-SSW regime. E) shows resistive sets under a NW-SE regime. F) shows resistive fractures under a NW-SE regime. G) shows all fractures under an isotropic stress regime.
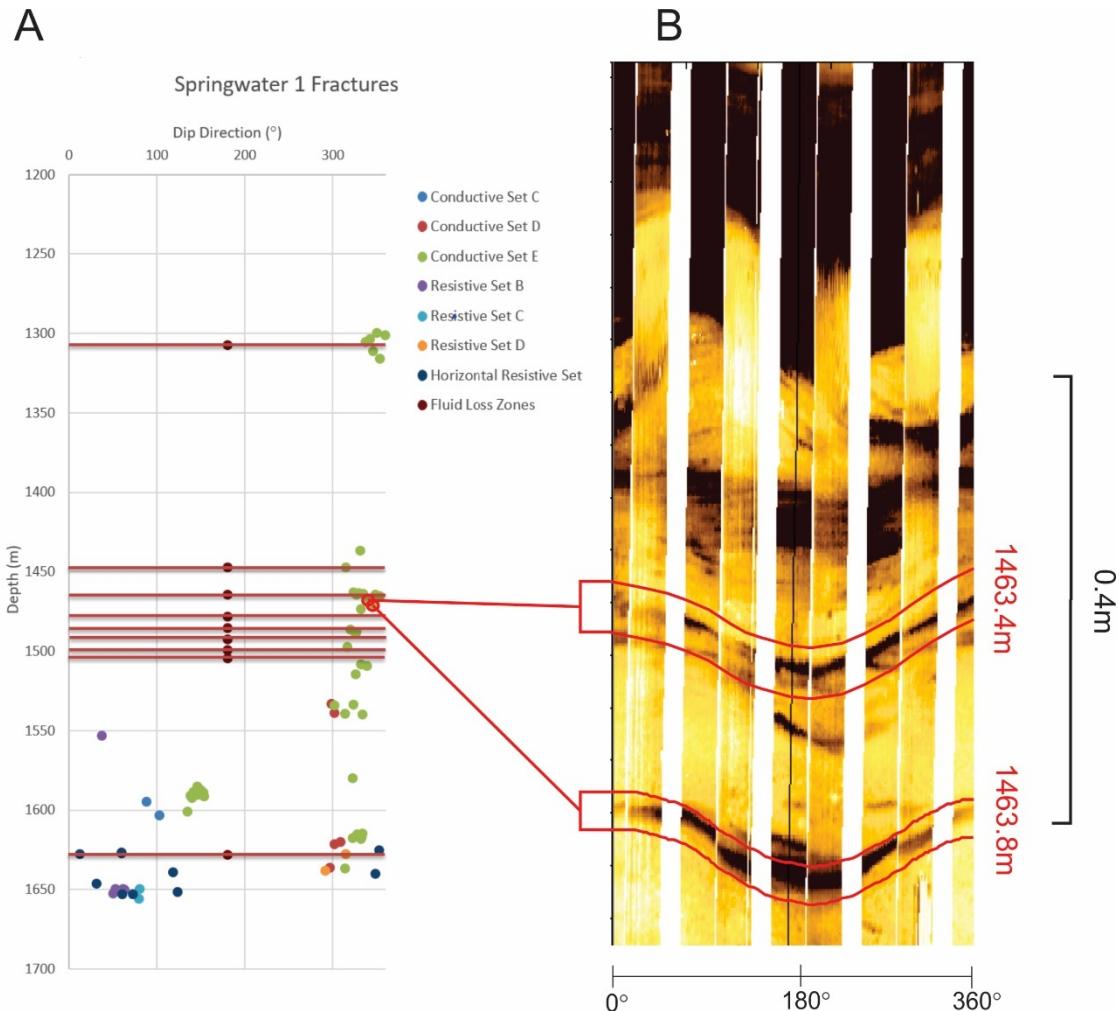
Figure 11: A) Graph showing fractures measured in Springwater 1 plotted by their dip direction vs depth. Also shown are the depths at which significant fluid losses were observed taken from the well completion report. B) A metre long section of the image log from well Springwater 1 showing two conductive fractures that occurred at the same depths as significant fluid losses.

5 DISCUSSION

5.1 FRACTURE ORIENTATION VARIABILITY AND DISTRIBUTION

There is a high level of variation in the strike and dip angle of fractures throughout the

Bowen-Surat basins however the fractures were able to be divided into sets based on

their orientations, degree of dip, and whether they were electrically conductive or

resistive on image logs.

Many of the structures seen in the Surat Basin are influenced by the underlying Bowen

Basin, for example the large synform running through the west of the Surat Basin was once the Taroom Trough, a major depocentre of the Bowen Basin (Figure 1) (Cadman et al., 1997);(Brook-Barnett et al., 2015). Regional scale structures can also effect smaller fractures such that the fractures will be aligned approximately parallel (±26°) to structures such as faults and folds (Healy et al., 2006);(Burberry, 2015). Therefore structures such as the Taroom Trough, and other large folds and faults in the Bowen-Surat Basin are a likely cause for the variable fracture orientations observed in the basins (Figures 1 and 9)

It is also possible that fractures of differing orientations were formed by the same event, and under the same stress regime, and some of the fractures have simply been rotated by a subsequent deformation event, or have simply followed a plane of weakness within a different lithology (Martel, 1999);(Twiss and Moores, 2007). This also could be the cause for the variation in fracture orientations in the Bowen-Surat Basins as well as the lack of an obvious stratigraphic control over the fractures.

There did not appear to be any obvious geographical or stratigraphic controls on the distribution of fractures, and fracture sets in the Bowen-Surat Basins. Conductive Set E appeared to be concentrated in the central region of the Bowen-Surat basins, exhibiting 51 fractures in well Emu Nest 1, and 46 fractures in well Springwater 1, suggesting that different regions of the basins have been effected by different stress regimes or fracture forming events (Figure 1) (Table 2). However, Conductive Set E, as well as fractures belonging to every set, were identified as far north as well Monslatt 9, and as far south as well Fantome 1, spanning the entire study area and making it difficult to determine a major geographical control on fracture distribution (Figure 1) (Table 2).

It is likely that the different fracture sets defined for the Bowen-Surat Basins each

formed under differing stress regimes at different times during the structural evolution of the basin and are possibly related to different tectonic events (Peacock et al, 2016). There was no obvious recurring pattern in the distribution of fracture sets in particular formations, for example, almost every set could be identified in well Monslatt 9 in the northern region of the basins, as well as in well Fantome 1 in the southern region. This may suggest that while different sections of the stratigraphy may exhibit different fracture sets in some wells, overall the stratigraphy of the basins does not exert a major control over the distribution of fractures. This is contrary to Di Naccio et al., 2005, and Burberry, 2015, which state that fracture density is controlled by rock properties and that large scale lithological variations in the stratigraphy does exert a control on fracture distribution.

There were however some sets which appeared to be concentrated in deeper, or shallower sections of the stratigraphy which may have implications for the relative age of the sets. For example, Conductive Sets A, B and E were all seen throughout most of the basins stratigraphy, however Conductive Set D was only seen at relatively shallow depths (<~1850m) and so while it is difficult to make an inference on the relative ages of Sets A, B and E, it could be said that Set D is the youngest set. All six of the resistive fracture sets were seen throughout most of the stratigraphy. As they are resistive, they have had time to form and subsequently become closed through compaction and diagenesis, therefore all of the resistive sets may be older than the conductive sets, however their relative ages cannot be determined (Barton and Zoback, 2000). This may suggest that if sets were formed under particular stress regimes, then those regimes must have remained fairly constant throughout the structural evolution of the basins. This is unlikely as the Bowen Basin was relatively tectonically active during sediment

deposition which would suggest highly variable stress conditions and therefore changing fracture orientations within the stratigraphy (Cadman et al., 1997);(Dickins and Malone, 1973). Due to the nature of natural fractures being formed, closed, and potentially reactivated, it is difficult to determine an absolute age for a fracture or fracture set.

5.2 STRESS ORIENTATION VARIABILITY

Measurements of BOs and DITFs showed that across the Bowen-Surat basins there was a high variability in the orientation of the present day in-situ σ_{Hmax} (Figure 9). In-situ σ_{Hmax} determined by the World Stress Map Project, and Brook-Barnett et al., 2015 also indicate variable orientations throughout and near to the Bowen-Surat Basins. Brook-Barnett et al., 2015, suggests that variations in in-situ stress orientations across the Surat Basin could be due to either influence of basement structures such as the Taroom Trough of the Bowen Basin, or due to complex interactions at the Indo-Australian Plate Boundary. Figure 1 shows five wells situated in close proximity to the Taroom Trough, one of the past depocentres of the Bowen basin. Brook-Barnett et al., 2015, presents observations which suggest a rotation of the stress field around the Taroom trough, resulting in highly variable σ_{Hmax} orientations in and around the trough. This may explain the highly variable σ_{Hmax} orientations seen between wells Emu Nest 1, Woleebee Creek 9, and Waddy Brae 1 despite their proximity to one another in the central region of the Bowen-Surat Basins (Figures 2 and 9). King et al., 2008 also describes stress fields aligning approximately parallel with regional scale structures such as faults, and as such fractures are seen to be forming parallel to large scale faults. This is seen in Fantome 1, which as shown in figure 1 comes into close proximity with a regional scale fault. The σ_{Hmax} orientation measured in Fantome 1 is approximately

parallel to the fault and many of the conductive fractures measured in this well are also oriented parallel to the fault thus supporting Burberry, 2015, and King et al., 2008, which state that fractures will form in the same orientation as regional scale structures (Figures 1 and 9).

Being that there is no obvious geographic or stratigraphic control on the distribution of fractures, it is more likely that their distribution, and orientation variability, in the Bowen-Surat Basins is dependent on variations in the in-situ stress as fractures will form within 26° of the in-situ σ_{Hmax} (Healy et al, 2006). This can be seen in the orientations of the conductive fractures identified in well Springwater 1, which are close to parallel with the in-situ σ_{Hmax} measured in the well (Figure 9).

All ten wells had a D quality ranking based on BO measurements meaning the σ_{Hmax} orientation measured in these wells have an uncertainty of ± 40°. Based on DITF measurements there were three wells of C quality (± 25°), and one well of B quality (± 20°)(Table 3). Zoback, 1992, states that only measurements from wells of C quality or better are reliable enough to make inferences from, however both King et al., 2008, and Tingay et al., 2008, both present evidence to suggest that measurements from D quality wells are reliable.

5.3 STRUCTURAL PERMEABILITY

Structural permeability is defined as the ability for fluid to flow through fractures in rocks, therefore rocks which are highly fractured can act as exceptional reservoirs for fluid flow (Sibson, 1996);(Bailey et al., 2012). Image logs were used to identify electrically resistive and electrically conductive fractures in the Bowen-Surat Basins. Fractures which are electrically conductive on image logs are likely to be open as they have allowed the conductive drilling mud to flow into them (Barton et al., 1995).

However, as fractures can be closed to become inactive, possibly by the cementation of electrically conductive minerals, they cannot be assumed to be hydraulically conductive and able to serve as a pathway for fluid flow (Bailey et al, 2012);(Laubach, 2003). Therefore, it is important to distinguish fractures which are electrically conductive, and fractures which are hydraulically conductive. To do this, fractures were analysed for their likelihood to be critically stressed and active based on predetermined stress conditions from Schadler, 2013, and whether they were seen at depths corresponding to significant fluid loss during drilling.

The fracture susceptibility diagrams in figure 10 showed that certain fracture sets were more likely to be critically stress or reactivated under stress regimes with particular σ_{Hmax} orientations. For example, under a NNE-SSW regime Conductive Sets B, D and E exhibited a number of fractures likely to be critically stressed, under a NW-SE regime Conductive Sets B and D exhibited a number of fractures likely to be critically stressed and under a NE-SW regime Conductive Sets D and E showed a large number of fractures likely to be critically stressed. Therefore, wells within a present day stress regime of the same orientation, and containing fractures belonging to these sets, will then exhibit fractures which are critically stress to remain open.

This does not confirm that the conductive fractures can serve as pathways for fluid flow. Figure 11 shows the fractures in well Springwater 1, their orientations, and the depths at which they were identified. Also shown are the depths at which significant fluid losses were observed by the drillers. Each zone of significant fluid losses was accompanied by a number of electrically conductive fractures at the same depth, suggesting that fluids were being lost through these open fractures. These fractures belong mostly to Conductive Set E which is oriented approximately NE-SW, approximately parallel to

the in-situ σ_{Hmax} orientation measured in Springwater 1, and as shown in figure 8c, a large number of the fractures belonging to Conductive Set E are highly likely to be optimally aligned with the σ_{Hmax} under a NE-SW oriented stress regime.

Therefore it can be said that conductive fractures which are optimally aligned with the present day σ_{Hmax} will serve as an effective pathway for fluid flow, thus contributing to the structural permeability of the rock or rock formation.

6 CONCLUSIONS

The 1708 fractures measured from ten wells in the Bowen-Surat basins showed highly variable orientations, although could be separated into six sets of electrically conductive fractures and six sets of electrically resistive fractures:

- Conductive Set A was oriented WNW-ESE.

- Conductive Set B was oriented NW-SE

- Conductive Set C was oriented N-S

- Conductive Set D was orient NW-SE

- Conductive Set E was oriented ENE-WSW

- Conductive Set F had no specific orientation as it was comprised of approximately horizontal fractures

- Resistive Set A was oriented WNW-ESE.

- Resistive Set B was oriented NW-SE

- Resistive Set C was oriented N-S

- Resistive Set D was orient NW-SE

- Resistive Set E was oriented ENE-WSW

- Resistive Set F had no specific orientation as it was comprised of approximately horizontal fractures

The stratigraphy of the Bowen-Surat Basins did not appear to exert a control over the distribution or density of fractures which is contrary to previous studies (Di Naccio et al, 2005). The high variability of fracture orientations across the basins, and the lack of obvious geographical control over their distribution, is likely due to the highly variable σ_{Hmax} orientations. The variable orientations were also likely due to the influence of regional scale structures such as folds and faults, which as stated by Burberry, 2015, can result in the formation of fractures approximately parallel with them.

Measurements of BOs and DITFs provided orientations for the in-situ σ_{Hmax} at the location of each well which tended to vary throughout the basins (Figures 1 and 9). The basin wide variation in σ_{Hmax} is most likely due to the effect of regional scale structures on the orientation of σ_{Hmax} (Brook-Barnett et al, 2015). This was shown by the in situ σ_{Hmax} orientation measured from Fantome 1 (Figure 9), being aligned parallel to the fault which is proximal to the well (Figure 1) as well as the variability in σ_{Hmax} orientations measured from wells which are proximal to the Taroom Trough (Figure 1). The in-situ σ_{Hmax} orientation is rotated by regional scale structures and therefore these structures exert a major control over fracture orientation and distribution (King et al, 2008).

The in-situ stress regime also exerts a major control on the structural permeability of a rock or rock formation. Analysis of fracture susceptibility of each fracture set showed that Conductive Sets B, D and E all showed a number of critically stressed fractures that were likely to be aligned with the in situ σ_{Hmax} orientation under certain stress regimes.

Springwater 1, exhibited a large number of fractures belonging to Conductive Set E (Table 2), which is oriented approximately NW-SE and the σ_{Hmax} measured from Springwater 1 was also oriented approximately NW-SE (Figure 9). Figure 10 then shows that under a NW-SE oriented stress regime, Conductive Set D will have a large number of fractures which are optimally aligned with the in situ σ_{Hmax} suggesting they are open to fluid flow. This was confirmed by the significant fluid losses experienced at the same depth as these NW-SE oriented conductive fractures. Therefore, conductive fractures which are optimally aligned with the present day in situ σ_{Hmax} will be able to serve as pathways for fluid flow, and so rock formations containing fractures of this nature will be highly structurally permeable.

7 RECCOMMENDATIONS

While this paper, along with the World Stress Map Project, Schadler, 2013 and Brook-Barnett, 2015, have presented measurements for in-situ stresses in the Bowen-Surat Basins, it remains an incomplete field of study. Schadler, 2013, presents stress magnitudes in the Bowen Basin which are indicative of a strike-slip faulting stress regime, however the stress regime may be varied in different regions of the Bowen-Surat Basins and so a further investigation in to in-situ stress orientations and magnitudes is necessary to better understand the regimes effecting the basins on a wider scale.

8 ACKNOWLEDGMENTS

REFERENCES

AADNOY B. S. & BELL J. S. 1998. Classification of drilling induced fractures and their relationship to in-situ stress directions. Log Analyst 39, 27–42

ANDERSON, E. (1905). The dynamics of faulting. *Transactions Of The Edinburgh Geological Society*, *8*(3), 387-402. http://dx.doi.org/10.1144/transed.8.3.387

BAILEY, A.H.E., King, R.C. & Backé, G., (2012). Integration of structural, stress, and seismic data to define secondary permeability networks through deep-cemented sediments in the Northern Perth Basin. The APPEA Journal, 52, 455–74.

BARTON, C. A., ZOBACK, M. D., & MOOS, D. (1995). Fluid flow along potentially active faults in crystalline rock. Geology, 23(8), 683-686.

BARTON C. A. & ZOBACK M. D. 2000. Discrimination of natural fractures from drilling-induced wellbore failures in wellbore image data—implications for reservoir permeability. SPE Reservoir Evaluation and Engineering 5, 249–254

BELL J. S. 1996a. In situ stresses in sedimentary rocks (Part 2): applications of stress measurements. Geoscience Canada 23, 135– 153.

BELL J. S. 1996b. In situ stresses in sedimentary rocks (Part 1): measurement techniques. Geoscience Canada 23, 85–100.

BELL, J. & GOUGH, D. (1979). Northeast-southwest compressive stress in Alberta evidence from oil wells. *Earth And Planetary Science Letters*, *45*(2), 475-482. http://dx.doi.org/10.1016/0012-821x(79)90146-8

BROOKE-BARNETT, S., FLOTTMANN, T., PAUL, P., BUSETTI, S., HENNINGS, P., REID, R., & ROSENBAUM, G. (2015). Influence of basement structures on in situ stresses over the Surat Basin, southeast Queensland. *J. Geophys. Res. Solid Earth*, *120*(7), 4946-4965. http://dx.doi.org/10.1002/2015jb011964

BRUDY M. & ZOBACK M. D. 1999. Drilling-induced tensile wall fractures: implications for determination of in-situ stress orientation and magnitude. International Journal of Rock Mechanics and Mining Sciences 36, 191–215

BUCK, A., KEOGH, S., WHITEHORN, S., & YASO, H. (2009). Emu Nest 1 Well Completion Report, *Santos Toga PTY LTD*

CADMAN, S. J & PAIN, L. (Leonard) & VUCKOVIC, V. (Velimir) & Australia. Bureau of Resource Sciences (1997). Bowen and Surat Basins, Clarence-Moreton Basin, Sydney Basin, Gunnedah Basin and other minor onshore basing, Qld, NSW and NT. Dept. of Primary Industries and Energy, Bureau of Resource Sciences, [Kingston, A.C.T.]

CORCORAN, D. & DORE, A. (2002). Depressurization of hydrocarbon-bearing reservoirs in exhumed basin settings: evidence from Atlantic margin and borderland basins. *Geological Society, London, Special Publications*, *196*(1), 457-483. http://dx.doi.org/10.1144/gsl.sp.2002.196.01.25

COSGROVE, J. & ENGELDER, T. (2004). *The initiation, propagation, and arrest of joints and other fractures*. London: Geological Society.

DICKINS, J. & MALONE, E. (1973). *Geology of the Bowen Basin, Queensland*. Canberra: Australian Govt. Pub. Service.

DI NACCIO, D., BONCIO, P., CIRILLI, S., CASAGLIA, F., MORETTINI, E., LAVECCHIA, G., & BROZZETTI, F. (2005). Role of mechanical stratigraphy on fracture development in carbonate reservoirs: Insights from outcropping shallow water carbonates in the Umbria–Marche Apennines, Italy. *Journal Of Volcanology And Geothermal Research*, *148*(1-2), 98-115. http://dx.doi.org/10.1016/j.jvolgeores.2005.03.016

EXON, N. F. & Australia. Bureau of Mineral Resources, Geology and Geophysics. (1976). Geology of the Surat Basin in Queensland. Canberra : Australian Govt. Pub. Service

FOSSEN, H. (2010). *Structural geology*. Cambridge: Cambridge University Press.

GRAY, I. (1987a), Reservoir engineering in coal seams: Part 1—The physical process of gas storage and movement in coal seams,SPE Reservoir Eng., 2(1),28–34.

GRAY, I. (1987b), Reservoir engineering in coal seams: Part 2—Observations of gas movement in coal seams, SPE Reservoir Eng., 2(1), 35–40

HEALY, D., JONES, R., & HOLDSWORTH, R. (2006). New insights into the development of brittle shear fractures from a 3-D numerical model of microcrack interaction. Earth And Planetary Science Letters, 249(1-2), 14-28. http://dx.doi.org/10.1016/j.epsl.2006.06.041

HEIDBACH, O., TINGAY, M.R.P., BARTH, A., REINECKER, J., KURFEB, D., MÜLLER, B., 2010. Global crustal stress pattern based on the 2008 World Stress Map database release. Tectonophysics 482, 3–15 doi:10.1016/j.tecto.2009.07.023.

HILLIS, R.R and S.D. REYNOLDS (2000): The Australian Stress Map. - J. Geol. Soc., London, 157, 915- 921.

KING, R., HILLIS, R., & REYNOLDS, S. (2008). In situ stresses and natural fractures in the Northern Perth Basin, Australia. *Australian Journal Of Earth Sciences*, *55*(5), 685-701. http://dx.doi.org/10.1080/08120090801982843

KIRSCH V. 1898. Die Theorie der Elastizitat und die Beddurfnisse der Festigkeitslehre. Zeitschrift des Vereines Deutscher Ingenieure 29, 797–807

LACAZETTE, A. (2001). *Natural Fractures*. *Naturalfractures.com*. Retrieved 17 September 2016, from http://www.naturalfractures.com/1.1.htm

LAUBACH, S. E., 1988, Subsurface fractures and their relationship to stress history in east Texas basin sandstone: Tectonophysics, v. 156, p. 37–49.

LAUBACH, S. E. (2003). Practical approaches to identifying sealed and open fractures. AAPG bulletin, 87(4), 561579.

MARTEL, S. (1999). Analysis of Fracture Orientation Data From Boreholes. *Environmental & Engineering Geoscience*, *V*(2), 213-233. http://dx.doi.org/10.2113/gseegeosci.v.2.213

National Research Council, 1996, *Rock fractures and fluid flow*. Washington, DC : National Academy Press.

NELSON, R. (2001). *Geologic analysis of naturally fractured reservoirs*. Boston: Gulf Professional Pub.

42

PEACOCK, D., Nixon, C., Rotevatn, A., Sanderson, D., & Zuluaga, L. (2016). Glossary of fault and other fracture networks. *Journal Of Structural Geology*, *92*, 12-29. http://dx.doi.org/10.1016/j.jsg.2016.09.008

PESKA P. & ZOBACK M. D. 1995. Compressive and tensile failure of inclined well bores and determination of in situ stress and rock strength. Journal of Geophysical Research 100, 12791–12811.

RIDER, M. H and Martin KENNEDY. *The Geological Interpretation Of Well Logs*. Scotland: Rider-French Consulting Limited, 2011. Print.

SCHADLER, M. (2013). In Situ Stress and Fracture characterisation in the Fairview Area, Bowen Basin. *The University Of Adelaide Thesis*.

SIBSON, R. H. (1977). Fault rocks and fault mechanisms. Journal of the Geological Society, 133(3), 191-213

SIBSON, R. (1996). Structural permeability of fluid-driven fault-fracture meshes. *Journal Of Structural Geology*, *18*(8), 1031-1042. http://dx.doi.org/10.1016/0191-8141(96)00032-6

TERZAGHI, K. and PECK, R.B. 1948. Soil Mechanics in Engineering Practice. New York: John Wiley & Sons

TINGAY, M., REINECKER, J., & MULLER, B. (2008). Borehole breakout and drilling-induced fracture analysis from image logs. *World Stress Map Project*.
TOTTERDELL, J., MOLONEY, J., KORSCH, R., & KRASSAY, A. (2009). Sequence stratigraphy of the Bowen–Gunnedah and Surat Basins in New South Wales. *Australian Journal Of Earth Sciences*, *56*(3), 433-459. http://dx.doi.org/10.1080/08120090802698729

TWISS, R. & MOORES, E. (2007). *Structural geology*. New York, NY: W.H. Freeman.

WHITE, A., TRAUGOTT, M., & SWARBRICK, R. (2002). The use of leak-off tests as means of predicting minimum in-situ stress. *Petroleum Geoscience*, *8*(2), 189-193. http://dx.doi.org/10.1144/petgeo.8.2.189

ZANG, A. & STEPHANSSON, O. (2008). *Stress field of the Earth's crust*. Dordrecht: Springer.

ZOBACK, M., BARTON, C., BRUDY, M., CASTILLO, D., FINKBEINER, T., & GROLLIMUND, B. et al. (2003). Determination of stress orientation and magnitude in deep wells. *International Journal Of Rock Mechanics And Mining Sciences*, *40*(7-8), 1049-1076. http://dx.doi.org/10.1016/j.ijrmms.2003.07.001

ZOBACK, M. (2007). *Reservoir geomechanics*. Cambridge: Cambridge University Press.

ZOBACK M.. 1992. First- and second-order patterns of stress in the lithosphere: the World Stress Map Project. Journal of Geophysical Research 97, 11703–11728.

ZOBACK, M.D., D. MOOS, L.G. MASTIN AND R.N. ANDERSON (1985): Well bore breakouts and in situ stress. - J. Geophys. Res., 90, 5523-5530.

APPENDIX A: EXTENDED METHOD

Using RokDoc to Analyse Image Logs

Ikon Science's 'RokDoc' software was used to load and display image logs, and measure natural fractures, DITFs, and BOs. Initially, Image log files 'DLIS' files were obtained from the Queensland Government's Department of Natural Resources and Mines online database. These files could then be read by RokDoc under the 'Well Management' tab. Once the file had been read, a dialogue would display the tool types recognised by RokDoc, and the associated image logs. The image log could then be selected and imported to the RokDoc project.

Once image logs from a number of wells had been imported, they could be displayed in a separate window for analysis, alongside other wireline logs if need. The scale bar can be used to zoom in and out of the image log in order to display an appropriate scale on screen. For the sake of identifying fractures, BOs and DITFs, a 1-2m scale was ideal. The surface picking tool was then used to mark fractures throughout the image log, overlaying a sinusoid shape to be fit to identified fractures. The DITF and BO picking tools fit rectangles around the identified features. Once features had been identified RokDoc provides 'surface sets' with related data, including the depth at which features were picked, their azimuthal orientation, and in the case of fractures their dip angles. This data was exported to Microsoft Excel for further analysis.

APPENDIX B: RAW DATA

Monslatt 9

Top Depth (m)	Bottom Depth (m)	Depth (m)	True Dip (deg)	True Azimuth (deg)	Surface Type
227.8854	228.2641	228.0748	67.65652	248.0198	ConFracC
244.8819	244.986	244.9339	33.78481	53.76238	ConFracC
245.0014	245.0653	245.0334	22.32191	217.1287	ConFracC
245.9304	246.276	246.1032	65.75181	315.1485	ConFracC
246.6499	246.8913	246.7706	57.18889	27.62376	ConFracC
249.3979	249.457	249.4274	20.81503	157.1287	ConFracC
249.2949	249.3446	249.3198	17.71037	328.2178	ConFracC
252.0535	252.47	252.2618	69.51171	247.4257	ConFracC
261.4854	261.5209	261.5032	12.84951	319.901	ConFracC
264.4499	265.4677	264.9588	81.30474	89.40594	ConFracC
288.56	288.7588	288.6594	51.94312	70.39604	ConFracC
301.2168	301.3589	301.2878	42.37666	41.88119	ConFracC
302.889	303.3553	303.1222	71.53991	305.6436	ConFracC
302.6997	302.9908	302.8452	61.86858	306.8317	ConFracC
321.4654	321.5861	321.5257	37.79443	260.495	ConFracC
334.8867	334.9743	334.9305	29.36376	254.5545	RFracC
345.8725	346.0382	345.9553	46.78786	81.08911	ConFracC
345.7281	345.9056	345.8169	48.75471	51.38614	ConFracC
350.2796	350.4548	350.3672	48.37315	28.81188	ConFracC
358.0997	358.2749	358.1873	48.37315	72.77228	ConFracC
358.2536	358.5802	358.4169	64.52029	75.14851	ConFracC
360.4086	360.9459	360.6772	73.84349	79.90099	RFracC
361.0867	361.4394	361.263	66.18525	63.26733	RFracC
361.6181	361.9116	361.7648	62.06105	75.14851	ConFracC
362.9719	363.1116	363.0417	41.89759	267.6238	ConFracC

363.1909	363.4915	363.3412	62.62417	255.7426	RFracC
363.3163	363.5601	363.4382	57.44295	258.1188	RFracC
363.5802	363.6678	363.624	29.36376	270	RFracC
363.7494	363.837	363.7932	29.36376	280.6931	RFracC
364.6832	364.8725	364.7778	50.57878	52.57426	ConFracC
364.2986	364.3648	364.3317	23.06348	47.82178	ConFracC
365.3329	365.5293	365.4311	51.60958	76.33663	ConFracC
367.6287	367.7542	367.6915	38.86659	58.51485	ConFracC
368.0678	368.1719	368.1199	33.78572	68.0198	ConFracC
371.6181	372.1719	371.895	74.30264	265.2475	RFracC
374.6311	375.2631	374.9471	76.16331	73.9604	RFracC
376.824	377.456	377.14	76.16331	271.1881	RFracC
383.9057	384.1116	384.0086	52.91473	13.36634	ConFracC
393.166	393.353	393.2595	50.22482	202.2772	RFracC
393.9341	394.1187	394.0264	49.86552	119.1089	ConFracC
397.5862	397.8086	397.6974	55.02334	198.7129	RFracC
397.4359	397.682	397.5589	57.69353	184.4554	RFracC
398.7802	398.837	398.8086	20.04998	315.1485	ConFracC
398.8264	398.8714	398.8489	16.11548	285.4455	ConFracC
410.9353	411.0797	411.0075	42.84854	201.0891	RFracC
411.9945	412.1483	412.0714	44.66602	255.7426	RFracC
411.8335	411.8714	411.8524	13.67489	274.7525	RFracC
412.6442	412.959	412.8016	63.68964	132.1782	ConFracC
414.0584	414.1436	414.101	28.69669	16.33663	ConFracC
416.9448	417.0087	416.9767	22.32078	348.4158	RFracC
417.0619	417.1211	417.0915	20.81387	66.83168	RFracC
417.6844	417.7436	417.714	20.81387	79.90099	RFracC
444.3803	444.8158	444.598	70.33265	54.9505	ConFracC
448.2986	448.372	448.3353	25.23817	125.0495	RFracC
459.959	460.3945	460.1767	70.33265	78.71287	ConFracC
476.3401	477.0904	476.7152	78.27997	76.33663	RFracC
476.8998	477.8608	477.3803	80.79925	73.9604	RFracC
478.0726	478.901	478.4868	79.3585	75.14851	RFracC
479.2998	480.1282	479.714	79.3585	73.9604	RFracC
481.4262	482.1197	481.7729	77.35044	87.0297	ConFracC
482.5557	483.0919	482.8238	73.81205	313.9604	ConFracC
484.236	485.0981	484.6671	79.76573	332.9703	ConFracC
498.1246	498.4498	498.2872	64.42081	308.0198	RFracC
519.2937	520.7244	520.0091	83.79113	73.9604	ConFracC
519.8332	521.6123	520.7228	85.00013	71.58416	ConFracC
533.8936	534.6612	534.2774	78.53742	77.52475	ConFracC
551.4662	551.9978	551.732	73.67986	106.0396	ConFracC
553.6298	553.9141	553.7719	61.30222	116.7327	ConFracC
556.6475	557.0218	556.8347	67.4171	49.0099	ConFracC
555.917	556.0664	555.9917	43.83715	43.06931	ConFracC
556.3778	556.5272	556.4525	43.83715	39.50495	ConFracC
558.0862	558.2693	558.1778	49.64421	54.9505	ConFracC
553.6972	554.2288	553.963	73.67986	106.0396	ConFracC
555.709	555.9484	555.8287	56.96613	98.91089	ConFracC
565.8694	566.165	566.0172	62.22794	57.32673	ConFracC
567.3642	567.5474	567.4558	49.64421	45.44554	ConFracC
568.0835	568.6039	568.3437	73.34669	335.3465	ConFracC

563.5766	563.6586	563.6176	27.78762	49.0099	ConFracC
562.8966	563.1022	562.9994	52.87942	59.70297	ConFracC
562.2278	562.4335	562.3307	52.87942	22.87129	ConFracC
561.3737	561.5793	561.4765	52.87942	50.19802	ConFracC
561.6378	561.8434	561.7406	52.87942	65.64356	ConFracC
564.9646	565.5075	565.236	74.00031	318.7129	ConFracC
566.9933	567.1428	567.068	43.83715	266.4356	ConFracC
570.5449	570.7618	570.6534	54.3353	310.396	ConFracC
571.9274	572.3129	572.1201	68.01196	252.1782	ConFracC
587.994	588.1322	588.0631	41.60518	252.1782	ConFracC
589.545	590.1328	589.8389	75.16804	113.1683	ConFracC
593.3888	593.617	593.5029	55.69492	298.5149	ConFracC
595.0466	595.5895	595.318	74.00031	100.099	ConFracC
598.8568	599.2085	599.0326	66.13122	110.7921	ConFracC
611.782	612.2236	612.0028	70.5871	57.32673	ConFracC
613.0014	613.3644	613.1829	66.79097	311.5842	ConFracC
612.1753	612.8643	612.5198	77.26901	306.8317	ConFracC
619.6692	619.7842	619.7267	36.45951	266.4356	ConFracC
626.8837	627.2115	627.0476	64.5961	245.0495	ConFracC
645.0197	645.2039	645.1118	49.79341	321.0891	ConFracC
646.9211	647.7381	647.3296	79.21403	209.4059	ConFracC
648.1776	648.4734	648.3255	62.24906	254.5545	ConFracC
649.4808	650.9409	650.2108	83.91507	107.2277	ConFracC
651.8454	651.9848	651.9151	41.84091	257.5248	ConFracC
657.163	657.568	657.3655	68.97616	44.25743	ConFracC
669.1583	669.9715	669.5649	79.16518	305.6436	ConFracC
670.1754	670.9775	670.5765	79.01702	120.297	ConFracC
672.5638	672.9162	672.74	66.17299	308.0198	ConFracC
672.7717	673.4838	673.1278	77.67041	306.8317	ConFracC
674.265	674.4183	674.3416	44.56533	246.8317	ConFracC
668.2913	668.9166	668.604	76.02306	231.9802	ConFracC
678.5809	679.2287	678.9048	76.48996	63.26733	ConFracC
680.3454	680.5437	680.4446	51.86562	230.7921	ConFracC
694.7614	696.4851	695.6232	84.83999	252.7723	ConFracC
697.7736	698.3958	698.0847	75.95499	310.396	ConFracC
697.0936	697.5022	697.2979	69.14881	82.27723	ConFracC
748.519	748.9277	748.7234	69.14881	68.0198	RFracC
756.8249	757.1549	756.9899	64.74679	62.07921	ConFracC
765.0352	765.1629	765.099	39.36048	19.30693	ConFracC
777.9154	778.1892	778.0523	60.38095	256.9307	ConFracC
780.5286	780.8024	780.6655	60.38095	245.0495	ConFracC
785.8729	786.2029	786.0379	64.74679	267.6238	ConFracC
814.4657	814.7957	814.6307	64.74679	250.9901	ConFracC
816.3089	816.8187	816.5638	73.02186	94.15842	ConFracC
820.4394	821.2414	820.8404	79.01702	78.71287	ConFracC
827.8629	828.9572	828.4101	81.90428	65.64356	ConFracC
829.7343	830.1654	829.9498	70.14899	78.71287	ConFracC
836.4217	837.0101	836.7159	75.18476	70.39604	ConFracC
839.8496	840.1347	839.9922	61.36102	70.39604	ConFracC
840.6982	840.9832	840.8407	61.36102	68.0198	ConFracC
841.367	841.652	841.5095	61.36102	68.0198	ConFracC
841.2883	841.4721	841.3802	49.75111	91.78218	ConFracC

845.7334	846.0184	845.8759	61.36102	233.1683	ConFracC
860.9852	861.495	861.2401	73.02186	78.71287	ConFracC
914.1246	914.4209	914.2727	62.28331	153.5644	ConFracC
914.4168	914.7131	914.565	62.28331	191.5842	RFracC
936.4627	936.9388	936.7008	71.89554	237.9208	ConFracC
940.3853	940.6253	940.5053	57.0419	129.802	RFracC
262.2305	262.5568	262.3936	56.09262	21.97138	RFracC
369.4347	369.7609	369.5978	55.10057	72.02112	RFracC
371.1342	371.4604	371.2973	55.44392	50.46604	RFracC
376.0653	376.3916	376.2285	57.01582	349.0341	RFracC
415.9716	416.0017	415.9866	6.708918	135.4036	ConFracC
416.9501	417.0059	416.978	15.35887	330.4463	ConFracC
417.0531	417.1218	417.0875	16.24949	78.3937	ConFracC
417.6711	417.7398	417.7055	16.94315	34.568	ConFracC
524.0448	524.6543	524.3495	72.62124	265.2416	ConFracC
536.4692	536.7826	536.6259	53.7828	65.2332	ConFracC
545.1856	545.4475	545.3166	48.93315	61.17984	ConFracC
546.7757	547.2822	547.029	65.48495	54.22614	ConFracC
559.4126	560.4083	559.9105	75.66846	83.53078	ConFracC
569.0882	570.0839	569.5861	75.70547	137.7879	ConFracC
605.6469	606.4881	606.0675	73.57127	65.81395	ConFracC
615.5285	616.138	615.8333	72.87635	303.4705	ConFracC
626.1247	626.438	626.2814	57.76064	258.2435	ConFracC
683.7148	683.8737	683.7942	37.84046	226.6601	ConFracC
684.6804	684.7621	684.7212	18.01772	95.5574	ConFracC
688.2919	688.3606	688.3263	14.94039	96.88681	ConFracC
687.97	688.0388	688.0044	15.02263	105.6937	ConFracC
703.4265	703.727	703.5768	56.99422	278.8783	ConFracC
704.2055	704.506	704.3557	56.94187	270.3993	ConFracC
720.0675	720.2006	720.1341	29.2697	80.75564	RFracC

Ironbark Gully 2

Top Depth (m)	Bottom Depth (m)	Depth (m)	True Dip (deg)	True Azimuth (deg)	Surface Type
519.7709	520.0451	519.908	52.46921	342.6228	ConFracC
527.2903	527.318	527.3041	10.60398	69.77482	ConFracC
527.3265	527.3542	527.3404	10.55067	73.22881	ConFracC
534.0604	534.1074	534.0839	13.84455	117.411	RFracC
566.5622	566.6092	566.5857	15.1196	46.73397	RFracC
566.5912	566.6382	566.6147	15.1196	46.73397	RFracC
566.7434	566.7712	566.7573	10.3077	67.49136	RFracC
566.4171	566.4594	566.4383	14.03678	55.03313	RFracC
566.1706	566.2128	566.1917	14.04209	55.95981	RFracC
567.6039	567.6364	567.6202	11.48956	74.13303	ConFracC
567.6885	567.721	567.7048	11.47793	75.06685	ConFracC
574.3958	574.467	574.4314	17.4552	166.2356	RFracC
574.3498	574.4211	574.3854	17.64424	162.3909	RFracC
594.5852	594.6178	594.6015	10.88657	38.86022	ConFracC
614.2018	614.2489	614.2254	9.725052	237.2719	ConFracC
614.0665	614.1135	614.09	10.51111	197.7728	ConFracC
616.6019	616.7022	616.6521	23.45187	308.5444	RFracC
619.8118	619.854	619.8329	10.06164	324.236	RFracC

621.1725	621.2148	621.1937	8.5187	266.2712	RFracC
628.6194	628.652	628.6357	6.513489	294.178	RFracC
629.608	629.6647	629.6363	16.29719	120.1145	RFracC
629.7264	629.7831	629.7548	16.64571	109.0365	RFracC
646.2807	646.3084	646.2945	5.09113	281.1298	ConFracC
650.3461	650.3835	650.3648	12.19114	63.9698	ConFracC
653.2199	653.2477	653.2338	8.836112	118.2194	ConFracC
653.5414	653.5836	653.5625	13.13688	104.1796	ConFracC
654.4792	654.5746	654.5269	25.57831	116.4519	RFracC
670.2189	670.3095	670.2642	24.09139	129.3601	RFracC
674.4777	674.5199	674.4988	8.785992	270.2232	ConFracC
674.0523	674.0945	674.0734	9.356878	303.5392	ConFracC
685.7902	685.8352	685.8127	11.70639	350.8495	RFracC
686.1021	686.1637	686.1329	13.65042	254.6912	ConFracC
686.2139	686.2755	686.2447	13.75623	238.7853	ConFracC
692.1861	692.2863	692.2362	22.76517	271.1657	RFracC
717.0726	717.0927	717.0827	3.368513	272.5481	RFracC
720.9068	721.0788	720.9928	38.73879	163.8018	RFracC
721.9089	722.0615	721.9852	33.29097	249.4863	RFracC
725.8446	725.8659	725.8553	4.18495	306.9839	ConFracC
726.0246	726.0475	726.0361	4.224518	240.1901	ConFracC
725.6147	725.6266	725.6206	2.15945	338.2871	ConFracC
726.3103	726.3746	726.3425	17.07762	7.379407	RFracC
737.2816	737.3073	737.2944	8.35214	104.5964	ConFracC
742.3773	742.4168	742.3971	11.18238	20.59559	ConFracC
742.761	742.8005	742.7808	9.994509	341.9838	RFracC
743.1227	743.1621	743.1424	11.98053	60.47335	RFracC
743.0012	743.0406	743.0209	11.98356	57.1676	RFracC
744.3745	744.4139	744.3942	11.77737	46.40771	RFracC
744.0474	744.0979	744.0726	12.09989	313.6469	ConFracC
744.9487	745.0157	744.9822	16.53143	326.3797	ConFracC
744.8672	744.8956	744.8814	7.256509	347.0517	ConFracC
755.7184	755.7689	755.7437	12.32648	322.8638	RFracC
762.9976	763.015	763.0063	5.422286	132.2973	RFracC

Moa 1

Top Depth (m)	Bottom Depth (m)	Depth (m)	True Dip (deg)	True Azimuth (deg)	Surface Type
912.2951	912.3206	912.3078	6.462287	331.5692	ConFracC
914.4792	914.572	914.5256	23.1379	275.3545	ConFracC
938.9661	939.0252	938.9957	15.07676	340.9148	ConFracC
948.7787	948.8378	948.8082	15.11632	315.6431	ConFracC
952.7374	952.7966	952.767	15.44436	228.245	ConFracC
988.6358	988.6709	988.6534	9.189318	288.6695	RFracC
987.9977	988.0328	988.0152	9.198222	281.827	RFracC
1008.634	1008.669	1008.652	9.204019	285.4843	RFracC
1008.889	1008.973	1008.931	21.01812	292.6364	RFracC
1010.549	1010.796	1010.672	48.51907	350.2589	ConFracC
1038.64	1038.743	1038.692	25.0943	1.644931	RFracC
1060.317	1060.357	1060.337	10.83583	251.2905	ConFracC
1062.398	1062.422	1062.41	6.648625	210.4588	RFracC
1079.078	1079.113	1079.096	9.043291	322.2112	RFracC

1076.387	1076.407	1076.397	5.593756	269.0019	ConFracC
1080.516	1080.545	1080.53	7.734815	296.2363	ConFracC
1081.16	1081.189	1081.175	7.909181	267.6261	ConFracC
1082.056	1082.085	1082.07	7.85952	273.3261	ConFracC
1081.846	1081.875	1081.86	7.996183	250.7242	ConFracC
1081.309	1081.339	1081.324	7.973236	255.6804	RFracC
1093.673	1093.702	1093.688	7.776896	291.0827	RFracC
1192.427	1192.595	1192.511	37.89303	290.5068	ConFracC
1208.963	1209.048	1209.005	21.16666	83.37259	ConFracC
1216.934	1216.963	1216.948	8.06281	215.2043	RFracC
1217.354	1217.427	1217.391	19.13371	210.4933	RFracC
1220.163	1220.209	1220.186	12.02545	143.049	ConFracC
1220.459	1220.505	1220.482	12.21616	175.7508	ConFracC
1243.492	1243.593	1243.542	24.79005	79.52646	ConFracC
1250.478	1250.662	1250.57	40.3086	344.2777	ConFracC
1255.95	1256.04	1255.995	22.45387	0.601729	ConFracC
1282.823	1282.913	1282.868	22.95149	206.0427	ConFracC
1297.534	1297.707	1297.621	38.34865	81.64434	RFracC
1357.299	1358.259	1357.779	77.6812	235.6678	ConFracC
1367.979	1368.077	1368.028	24.14595	124.6744	ConFracC
1378.982	1379.08	1379.031	24.08892	65.68532	RFracC
1385.098	1385.196	1385.147	24.26348	140.4785	RFracC
1434.606	1434.704	1434.655	24.35049	221.0951	ConFracC
1434.523	1434.621	1434.572	24.3485	221.1624	ConFracC
1441.189	1441.287	1441.238	24.35854	216.8709	RFracC
1490.974	1491.072	1491.023	24.54539	63.13653	ConFracC
1508.812	1508.855	1508.833	11.15805	57.74959	ConFracC
1509.641	1509.684	1509.663	11.15075	53.88493	ConFracC
1509.475	1509.518	1509.497	11.11879	30.11908	ConFracC
1508.549	1508.592	1508.571	11.15257	52.98932	ConFracC
1507.734	1507.776	1507.755	11.18691	74.2077	ConFracC
1510.872	1510.914	1510.893	11.14036	48.11566	ConFracC
1513.495	1513.577	1513.536	20.60166	39.52733	ConFracC
1514.477	1514.558	1514.518	20.63274	58.90106	ConFracC
1547.386	1547.428	1547.407	11.27866	186.8819	RFracC
1562.31	1562.424	1562.367	28.13841	95.86354	ConFracC
1573.811	1573.854	1573.832	10.91922	267.2339	RFracC
1579.056	1579.12	1579.088	16.42178	5.683906	RFracC
1585.987	1586.052	1586.019	16.4451	252.3393	RFracC
1592.542	1592.568	1592.555	6.681425	240.4909	ConFracC
1597.845	1597.982	1597.913	31.94738	318.7509	RFracC
1598.204	1598.258	1598.231	14.33086	117.5412	RFracC
1596.537	1596.978	1596.758	63.97237	43.06866	RFracC
1602.68	1603.055	1602.868	60.4028	147.075	ConFracC
1606.429	1606.489	1606.459	15.44167	194.9772	ConFracC
1633.665	1633.813	1633.739	34.46221	75.4731	RFracC
1636.579	1636.727	1636.653	34.63054	104.6693	RFracC
1682.794	1682.859	1682.827	16.58571	32.07588	RFracC
1682.725	1682.79	1682.758	16.541	23.26861	RFracC
1716.566	1716.874	1716.72	54.62267	281.6188	RFracC
1732.911	1732.987	1732.949	19.27407	61.52015	RFracC
1738.227	1738.303	1738.265	19.6628	118.1317	ConFracC

1742.93	1743.006	1742.968	19.58666	107.594	ConFracC
1742.872	1742.948	1742.91	19.61924	112.4735	ConFracC
1743.34	1743.415	1743.377	19.42751	86.80596	ConFracC
1744.454	1744.529	1744.492	19.1082	46.25595	ConFracC
1749.541	1749.572	1749.557	7.819061	352.7539	RFracC
1754.577	1754.65	1754.613	19.05361	225.6186	RFracC
1780.17	1780.243	1780.207	18.50059	286.6856	RFracC
1785.334	1785.408	1785.371	18.29068	342.4622	RFracC
1794.217	1794.291	1794.254	18.67804	82.11319	RFracC
1797.983	1798.057	1798.02	18.87092	106.7043	RFracC
1800.413	1800.514	1800.464	25.14712	279.7349	RFracC
1807.242	1807.343	1807.293	24.99827	302.002	RFracC
1815.423	1815.524	1815.474	24.72736	333.6004	RFracC
1817.831	1817.932	1817.882	24.51781	34.11151	RFracC
1818.893	1818.994	1818.943	24.79623	333.9359	RFracC
1857.209	1857.288	1857.249	20.0409	292.865	ConFracC
1901.639	1901.718	1901.678	20.09712	117.0931	RFracC
1938.993	1939.1	1939.046	26.22211	355.4925	ConFracC
1943.579	1943.677	1943.628	24.32872	197.798	ConFracC
1969.13	1969.162	1969.146	8.250479	327.1085	ConFracC
1970.93	1970.962	1970.946	8.452042	20.17314	ConFracC
2005.224	2005.278	2005.251	13.91569	10.73322	RFracC
2025.111	2025.165	2025.138	13.97655	358.2593	RFracC
2026.112	2026.165	2026.139	13.82269	199.403	ConFracC
2048.946	2048.999	2048.973	13.66384	306.3186	ConFracC
2119.837	2119.957	2119.897	29.72766	121.1923	RFracC
2126.887	2126.946	2126.916	15.23058	10.57212	RFracC

Woleebee Creek 9

Top Depth (m)	Bottom Depth (m)	Depth (m)	True Dip (deg)	True Azimuth (deg)	Surface Type
415.6089	415.6862	415.6475	20.42319	169.5387	ConFracC
415.8474	415.9296	415.8885	21.59123	165.9668	ConFracC
415.2901	415.3303	415.3102	11.30318	174.7024	ConFracC
420.7245	420.7845	420.7545	15.17469	266.2684	ConFracC
421.3498	421.4024	421.3761	14.00991	212.1956	ConFracC
421.7995	421.8694	421.8345	18.50452	190.9404	ConFracC
423.0871	423.157	423.1221	18.13908	78.33316	RFracC
426.3023	426.3722	426.3372	18.26583	90.61342	RFracC
431.4587	431.4743	431.4665	3.583578	15.24112	RFracC
436.9191	436.9371	436.9281	4.986799	82.23316	RFracC
443.9327	443.9853	443.959	13.38776	26.13499	RFracC
444.4221	444.5883	444.5052	38.05466	189.412	RFracC
444.8064	444.8392	444.8228	8.616089	234.5576	RFracC
447.7855	447.8184	447.802	8.066165	335.6783	RFracC
466.2068	466.2396	466.2232	9.052815	94.28672	RFracC
492.2509	492.2837	492.2673	9.158757	104.7546	ConFracC
517.7513	517.7841	517.7677	9.163927	140.9288	RFracC
523.3859	523.4187	523.4023	8.237485	15.72208	RFracC
523.2648	523.2976	523.2812	8.177007	357.3025	RFracC
534.5563	534.6015	534.5789	11.38505	337.1998	RFracC
544.3069	544.3521	544.3295	12.16615	205.1798	RFracC

547.2033	547.2361	547.2197	8.7619	98.89386	RFracC
550.2109	550.2437	550.2273	8.784135	238.9444	RFracC
555.1103	555.1901	555.1502	20.37358	245.3572	RFracC
567.3137	567.3639	567.3388	13.31845	231.4997	RFracC
570.1323	570.1824	570.1574	13.36472	220.5122	RFracC
574.8216	574.8569	574.8393	8.936835	7.386082	RFracC
582.4173	582.4353	582.4263	4.376192	20.38115	RFracC
586.9707	587.0727	587.0217	25.65423	209.7536	RFracC
597.4034	597.4486	597.426	12.10388	140.1223	RFracC
600.6902	600.7601	600.7252	18.2924	125.5134	ConFracC
606.7784	606.826	606.8022	12.81592	136.055	RFracC
616.0285	616.0539	616.0412	6.71793	86.17616	RFracC
616.0557	616.0811	616.0684	6.792721	96.09245	RFracC
622.4775	622.5399	622.5087	15.98524	287.4197	RFracC
645.8352	645.8903	645.8627	14.19178	277.4038	ConFracC
649.7449	649.8197	649.7823	19.30946	208.1947	ConFracC
655.0162	655.0713	655.0437	14.44169	232.6878	ConFracC
659.451	659.4863	659.4686	9.343454	73.56374	RFracC
661.6727	661.708	661.6904	9.323663	126.1534	RFracC
661.6319	661.6672	661.6496	9.468553	141.9147	RFracC
679.3229	679.3582	679.3406	9.11901	328.2338	ConFracC
695.7214	695.8061	695.7638	21.75517	190.2	ConFracC
695.8932	695.9433	695.9182	13.39353	207.4645	ConFracC
696.6791	696.7514	696.7152	18.89682	203.7458	ConFracC
696.7829	696.8552	696.819	18.88571	201.3168	ConFracC
708.6304	708.6558	708.6431	6.664252	290.9791	RFracC
708.6959	708.7213	708.7086	6.594674	303.6211	RFracC
715.4179	715.468	715.443	13.08827	287.3429	RFracC
715.8405	715.8906	715.8655	12.98889	307.4829	RFracC
716.9205	716.9434	716.9319	6.145077	274.9656	RFracC
732.8395	732.855	732.8473	4.269759	246.4974	ConFracC
732.8716	732.8797	732.8757	2.310361	241.9178	ConFracC
733.1101	733.1429	733.1265	8.851584	221.7078	ConFracC
746.6703	746.7501	746.7102	20.46353	284.5551	RFracC
760.3862	760.4659	760.426	20.38314	137.2469	RFracC
786.5563	786.5866	786.5714	8.396274	232.3141	ConFracC
790.047	790.0749	790.061	7.846863	203.7865	ConFracC
807.5341	807.6114	807.5728	20.31548	195.2561	RFracC
813.558	813.6353	813.5966	20.23432	231.5218	RFracC
816.0133	816.0461	816.0297	8.681377	284.5007	RFracC
819.394	819.4269	819.4104	8.90902	265.9368	RFracC
818.9344	818.9672	818.9508	8.678564	284.3503	RFracC
822.3794	822.4122	822.3958	8.059541	350.1598	RFracC
826.4472	826.48	826.4636	8.903317	268.5693	RFracC
872.0487	872.2509	872.1498	42.27793	35.14358	ConFracC
897.9641	898.0282	897.9961	17.37208	201.7694	ConFracC

Emu Nest 1

Top Depth (m)	Bottom Depth (m)	Depth (m)	True Dip (deg)	True Azimuth (deg)	Surface Type
53.13122	53.20886	53.17004	21.10355	158.7025	ConFracD
55.75844	55.90583	55.83213	36.39026	279.0011	ConFracC

56.03614	56.20507	56.1206	40.39943	4.946583	ConFracC
56.5893	56.72201	56.65566	33.6194	271.6222	ConFracC
56.41335	56.51014	56.46174	26.05585	337.6051	ConFracC
56.92207	57.01168	56.96687	24.25644	287.9504	ConFracC
58.97473	59.15564	59.06518	41.86215	167.5252	ConFracC
59.17463	59.28371	59.22917	28.35805	168.7622	ConFracC
59.32904	59.48361	59.40633	37.44908	181.313	ConFracC
59.5445	59.70864	59.62657	39.15286	178.7767	ConFracC
59.91317	60.07732	59.99524	39.15292	185.0564	ConFracC
60.09511	60.23771	60.16641	35.24021	187.6432	ConFracC
64.05593	64.0932	64.07456	10.33869	167.0905	ConFracC
66.22846	66.35669	66.29258	32.44633	184.9789	ConFracD
66.04771	66.21904	66.13338	40.36979	221.4361	ConFracD
70.95654	71.04648	71.00151	23.91681	155.8132	ConFracD
72.26126	72.32246	72.29186	16.68314	163.4508	ConFracC
73.17575	73.26329	73.21952	23.573	105.5182	ConFracC
74.67557	74.7296	74.70259	14.87115	153.1808	ConFracC
78.80517	78.85919	78.83218	14.81894	177.3173	ConFracC
79.91238	79.94965	79.93101	10.25327	151.5598	ConFracC
81.83354	82.05275	81.94314	47.92367	2.482891	ConFracC
81.93768	82.09704	82.01736	38.88374	356.2911	ConFracC
82.12441	82.22631	82.17536	27.29969	337.7638	ConFracC
83.47117	83.55121	83.51119	21.44498	181.1806	ConFracC
83.94981	84.02538	83.98759	20.34848	160.8344	ConFracC
84.1355	84.31608	84.22579	41.7966	167.3631	ConFracC
86.1774	86.29845	86.23792	30.88173	171.1609	ConFracC
86.64901	86.72697	86.68799	20.99437	155.8887	ConFracC
87.51578	87.60061	87.5582	22.63507	155.8773	ConFracC
87.96928	88.05443	88.01185	23.33744	27.14813	ConFracC
91.01337	91.13889	91.07613	31.81365	157.1679	ConFracC
91.59135	91.73156	91.66146	35.06376	286.727	ConFracC
91.7326	91.88956	91.81108	38.14794	285.4152	ConFracC
92.01987	92.15529	92.08758	33.8516	237.8695	ConFracC
92.25209	92.34921	92.30065	25.72397	255.6943	ConFracC
92.66162	92.83502	92.74832	40.60094	173.6175	ConFracC
92.33843	92.53817	92.4383	44.61747	189.9628	ConFracC
92.46635	92.64247	92.55441	41.03048	179.9129	ConFracC
93.13427	93.4636	93.29893	58.43441	154.9008	ConFracC
93.26833	93.63357	93.45095	60.99208	158.67	ConFracC
93.38444	93.74968	93.56706	60.97488	158.6553	ConFracC
94.86271	94.93589	94.8993	19.76082	168.3298	ConFracC
95.04824	95.10945	95.07885	16.66419	169.5591	ConFracC
95.14879	95.22676	95.18777	20.91657	182.3605	ConFracC
95.3032	95.37638	95.33979	19.74207	173.3908	ConFracC
97.67698	97.77138	97.72418	24.867	172.2623	ConFracC
98.75906	98.81994	98.7895	16.6023	159.2614	ConFracC
106.4569	106.5034	106.4801	12.70002	210.6693	ConFracC
106.2113	106.3563	106.2838	36.33533	22.3716	ConFracC
106.0832	106.1995	106.1414	30.35746	66.85772	ConFracC
108.3467	108.4103	108.3785	17.28494	156.8767	ConFracC
108.7765	108.8712	108.8238	25.02041	151.9905	ConFracC
109.2421	109.3177	109.2799	20.48704	121.4535	ConFracC

127.8001	127.9715	127.8858	40.95277	340.1616	ConFracC
127.933	128.0612	127.9971	32.74574	80.65066	ConFracD
127.8995	128.0277	127.9636	32.94597	47.07031	ConFracD
127.8516	127.9966	127.9241	36.32969	9.914504	ConFracD
131.4425	131.5468	131.4947	27.44952	248.1303	ConFracC
131.3541	131.4509	131.4025	25.4938	193.9821	ConFracC
131.6905	131.7226	131.7066	9.131236	268.3399	ConFracC
132.4206	132.4887	132.4547	19.10669	345.0989	ConFracC
145.694	145.8195	145.7568	31.87822	177.565	ConFracC
146.0316	146.0972	146.0644	17.9531	171.2338	ConFracC
146.0902	146.1559	146.123	17.95308	173.7641	ConFracC
146.1285	146.2301	146.1793	26.69727	173.7489	ConFracC
146.2662	146.3917	146.3289	31.91786	151.1268	ConFracC
146.4349	146.4527	146.4438	5.280281	356.1435	ConFracC
146.5654	146.6119	146.5887	13.23332	45.42079	ConFracC
152.7023	152.9571	152.8297	52.05672	7.439574	ConFracC
153.1297	153.2073	153.1685	21.31522	55.83701	ConFracC
153.6085	153.7819	153.6952	40.9465	71.10813	ConFracC
157.1946	157.6074	157.401	64.06106	171.2488	ConFracC
178.3322	178.4792	178.4057	36.41719	70.95597	ConFracC
187.5525	187.6517	187.6021	26.54598	80.67616	ConFracC
199.0675	199.1715	199.1195	27.12174	209.1835	ConFracC
296.7764	297.0063	296.8914	48.45903	150.2081	ConFracC
340.0078	341.9353	340.9715	85.24927	338.7073	DITF
351.1095	351.515	351.3123	65.17881	319.8571	ConFracC
355.4206	355.7424	355.5815	56.828	149.0605	ConFracC
372.1422	372.3637	372.2529	46.26262	145.5441	ConFracC
440.5213	440.9017	440.7115	62.26479	40.6709	ConFracC
442.1478	442.4113	442.2795	53.71538	274.2657	ConFracC
443.3813	443.6866	443.534	56.32658	65.56505	ConFracC
449.5447	450.009	449.7769	66.27443	78.45527	ConFracC
449.1391	449.6452	449.3922	68.23867	64.71314	ConFracC
446.9523	447.0819	447.0171	33.48042	261.032	ConFracC
450.8244	451.3469	451.0857	68.83109	63.43099	ConFracC
466.3166	467.065	466.6908	75.07178	48.53031	ConFracD
466.2748	466.6134	466.4441	59.58619	36.99171	ConFracC
466.7097	466.9981	466.8539	55.39905	38.19853	ConFracC
466.7975	467.4288	467.1131	72.34382	53.48301	ConFracC
467.4372	467.8846	467.6609	65.99215	44.60823	ConFracC
592.0734	592.7467	592.41	71.42643	196.4865	ConFracC
55.94034	56.08293	56.01163	35.66972	332.6251	ConFracC
56.07322	56.1597	56.11646	23.49701	294.1793	ConFracC
59.31198	59.55623	59.4341	50.43782	181.2898	ConFracC
59.21601	59.36871	59.29236	37.12002	177.5336	ConFracC
59.70473	59.87515	59.78994	40.23091	208.9635	ConFracC
60.23035	60.31514	60.27274	22.7559	201.602	ConFracC
62.83043	62.86797	62.8492	10.43914	150.5549	ConFracC
65.91183	66.05273	65.98228	35.04538	246.5702	ConFracC
65.94136	66.13246	66.03691	43.44585	195.051	ConFracC
66.03291	66.21514	66.12402	42.26406	110.9678	ConFracC
66.39907	66.46909	66.43408	19.06634	174.9397	ConFracC
66.45961	66.52963	66.49462	19.04588	167.3672	ConFracC

70.69562	70.75973	70.72768	17.81819	85.23485	RFracC
71.41466	71.47878	71.44672	17.52017	143.0428	ConFracC
71.5003	71.56441	71.53236	17.53168	141.896	ConFracC
71.69667	71.78736	71.74202	24.09028	159.7327	ConFracC
73.35623	73.40853	73.38238	14.39049	144.2103	ConFracC
157.9227	158.2544	158.0885	58.96073	346.2782	ConFracC
222.6207	222.6355	222.6281	4.371762	63.50994	RFracC
329.8806	329.9971	329.9389	31.31185	331.8434	RFracC
331.0377	331.1183	331.078	22.93115	346.0437	RFracC
341.2775	341.4359	341.3567	39.64626	322.3417	RFracC
340.8111	340.9695	340.8903	39.58268	335.7296	RFracC
342.1625	342.4284	342.2955	54.33934	327.3581	RFracC
351.64	352.6892	352.1646	79.29585	34.72038	ConFracC
352.8777	352.9105	352.8941	10.76557	307.9462	RFracC
354.83	354.8628	354.8464	10.58566	283.8657	RFracC
364.6663	364.7768	364.7215	28.15766	187.4494	ConFracC
364.8845	364.995	364.9398	30.40935	314.5958	RFracC
377.1425	377.4084	377.2754	51.34808	142.8854	ConFracC
384.9218	385.0203	384.971	27.99786	290.811	ConFracC
416.7266	416.7953	416.761	17.66899	99.79991	RFracC
418.0959	418.1586	418.1273	16.51016	71.61953	RFracC
435.4783	435.8399	435.6591	59.84712	118.7172	ConFracC
451.1206	451.2969	451.2088	41.34749	52.77679	ConFracC
453.7935	453.9697	453.8816	41.46165	232.2237	ConFracC
457.0014	457.1119	457.0567	28.66117	73.68889	ConFracC
458.885	458.9237	458.9043	10.35072	109.1402	RFracC
518.0759	518.1146	518.0952	11.35151	47.7903	RFracC
519.2837	519.3225	519.3031	12.34301	355.0689	RFracC
564.39	564.4885	564.4392	27.55168	39.36999	RFracC
564.387	564.4855	564.4362	27.48284	41.75654	RFracC
581.7155	581.7662	581.7409	13.81594	94.11804	RFracC
586.1254	586.1761	586.1507	13.9564	89.13443	RFracC
598.6283	599.0739	598.8511	64.1651	204.2043	RFracC
600.5926	601.0442	600.8184	64.18447	173.7318	RFracC

Waddy Brae 1

Top Depth (m)	Bottom Depth (m)	Depth (m)	True Dip (deg)	True Azimuth (deg)	Surface Type
1433.506	1433.603	1433.554	17.03793	90.33	RFracC
1441.7	1442.335	1442.018	65.21322	38.43648	ConFracC
1441.442	1441.709	1441.576	58.08896	244.4942	ConFracC
1441.258	1441.525	1441.392	57.86766	236.4655	ConFracC
1443.353	1443.388	1443.371	5.293945	159.4711	ConFracC
1444.059	1444.096	1444.077	3.907631	128.7159	ConFracC
1444.692	1444.709	1444.701	3.829518	215.202	ConFracC
1449.432	1449.667	1449.55	49.25824	321.5673	ConFracC
1446.113	1446.629	1446.371	63.34726	14.85475	ConFracC
1445.233	1446.188	1445.71	77.24582	340.9064	ConFracC
1445.62	1446.269	1445.945	70.43785	350.1244	ConFracC
1451.341	1452.088	1451.715	75.44019	325.6692	ConFracC
1454.941	1455.659	1455.3	66.83139	58.25874	ConFracC

1455.833	1456.418	1456.126	63.78523	45.09268	ConFracC
1491.773	1491.801	1491.787	2.043482	94.58361	RFracC
1508.002	1508.057	1508.029	10.28432	107.4016	ConFracC
1515.351	1515.541	1515.446	45.4462	209.1073	ConFracC
1521.261	1521.43	1521.345	41.37333	194.2168	ConFracC
1522.923	1523.225	1523.074	55.45834	163.2597	ConFracC
1523.567	1524.01	1523.789	65.45091	167.1285	ConFracC
1525.119	1525.562	1525.341	66.3685	178.1503	ConFracC
1527.425	1527.868	1527.647	65.25476	163.4196	ConFracC
1532.329	1533.143	1532.736	75.86098	153.7222	ConFracC
1540.464	1540.549	1540.507	18.59628	109.6126	ConFracC
1540.86	1541.096	1540.978	44.2333	101.0941	ConFracC
1563.158	1563.364	1563.261	46.61393	279.2885	RFracC
1565.076	1565.14	1565.108	21.94125	230.7708	RFracC
1564.942	1565.015	1564.979	23.17211	194.388	RFracC
1565.981	1566.141	1566.061	42.06495	223.9467	RFracC
1566.173	1566.319	1566.246	39.40068	219.5577	RFracC
1565.689	1565.795	1565.742	30.96428	252.5446	ConFracC
1568.099	1568.262	1568.181	31.94154	26.1834	ConFracC
1569.186	1569.268	1569.227	22.73588	162.8345	RFracC
1569.691	1569.909	1569.8	48.06313	169.3995	RFracC
1570.167	1570.337	1570.252	39.89241	157.6411	RFracC
1571.921	1571.994	1571.957	23.99253	210.349	RFracC
1571.974	1572.047	1572.01	22.92347	189.4147	RFracC
1572.076	1572.179	1572.128	31.04853	220.8481	RFracC
1572.875	1572.93	1572.903	19.7513	228.7351	RFracC
1573.062	1573.117	1573.089	19.67602	216.8813	RFracC
1573.238	1573.293	1573.266	19.74245	218.7792	ConFracC
1574.417	1574.508	1574.462	27.52466	196.13	ConFracC
1575.65	1575.741	1575.695	28.0905	210.7107	ConFracC
1579.222	1579.385	1579.303	31.70058	44.96032	RFracC
1580.168	1580.332	1580.25	32.07219	67.84911	RFracC
1579.878	1580.081	1579.979	37.90863	58.94352	RFracC
1579.876	1580.079	1579.978	38.08462	65.88645	RFracC
1595.768	1595.971	1595.869	38.73715	78.37229	ConFracC
1595.651	1595.799	1595.725	30.1567	81.0896	ConFracC
1598.264	1598.479	1598.371	50.07329	232.9536	ConFracC
1598.433	1598.647	1598.54	49.91656	207.6636	ConFracC
1599.393	1599.608	1599.5	40.10066	71.2872	ConFracC
1600.448	1600.63	1600.539	43.98282	183.9013	ConFracC
1396.678	1396.732	1396.705	10.69857	100.1678	ConFracC
1400.782	1400.815	1400.799	5.378185	105.5703	RFracC
1400.919	1400.982	1400.951	13.30738	115.6159	RFracC
1414.346	1414.38	1414.363	5.162599	130.504	RFracC
1415.106	1415.14	1415.123	4.34689	109.1646	RFracC
1415.965	1415.999	1415.982	5.385578	137.0048	RFracC

Springwater 1

Top Depth (m)	Bottom Depth (m)	Depth (m)	True Dip (deg)	True Azimuth (deg)	Surface Type
1298.406	1300.406	1299.406	84.85276	350.0334	ConFracC
1299.978	1301.978	1300.978	84.84019	358.7729	ConFracC

55

1301.967	1304.015	1302.991	84.87836	341.2852	ConFracC
1304.091	1306.014	1305.052	84.54612	336.2938	ConFracC
1310.217	1311.699	1310.958	82.69704	345.0429	ConFracC
1314.973	1316.51	1315.741	83.10973	352.5379	ConFracC
1435.97	1436.894	1436.432	78.29852	330.121	ConFracC
1446.652	1447.278	1446.965	72.53416	314.0773	ConFracC
1462.535	1463.161	1462.848	72.78848	322.8341	ConFracC
1462.834	1463.46	1463.147	72.89229	329.0617	ConFracC
1463.096	1463.721	1463.408	72.99187	334.0385	ConFracC
1463.497	1464.291	1463.894	76.80343	347.6905	ConFracC
1463.992	1465.01	1464.501	79.48229	326.4519	ConFracC
1464.58	1465.598	1465.089	79.88578	352.6261	ConFracC
1467.354	1468.371	1467.862	79.71699	340.1646	ConFracC
1468.334	1469.8	1469.067	83.15188	341.3706	ConFracC
1470.463	1471.088	1470.776	73.30156	345.2731	ConFracC
1472.461	1473.236	1472.849	76.25971	331.529	ConFracC
1485.889	1486.663	1486.276	76.34053	319.1101	ConFracC
1488.438	1489.754	1489.096	82.33747	325.196	ConFracC
1486.916	1487.952	1487.434	80.06181	326.4953	ConFracC
1496.412	1497.448	1496.93	79.86865	316.5542	ConFracC
1507.244	1508.28	1507.762	80.44551	331.5193	ConFracC
1508.458	1509.494	1508.976	80.61521	338.9794	ConFracC
1513.818	1514.854	1514.336	80.32738	325.3088	ConFracC
1533.389	1533.79	1533.59	65.11738	323.203	ConFracC
1533.744	1534.145	1533.945	64.47498	300.9528	ConFracC
1532.708	1533.109	1532.908	64.33542	298.4703	ConFracC
1538.441	1538.842	1538.641	64.42274	300.9753	ConFracC
1538.861	1539.262	1539.062	64.88319	313.3442	ConFracC
1539.188	1539.589	1539.388	65.42804	333.0772	ConFracC
1552.94	1553.157	1553.048	48.99321	37.55001	RFracC
1580.032	1580.338	1580.185	59.41064	15.80503	RFaultC
1580.919	1581.412	1581.166	70.60364	12.28553	RFaultC
1579.378	1579.715	1579.546	61.38872	322.1851	ConFracC
1584.643	1585.569	1585.106	75.48201	145.871	ConFracC
1585.858	1586.988	1586.423	77.59718	147.1912	ConFracC
1586.704	1587.811	1587.258	77.31709	149.7063	ConFracC
1587.835	1588.942	1588.389	77.55629	140.8886	ConFracC
1588.05	1589.157	1588.603	77.22503	152.225	ConFracC
1588.944	1590.051	1589.497	77.38256	145.9263	ConFracC
1589.804	1590.911	1590.358	77.30944	145.9222	ConFracC
1590.23	1591.337	1590.784	77.58471	137.1151	ConFracC
1590.481	1591.588	1591.035	77.07801	153.4925	ConFracC
1591.356	1592.355	1591.855	76.35134	139.5941	ConFracC
1599.643	1601.596	1600.619	81.8811	134.7355	ConFracC
1602.452	1604.1	1603.276	82.30539	102.1005	ConFracC
1614.422	1614.7	1614.561	57.30185	333.3218	ConFracC
1615.071	1615.36	1615.216	58.17008	327.2848	ConFracC
1616.05	1616.503	1616.276	69.14351	333.0284	ConFracC
1617.539	1617.992	1617.766	69.10276	331.7802	ConFracC
1619.621	1620.073	1619.847	68.43262	308.4954	ConFracC
1625.218	1625.258	1625.238	14.61947	352.3251	RFracC
1626.547	1626.588	1626.567	12.59714	58.88464	RFracC

1626.592	1626.633	1626.613	12.59714	58.88464	RFracC
1627.109	1627.149	1627.129	14.48623	11.87635	RFracC
1627.482	1627.537	1627.509	17.43711	313.946	RFracC
1637.906	1637.96	1637.933	16.20314	290.8722	RFracC
1638.691	1638.746	1638.719	13.50263	118.1588	RFracC
1640.257	1640.281	1640.269	9.762705	347.3085	RFracC
1645.809	1645.834	1645.821	9.266675	30.20325	RFracC
1649.616	1649.676	1649.646	18.25748	51.96376	RFracC
1652.482	1652.515	1652.499	9.739774	72.27705	RFracC
1652.336	1652.351	1652.343	5.233085	60.21354	RFracC
1655.213	1655.347	1655.28	34.34691	79.33454	RFracC
1594.408	1594.555	1594.481	36.10885	87.12383	ConFracC
1617.132	1617.455	1617.294	60.93565	322.3285	ConFracC
1621.415	1621.749	1621.582	61.00339	301.5122	ConFracC
1628.01	1628.141	1628.076	36.04756	18.15592	RFracC
1628.193	1628.28	1628.236	26.53432	16.22022	RFracC
1635.827	1636.08	1635.954	53.14701	295.7735	ConFracC
1636.106	1636.322	1636.214	49.35163	313.1092	ConFracC
1649.025	1649.118	1649.072	25.09439	80.00745	RFracC
1649.384	1649.445	1649.414	18.0168	61.16707	RFracC
1650.156	1650.216	1650.186	17.94963	62.41545	RFracC
1651.109	1651.17	1651.14	14.97612	122.8754	RFracC
1652.031	1652.091	1652.061	18.69644	50.07592	RFracC

Alderley 1

Top Depth (m)	Bottom Depth (m)	Depth (m)	True Dip (deg)	True Azimuth (deg)	Surface Type
241.9017	241.9896	241.9457	35.73347	149.6821	ConFracC
258.1638	258.2854	258.2246	45.47349	87.97813	ConFracC
321.9177	321.9503	321.934	14.74687	131.024	RFracC
162.536	162.6955	162.6158	53.39827	271.738	ConFracC
162.8038	162.8663	162.835	27.51096	241.2045	ConFracC
163.4644	163.5547	163.5095	36.74142	219.4536	ConFracC
164.5275	164.5734	164.5504	21.73393	334.1299	RFracC
167.8584	167.8876	167.873	14.13035	282.3689	ConFracC
170.6424	170.6994	170.6709	25.30928	87.53636	RFracC
185.0484	185.1054	185.0769	26.20189	314.3367	ConFracC
185.4537	185.5828	185.5183	46.69194	142.3126	ConFracC
189.9254	189.9768	189.9511	23.76372	289.7751	ConFracC
191.5075	191.5479	191.5277	18.22877	129.0929	RFracC
198.7799	198.9146	198.8473	48.53131	259.2123	ConFracC
201.2115	201.2685	201.24	25.43744	244.8638	ConFracC
205.7748	205.8206	205.7977	20.7956	105.0819	RFracC
205.7748	205.8206	205.7977	20.7956	105.0819	RFracC
273.5996	273.6899	273.6447	37.50671	288.3017	RFracC
288.4302	288.4872	288.4587	25.99142	291.342	ConFracC
295.6388	295.6791	295.659	18.49906	94.11235	ConFracC
299.7441	299.7844	299.7643	19.40204	347.6886	RFracC
305.3372	305.3775	305.3573	18.2085	124.4596	RFracC
317.7502	317.7683	317.7593	8.126384	207.9297	RFracC
318.136	318.1875	318.1618	23.29093	87.2033	ConFracC
323.3738	323.4086	323.3912	16.57725	51.63444	RFracC

328.5533	328.5826	328.568	13.66985	84.92949	RFracC
346.3346	346.3805	346.3576	20.7354	197.8502	ConFracC
357.8178	357.8581	357.838	18.59762	180.0001	RFracC
377.1424	377.1661	377.1542	10.94066	234.6906	RFracC
386.1579	386.2649	386.2114	42.40033	35.12186	RFracC
437.5154	437.5488	437.5321	15.32302	171.4927	RFracC
439.7509	439.8003	439.7756	22.11211	186.9828	ConFracC
443.3456	443.4003	443.373	24.36534	169.4309	RFracC
448.3462	448.4969	448.4215	51.81413	317.7879	RFracC
447.9154	448.0074	447.9614	37.35732	183.5772	RFracC
449.9721	450.0108	449.9915	18.03418	297.2148	RFracC
451.1806	451.2193	451.1999	17.70007	193.5279	RFracC
451.302	451.3406	451.3213	17.72693	199.8894	RFracC
451.6341	451.6728	451.6534	17.68667	203.729	RFracC
454.4685	454.4992	454.4838	14.34612	152.8432	RFracC
458.9675	458.9982	458.9829	14.29226	279.0132	RFracC
460.5241	460.5548	460.5395	14.60835	72.65451	ConFracC
461.6619	461.7592	461.7106	39.13944	341.407	ConFracC
462.8863	462.941	462.9137	24.74924	185.8508	RFracC
463.1878	463.2611	463.2245	31.60372	10.35205	RFracC
463.3252	463.3985	463.3619	31.57128	10.33176	RFracC
464.9405	464.9845	464.9625	20.22421	10.59585	ConFracC
475.5231	475.5431	475.5331	9.595826	237.9976	RFracC
487.4236	487.5023	487.463	33.73585	140.1717	RFracC
487.8278	487.9198	487.8738	37.92795	110.2977	RFracC
487.7584	487.8504	487.8044	38.04655	133.8296	RFracC
489.1936	489.2857	489.2396	37.46063	332.597	RFracC
495.6094	495.7281	495.6687	44.77589	17.79666	ConFracC
502.428	502.4666	502.4473	18.29429	185.132	ConFracC
497.6742	497.7128	497.6935	18.24102	180.4191	ConFracC
499.8723	499.9644	499.9183	37.44544	5.347976	RFracC
503.4937	503.5297	503.5117	16.37458	307.2758	RFracC
504.8009	504.8129	504.8069	6.182241	165.4657	RFracC
521.2778	521.2978	521.2878	9.309896	17.49701	RFracC
521.4311	521.4512	521.4411	9.201316	0.728127	RFracC
520.5855	520.6055	520.5955	9.10687	341.1307	RFracC
523.8014	523.8214	523.8114	9.209511	280.81	RFracC
530.1851	530.2051	530.1951	10.04977	159.6204	RFracC
163.7238	163.8359	163.7799	43.53343	60.57407	RFracC
165.3069	165.329	165.318	10.94383	295.4329	RFracC
169.6704	169.7002	169.6853	14.5929	12.1915	RFracC
175.1746	175.2224	175.1985	21.32008	162.6814	RFracC
178.1608	178.2086	178.1847	21.81373	77.23617	RFracC
178.8913	178.9391	178.9152	21.26944	154.8805	RFracC
184.4109	184.4407	184.4258	14.62808	14.78277	RFracC
198.5778	198.6488	198.6133	30.67404	92.88313	RFracC
212.8258	212.8813	212.8535	25.66174	342.6656	RFracC
231.4578	231.5133	231.4855	25.36004	55.01801	RFracC
234.3308	234.376	234.3534	20.38513	232.7872	ConFracC
236.5196	236.5648	236.5422	21.32143	38.85634	RFracC
237.7992	237.829	237.8141	14.00645	257.776	ConFracC
280.9764	281.0088	280.9926	15.26942	264.0896	ConFracC

286.7275	286.7496	286.7386	11.15768	19.26392	RFracC
312.9214	312.9409	312.9311	9.190175	88.0004	RFracC
326.309	326.4108	326.3599	39.95164	194.1335	RFracC
329.3954	329.4304	329.4129	17.00672	346.3157	RFracC
330.8782	330.9055	330.8918	13.35614	309.5616	ConFracC
335.4539	335.4709	335.4624	8.508549	293.3877	ConFracC
378.6903	378.7072	378.6988	7.78556	216.2409	RFracC
378.8909	378.9078	378.8994	7.790703	195.5278	RFracC
384.6176	384.6345	384.6261	7.758432	276.6534	RFracC
389.0891	389.1061	389.0976	7.69482	268.2013	RFracC
389.2782	389.3208	389.2995	20.01233	112.7012	ConFracC
392.5768	392.6169	392.5969	19.06146	56.09657	RFracC
395.2788	395.2983	395.2886	9.615906	85.87434	RFracC
397.096	397.1155	397.1057	9.526162	99.33304	RFracC
400.8525	400.8977	400.8751	20.68198	284.4627	ConFracC
402.7712	402.801	402.7861	13.93373	273.3624	RFracC
402.6015	402.6313	402.6164	13.9275	272.1163	RFracC
421.6013	421.6311	421.6162	14.16525	340.0629	RFracC
448.7069	448.7393	448.7231	15.21827	118.6296	RFracC
448.8355	448.9194	448.8775	35.48417	43.64331	ConFracC
462.5125	462.5449	462.5287	15.17215	208.1124	RFracC
473.5441	473.5636	473.5538	9.067858	302.6684	RFracC
485.4707	485.4902	485.4805	9.144549	5.56018	RFracC
487.963	487.9825	487.9728	9.000129	333.6107	RFracC
500.8053	500.8248	500.8151	9.499257	195.3536	RFracC
502.863	502.8825	502.8727	9.721062	158.922	RFracC
503.2745	503.294	503.2843	9.050592	14.9426	RFracC
503.8262	503.8457	503.836	9.239315	37.86123	CoalFracC
506.442	506.4615	506.4518	9.42679	56.64303	RFracC
506.7314	506.7509	506.7411	9.61146	82.23021	RFracC
510.403	510.4791	510.441	32.22292	316.2558	RFracC
524.8451	524.8723	524.8587	12.56536	1.24937	RFracC
329.7086	329.7255	329.7171	8.088906	79.05768	ConFracC
339.224	339.2409	339.2325	8.235203	63.08172	ConFracC
338.6574	338.6744	338.6659	8.15427	70.04747	ConFracC
338.5937	338.6106	338.6022	8.215248	65.12089	ConFracC
354.4532	354.5041	354.4786	23.25129	64.3884	RFracC
360.242	360.2731	360.2575	14.59231	260.3624	ConFracC
360.3723	360.4034	360.3878	14.55417	215.11	ConFracC
362.232	362.2915	362.2617	26.43406	162.2413	ConFracC
418.3216	418.381	418.3513	26.21133	283.1131	RFracC
419.9023	419.9787	419.9405	33.027	32.73857	RFracC
420.4858	420.5622	420.524	32.53001	175.7727	RFracC
441.9556	442.0972	442.0264	50.30566	52.36436	RFracC
455.9709	456.0133	455.9921	19.60363	135.6647	RFracC
455.9114	455.9539	455.9326	19.52087	159.4812	RFracC
458.7669	458.8093	458.7881	19.62949	350.3621	RFracC
522.9568	523.0134	522.9851	25.00708	295.8742	ConFracC
524.3789	524.4355	524.4072	25.0431	294.588	ConFracC

Daydream 1

Top Depth (m)	Bottom Depth (m)	Depth (m)	True Dip (deg)	True Azimuth (deg)	Surface Type
2889.396	2889.438	2889.417	11.08908	33.9517	RFracC
2889.464	2889.504	2889.484	10.88382	43.02019	RFracC
2898.354	2898.371	2898.362	6.483046	75.0946	RFracC
2909.206	2909.222	2909.214	5.143795	53.14259	RFracC
2911.55	2911.567	2911.559	4.574717	183.9493	RFracC
2916.227	2916.236	2916.232	2.069345	175.2073	RFracC
2921.74	2921.766	2921.753	8.954619	75.31421	RFracC
2923.799	2923.919	2923.859	26.29396	280.0086	RFracC
2923.036	2923.085	2923.06	15.22981	96.20012	RFracC
2925.954	2926.005	2925.98	12.66019	16.34319	RFracC
2931.858	2931.902	2931.88	14.10285	121.0347	RFracC
2947.464	2947.486	2947.475	4.211136	229.7549	RFracC
2948.25	2948.303	2948.276	12.89708	223.8293	RFracC
2948.294	2948.352	2948.323	13.93579	228.7	RFracC
2948.199	2948.257	2948.228	13.98441	227.3823	RFracC
2954.594	2954.636	2954.615	11.87241	175.7087	RFracC
2955.573	2955.615	2955.594	9.47302	359.6986	RFracC
2962.562	2962.603	2962.583	9.086173	243.314	RFracC
2973.912	2974.053	2973.983	31.54901	346.7805	RFracC
2996.311	2996.336	2996.324	6.579253	41.35572	RFracC
2997.835	2997.859	2997.847	8.723698	102.7557	RFracC
2997.939	2997.964	2997.951	8.209099	81.18954	RFracC
2997.381	2997.444	2997.413	17.32062	54.75456	RFracC
2999.653	2999.716	2999.684	13.92895	300.6012	RFracC
2999.775	2999.838	2999.806	18.69582	109.6747	RFracC
2999.35	2999.413	2999.382	18.44907	142.6298	RFracC
3004.791	3004.813	3004.802	4.965404	20.69134	RFracC
3007.736	3007.748	3007.742	2.043097	25.97326	RFracC
3007.617	3007.629	3007.623	1.832015	20.66956	RFracC
3010.344	3010.356	3010.35	1.114912	348.9463	RFracC
3010.722	3010.734	3010.728	0.822144	290.1104	RFracC
3011.196	3011.234	3011.215	7.906435	282.7038	ConFracC
3011.15	3011.175	3011.163	4.248967	267.9776	ConFracC
3011.281	3011.305	3011.293	4.27511	266.2179	ConFracC
3011.328	3011.365	3011.347	7.226953	290.618	ConFracC
3011.443	3011.494	3011.469	10.97953	286.7325	ConFracC
3011.508	3011.559	3011.533	10.98735	286.7567	ConFracC
3022.457	3022.474	3022.465	6.823281	117.6385	ConFracC
3023.38	3023.414	3023.397	11.27758	122.5383	ConFracC
3024.14	3024.174	3024.157	11.27357	112.6093	ConFracC
3026.178	3026.19	3026.184	5.465021	109.001	ConFracC
3036.539	3036.555	3036.547	6.127631	83.51377	ConFracC
3036.518	3036.535	3036.526	5.974716	79.12119	ConFracC
3038.658	3038.692	3038.675	10.42047	73.92205	RFracC
3042.036	3042.584	3042.31	67.82894	10.84751	RFracC
3044.013	3044.023	3044.018	0.466646	322.7186	RFracC
3044.788	3044.81	3044.799	3.699587	273.3713	ConFracC
3049.148	3049.453	3049.301	55.06751	195.9978	RFracC
3049.176	3049.545	3049.36	60.26578	188.803	RFracC

3049.159	3049.525	3049.342	59.96326	192.5192	ConFracC
3050.992	3051.024	3051.008	6.191055	284.1809	ConFracC
3050.093	3050.14	3050.117	12.76952	50.55896	ConFracC
3051.63	3051.661	3051.646	9.441828	64.34799	RFracC
3052.362	3052.396	3052.379	6.833374	312.4877	RFracC
3052.688	3052.708	3052.698	5.660554	181.3338	ConFracC
3055.986	3056.022	3056.004	7.655787	327.6959	ConFracC
3075.471	3075.519	3075.495	10.82771	272.0622	ConFracC
3083.203	3083.256	3083.23	13.7998	30.78577	RFracC
3083.689	3083.711	3083.7	4.151648	346.0373	RFracC
3090.139	3090.19	3090.164	11.5785	266.4123	ConFracC
3099.946	3099.971	3099.959	5.170712	245.2468	ConFracC
3100.017	3100.042	3100.029	6.156097	212.1986	ConFracC
3105.303	3105.35	3105.326	13.38521	170.5072	ConFracC
3106.524	3106.57	3106.547	12.39233	42.90851	RFracC
3106.713	3106.735	3106.724	4.703634	237.0237	RFracC
3106.988	3107.064	3107.026	17.90219	347.895	RFracC
3107.146	3107.17	3107.158	5.999421	26.58166	ConFracC
3107.276	3107.301	3107.288	6.172925	31.64621	ConFracC
3106.835	3106.859	3106.847	7.024506	55.11728	ConFracC
3108.169	3108.213	3108.191	12.5279	178.0857	ConFracC
3109.826	3109.851	3109.838	5.526242	231.9324	ConFracC
3110.438	3110.463	3110.45	7.443798	176.7256	ConFracC
3110.353	3110.368	3110.36	4.957495	73.68602	ConFracC
3111.216	3111.238	3111.227	5.63496	36.2055	ConFracC
3112.206	3112.228	3112.217	7.299446	160.366	ConFracC
3112.259	3112.281	3112.27	7.096278	167.2948	ConFracC
3114.666	3114.688	3114.677	4.07038	335.741	ConFracC
3114.967	3115.043	3115.005	20.15467	186.1595	ConFracC
3115.089	3115.165	3115.127	17.84669	346.4598	ConFracC
3116.085	3116.112	3116.099	8.359869	76.65037	ConFracC
3116.985	3117.012	3116.999	8.228934	173.7729	ConFracC
3118.161	3118.188	3118.174	8.649288	87.04381	ConFracC
3118.269	3118.284	3118.277	2.721405	12.31967	ConFracC
3120.482	3120.509	3120.496	7.366863	48.40184	ConFracC
3122.872	3122.934	3122.903	16.89315	179.145	ConFracC
3130.311	3130.343	3130.327	10.33857	102.4746	ConFracC
3131.734	3131.754	3131.744	4.461357	221.4134	ConFracC
3132.774	3132.84	3132.807	14.96211	291.1253	ConFracC
3133.231	3133.314	3133.273	19.16568	328.5841	ConFracC
3133.507	3133.58	3133.544	16.84386	326.1791	ConFracC
3136.26	3136.295	3136.277	7.799287	243.712	ConFracC
3141.288	3141.342	3141.315	14.50642	52.89823	ConFracC
3141.667	3141.694	3141.681	8.962815	102.1442	ConFracC
3142.116	3142.189	3142.153	20.0505	75.73377	ConFracC
3145.024	3145.112	3145.068	20.47189	343.4066	ConFracC
3144.977	3145.016	3144.996	11.82369	158.1943	ConFracC
3146.957	3147.008	3146.983	14.56648	172.0742	ConFracC
3147.905	3147.941	3147.923	11.49631	101.848	ConFracC
3148.83	3148.889	3148.859	13.20895	319.7972	ConFracC
3150.286	3150.31	3150.298	6.985317	54.72883	RFracC
3159.136	3159.163	3159.15	6.289068	227.4423	ConFracC

3159.255	3159.282	3159.268	6.918089	209.2843	ConFracC
3168.588	3168.615	3168.601	9.191039	113.4584	ConFracC
3172.554	3172.612	3172.583	13.16353	312.7975	ConFracC
3173.2	3173.219	3173.21	3.405875	339.019	ConFracC
3173.938	3173.991	3173.964	12.02018	320.2148	ConFracC
3180.385	3180.426	3180.405	11.20367	44.18026	ConFracC
3183.595	3183.652	3183.623	15.31883	53.50691	ConFracC
3186.693	3186.744	3186.718	12.19944	241.3015	ConFracC
3186.632	3186.661	3186.646	6.131034	252.3354	ConFracC
3186.683	3186.712	3186.697	6.306928	244.8009	ConFracC
3191.996	3192.025	3192.01	9.210612	80.68904	ConFracC
3198.453	3198.504	3198.478	11.61276	258.1772	ConFracC
3199.16	3199.182	3199.171	3.879761	328.4127	ConFracC
3202.5	3202.566	3202.533	15.80033	235.1597	ConFracC
3203.221	3203.272	3203.246	14.31608	58.77375	RFracC
3206.208	3206.259	3206.234	13.38057	32.63198	RFracC
3209.757	3209.839	3209.798	20.19607	6.428269	ConFracC
3215.362	3215.389	3215.375	8.943546	97.63059	ConFracC
3216.832	3216.888	3216.86	14.3602	25.60047	ConFracC
3216.782	3216.855	3216.819	18.31919	18.65232	ConFracC
3218.05	3218.099	3218.075	11.41269	238.4368	ConFracC
3217.974	3218.052	3218.013	20.13188	36.89699	ConFracC
3219.186	3219.25	3219.218	14.25666	303.4566	ConFracC
3220.293	3220.346	3220.32	14.3921	44.18823	ConFracC
3231.76	3231.848	3231.804	20.86837	244.8359	ConFracC
3234.669	3234.727	3234.698	13.20498	314.4071	ConFracC
3245.849	3245.877	3245.863	5.519354	330.6063	ConFracC
3249.974	3250.022	3249.998	11.38593	246.9176	ConFracC
3254.117	3254.144	3254.131	8.736649	141.5437	ConFracC
3260.069	3260.115	3260.092	11.0588	235.5612	ConFracC
3260.046	3260.087	3260.066	10.26601	219.9581	ConFracC
3261.357	3261.415	3261.386	14.28401	6.583745	ConFracC
3282.617	3282.656	3282.636	10.24065	34.7005	ConFracC
3287.275	3287.328	3287.301	11.92744	301.988	ConFracC
3293.866	3293.89	3293.878	4.347978	293.9931	ConFracC
3294.968	3294.992	3294.98	7.179975	174.7299	ConFracC
3295.991	3296.052	3296.022	15.67604	29.58244	ConFracC
3295.896	3295.957	3295.926	16.46932	52.62302	ConFracC
3296.365	3296.413	3296.389	13.40168	52.96318	ConFracC
3296.275	3296.324	3296.3	13.27559	49.45462	ConFracC
3305.552	3305.647	3305.599	23.36651	18.39465	ConFracC
3454.596	3454.655	3454.625	15.83878	41.23197	RFracC
3458.895	3458.954	3458.924	16.8944	73.35757	RFracC
3467.849	3467.88	3467.865	10.13356	90.65356	RFracC
3474.093	3474.607	3474.35	65.51813	251.9871	ConFracC
3482.037	3482.069	3482.053	8.249105	22.7436	ConFracC
3507.136	3507.399	3507.268	50.31109	203.4404	ConFracC
3507.051	3507.11	3507.08	15.2435	18.74874	RFracC
3548.61	3548.657	3548.634	13.413	130.8101	RFracC
3557.282	3557.297	3557.289	4.19594	177.4888	ConFracC
3561.629	3562.114	3561.872	66.91207	40.66715	ConFracC
3563.893	3563.914	3563.903	4.407682	331.8667	ConFracC

3580.52	3580.541	3580.53	6.269504	158.0699	ConFracC
3615.559	3615.615	3615.587	12.84689	298.0162	RFracC
3615.195	3615.234	3615.215	8.337107	291.8057	RFracC
3620.16	3620.182	3620.171	3.975808	290.7974	ConFracC
3620.051	3620.073	3620.062	4.152391	304.559	ConFracC
3625.454	3625.496	3625.475	12.49422	67.28745	ConFracC
3625.569	3625.61	3625.59	9.420277	241.6939	ConFracC
3625.258	3625.3	3625.279	9.337123	304.4463	ConFracC
3627.648	3627.689	3627.668	9.0879	273.9077	ConFracC
3628.91	3628.952	3628.931	10.46501	191.0206	ConFracC
3630.499	3630.541	3630.52	12.53138	112.2699	ConFracC
3633.026	3633.068	3633.047	9.944231	215.6027	ConFracC
3637.341	3637.383	3637.362	10.05655	347.4538	ConFracC
3639.188	3639.23	3639.209	12.08359	146.9234	ConFracC
3643.525	3643.566	3643.545	10.48139	197.8158	ConFracC
3644.86	3644.902	3644.881	9.014815	285.896	RFracC
3645.275	3645.303	3645.289	5.97709	223.7432	RFracC
3645.907	3645.934	3645.92	5.661954	321.2906	RFracC
3645.787	3645.814	3645.8	5.326145	291.9793	ConFracC
3646.325	3646.352	3646.338	7.719657	166.1016	ConFracC
3646.869	3646.979	3646.924	26.83831	193.8022	ConFracC
3647.207	3647.251	3647.229	12.02917	172.5633	ConFracC
3647.094	3647.149	3647.122	13.98728	357.0852	RFracC
3648.126	3648.182	3648.154	14.04734	359.5701	RFracC
3650.089	3650.124	3650.106	10.56157	49.935	RFracC
3651.556	3651.592	3651.574	10.62285	52.11893	RFracC
3651.682	3651.718	3651.7	11.1672	78.87158	RFracC
3660.113	3660.149	3660.131	11.37361	102.2218	RFracC
3666.038	3666.063	3666.051	8.248864	120.2932	RFracC
3692.064	3692.089	3692.076	8.137655	80.14103	RFracC
3693.446	3693.502	3693.474	15.93883	141.6164	RFracC
3693.272	3693.285	3693.279	2.488245	1.84252	ConFracC
3695.327	3695.348	3695.338	7.386529	126.4871	RFracC
3696.121	3696.186	3696.154	17.84116	151.4183	RFracC
3696.22	3696.285	3696.252	18.40824	123.9471	RFracC
3696.156	3696.22	3696.188	17.35015	167.8857	RFracC
3696.017	3696.081	3696.049	18.47932	87.90599	RFracC
3696.64	3696.664	3696.652	7.085238	40.41187	RFracC
3698.219	3698.26	3698.24	12.61486	80.39334	RFracC
3702.277	3702.296	3702.287	6.935251	94.24149	RFracC
3703.988	3704.007	3703.998	6.612249	128.5276	ConFracC
3703.532	3703.573	3703.552	12.29322	59.68945	ConFracC
3705.711	3705.732	3705.721	7.711408	108.4014	ConFracC
3706.747	3706.84	3706.794	23.83347	28.2353	ConFracC
3706.827	3706.895	3706.861	17.29373	13.99934	RFracC
3714.598	3714.935	3714.766	59.19613	114.6153	RFracC
3714.71	3714.786	3714.748	21.14891	121.3904	RFracC
3718.777	3718.819	3718.798	12.2132	50.62932	RFracC
3736.15	3736.203	3736.177	14.68866	163.4702	RFracC
3743.434	3743.473	3743.454	12.16901	105.3914	RFracC
3747.201	3747.26	3747.23	14.93248	12.73468	RFracC
3747.251	3747.31	3747.28	15.20703	20.22911	RFracC

3759.151	3759.178	3759.164	8.359212	50.30516	RFracC
3774.468	3774.486	3774.477	4.943114	179.8131	ConFracC
3781.699	3781.718	3781.708	3.262233	239.5206	RFracC
3787.526	3787.587	3787.557	13.8527	302.0185	RFracC
3789.487	3789.594	3789.541	27.85631	59.35192	RFracC
3802.881	3802.949	3802.915	19.28162	109.1345	RFracC
3803.017	3803.088	3803.053	19.45949	142.2474	RFracC
3803.184	3803.214	3803.199	9.516015	134.6543	ConFracC
3805.199	3805.247	3805.223	13.22848	159.9282	RFracC
3805.46	3805.499	3805.479	10.11914	186.6582	RFracC
3806.69	3806.728	3806.709	12.02244	110.8551	RFracC
3807.922	3807.932	3807.927	4.367538	82.55009	RFracC
3809.109	3809.142	3809.126	8.801852	181.4827	ConFracC
3809.494	3809.516	3809.505	6.798894	147.511	ConFracC
3809.537	3809.573	3809.555	9.819883	172.9901	ConFracC
3813.902	3813.927	3813.914	5.767765	0.977984	ConFracC
3824.833	3824.897	3824.865	18.45556	128.1054	ConFracC
3834.345	3834.369	3834.357	7.370922	54.61047	ConFracC
3854.881	3854.906	3854.894	8.393806	86.90911	ConFracC
3878.21	3878.234	3878.222	4.382041	307.8175	ConFracC
3880.634	3880.658	3880.646	4.459047	263.7477	ConFracC
3892.342	3892.377	3892.36	11.49216	98.09591	ConFracC
3893.962	3893.998	3893.98	10.02977	172.1217	ConFracC
3894.3	3894.322	3894.311	7.763532	105.9905	RFracC
3899.709	3899.762	3899.735	15.80513	97.1391	RFracC
3899.395	3899.425	3899.41	9.330165	145.2289	ConFracC
3899.853	3899.909	3899.881	16.52382	108.0879	ConFracC
3900.475	3900.531	3900.503	12.72893	314.1142	ConFracC
3900.652	3900.791	3900.722	34.56372	76.37739	ConFracC
3901.345	3901.424	3901.385	22.05435	93.34629	ConFracC
3901.49	3901.551	3901.521	17.78979	80.17578	ConFracC
3902.156	3902.2	3902.178	11.93767	27.26168	ConFracC
3905.203	3905.225	3905.214	7.265431	136.4439	RFracC
3905.017	3905.059	3905.038	10.4652	6.725591	RFracC
3905.332	3905.374	3905.353	12.80339	119.6073	RFracC
3905.405	3905.447	3905.426	12.55837	134.6059	RFracC
3918.406	3918.482	3918.444	21.12484	105.8399	RFracC
3918.181	3918.231	3918.206	14.70329	122.2514	RFracC
3932.217	3932.267	3932.242	15.02374	99.17521	RFracC
3937.378	3937.46	3937.419	22.39346	150.1382	RFracC
3939.465	3939.55	3939.508	22.4982	53.66539	RFracC
3940.07	3940.12	3940.095	14.70778	70.23529	RFracC
3941.941	3941.991	3941.966	14.99827	79.01563	ConFracC
3948.437	3948.468	3948.453	10.21836	128.0725	ConFracC
3954.098	3954.22	3954.159	27.48038	242.8896	RFracC
3954.46	3954.573	3954.517	28.37439	36.04597	RFracC
3956.2	3956.23	3956.215	8.501044	38.17973	ConFracC
3960.221	3960.24	3960.231	7.501321	87.98485	ConFracC
3968.062	3968.178	3968.12	25.49578	268.8585	ConFracC
3971.007	3971.298	3971.153	50.72357	259.211	RFracC
3971.18	3971.211	3971.195	10.76031	100.0404	RFracC
3985.849	3985.905	3985.877	15.77085	47.251	ConFracC

3986.057	3986.09	3986.073	9.178736	174.8457	ConFracC
3987.637	3987.704	3987.671	17.20845	194.1374	RFracC
3988.047	3988.088	3988.067	11.6021	173.7626	RFracC
3991.713	3991.743	3991.728	10.52051	101.3623	RFracC
3991.999	3992.044	3992.022	12.87601	53.16146	ConFracC
4049.518	4049.563	4049.54	14.09069	73.12111	ConFracC
4062.006	4062.022	4062.014	1.857614	216.1749	ConFracC
4066.225	4066.267	4066.246	13.83805	87.78908	ConFracC
4066.852	4066.874	4066.863	5.270241	25.67475	ConFracC
4075.67	4075.711	4075.691	8.32601	249.0211	ConFracC
4076.998	4077.017	4077.008	7.224385	72.47638	ConFracC
4077.863	4077.882	4077.873	6.257092	53.28805	ConFracC
4093.444	4093.462	4093.453	7.122828	71.79091	RFracC
4099.714	4099.739	4099.726	4.312501	348.5955	RFracC
4137.167	4137.243	4137.205	16.83508	330.9439	ConFracC

Fantome 1

Top Depth (m)	Bottom Depth (m)	Depth (m)	True Dip (deg)	True Azimuth (deg)	Surface Type
2886.194	2886.243	2886.219	15.29249	237.7775	RFracC
2886.344	2886.4	2886.372	17.2344	243.218	RFracC
2894.489	2894.509	2894.499	4.777113	137.9217	RFracC
2895.79	2895.799	2895.795	3.229819	293.6457	RFracC
2895.991	2896.069	2896.03	21.3147	173.4991	RFracC
2896.115	2896.146	2896.131	9.962801	276.3501	RFracC
2896.552	2896.601	2896.576	11.7104	81.95217	RFracC
2896.639	2896.637	2896.638	1.541894	249.1969	RFracC
2896.658	2896.669	2896.663	1.360317	109.5834	RFracC
3474.1	3474.178	3474.139	17.04393	83.55834	ConFracC
2869.947	2870.174	2870.061	47.89372	160.4413	ConFracC
2902.687	2902.991	2902.839	55.63673	344.9523	RFracC
2917.327	2917.415	2917.371	21.54155	36.49471	ConFracC
2951.144	2951.256	2951.2	26.75727	24.09756	ConFracC
3009.706	3009.749	3009.728	12.16432	157.7817	RFracC
3453.206	3453.267	3453.237	19.20348	290.7423	ConFracC
2954.516	2954.547	2954.531	8.077537	138.6373	RFracC
2955.44	2955.472	2955.456	6.646104	75.47435	RFracC
2976.761	2976.783	2976.772	8.027121	247.5398	ConFracC
2982.787	2982.798	2982.792	1.288998	89.38049	RFracC
3005.486	3005.498	3005.492	5.38661	245.9432	RFracC
3005.486	3005.498	3005.492	5.38661	245.9432	RFracC
3009.473	3009.519	3009.496	11.54593	120.4331	RFracC
3014.582	3014.591	3014.587	0.737363	119.5483	RFracC
3017.033	3017.043	3017.038	0.457607	89.25344	RFracC
3058.571	3058.583	3058.577	2.723854	150.0003	ConFracC
3089.269	3089.295	3089.282	8.576447	179.0759	RFracC
3128.854	3128.878	3128.866	7.62376	280.9795	ConFracC
3148.704	3148.728	3148.716	7.199616	156.4913	RFracC
3148.446	3148.531	3148.488	24.23633	185.9765	RFracC
3148.47	3148.555	3148.513	24.10403	181.3322	RFracC
3148.536	3148.594	3148.565	17.14445	172.7293	RFracC
3148.643	3148.701	3148.672	18.04981	210.6189	RFracC

3157.18	3157.238	3157.209	17.15629	170.4144	RFracC
3200.819	3200.834	3200.826	5.922254	251.3046	ConFracC
3200.959	3200.966	3200.963	0.450808	269.545	ConFracC
3215.64	3215.657	3215.649	5.205679	148.641	RFracC
3215.678	3215.693	3215.685	5.02686	160.9336	RFracC
3234.813	3234.891	3234.852	22.78022	240.7251	ConFracC
3273.039	3273.065	3273.052	4.815109	9.458108	RFracC
3333.638	3333.652	3333.645	3.234389	309.9676	ConFracC
3334.36	3334.374	3334.367	3.378133	306.5495	ConFracC
3334.489	3334.503	3334.496	6.725818	227.4181	ConFracC
3334.583	3334.597	3334.59	5.122903	177.3491	ConFracC
3334.771	3334.79	3334.78	2.695351	19.43415	ConFracC
3335.863	3335.924	3335.894	13.7212	30.82881	ConFracC
3338.695	3338.755	3338.725	14.12115	98.17307	ConFracC
3343.797	3343.857	3343.827	15.78196	326.7403	ConFracC
3344.193	3344.224	3344.208	11.44426	226.024	ConFracC
3344.26	3344.291	3344.275	7.360092	337.0853	ConFracC
3344.851	3344.857	3344.854	4.248117	224.3745	ConFracC
3347.998	3348.028	3348.013	10.57618	210.498	ConFracC
3348.245	3348.263	3348.254	7.671335	241.0473	ConFracC
3348.527	3348.556	3348.542	5.376047	54.84295	ConFracC
3348.526	3348.555	3348.54	10.98868	249.977	ConFracD
3348.225	3348.254	3348.24	6.645529	354.1201	ConFracD
3348.639	3348.669	3348.654	7.353542	340.0454	ConFracD
3349.425	3349.454	3349.44	5.633989	30.87012	ConFracD
3349.24	3349.269	3349.254	9.373348	185.5291	ConFracD
3350.792	3350.807	3350.799	1.301009	70.06306	ConFracD
3353.237	3353.293	3353.265	12.95061	29.74949	ConFracD
3352.42	3352.445	3352.433	8.286693	300.9873	ConFracC
3355.255	3355.28	3355.268	4.017673	86.69239	ConFracD
3354.377	3354.399	3354.388	6.849086	317.6047	ConFracD
3356.068	3356.105	3356.086	7.250741	69.7535	ConFracD
3355.804	3355.84	3355.822	7.27361	58.95276	ConFracD
3357.161	3357.173	3357.167	5.161762	205.6342	ConFracD
3356.916	3356.984	3356.95	17.94243	341.1667	ConFracD
3362.153	3362.19	3362.172	7.21912	48.14609	ConFracD
3363.809	3363.872	3363.841	14.15132	55.53406	ConFracD
3363.859	3363.874	3363.866	1.648382	1.419971	ConFracD
3363.884	3363.958	3363.921	16.91684	30.79455	ConFracD
3365.936	3365.972	3365.954	12.98207	229.387	ConFracD
3366.343	3366.406	3366.375	20.00949	227.1747	ConFracD
3366.396	3366.458	3366.427	19.96012	223.9688	ConFracD
3368.238	3368.3	3368.269	20.11023	237.4667	ConFracD
3368.201	3368.357	3368.279	40.16379	231.6446	ConFracD
3368.209	3368.248	3368.229	13.47634	216.9727	ConFracD
3372.287	3372.311	3372.299	9.6264	253.3308	ConFracD
3474.351	3474.375	3474.363	9.292527	286.6052	ConFracC
3474.487	3474.545	3474.516	18.864	279.62	ConFracC
3478.084	3478.147	3478.116	13.43	45.77923	ConFracC
3479.231	3479.292	3479.261	20.20897	253.2963	ConFracC
3479.371	3479.434	3479.403	20.79262	244.0792	ConFracC
3482.188	3482.229	3482.209	13.59774	202.8431	ConFracC

3487.491	3487.53	3487.51	12.84884	201.8562	ConFracC
3487.522	3487.561	3487.542	9.662112	345.2465	ConFracC
3492.383	3492.441	3492.412	16.81703	182.9508	ConFracC
3492.158	3492.216	3492.187	15.5837	334.6938	ConFracC
3497.874	3497.954	3497.914	22.8543	188.9897	ConFracC
3498.509	3498.55	3498.529	14.41927	218.1593	ConFracC
3499.098	3499.139	3499.119	8.036967	25.67264	ConFracC
3506.576	3506.627	3506.602	10.36055	34.82247	ConFracC
3509.999	3510.049	3510.024	17.81193	248.7929	ConFracC
3510.916	3510.933	3510.924	7.660074	287.2895	ConFracC
3511.089	3511.152	3511.12	20.29957	286.9164	ConFracC
3511.363	3511.387	3511.375	2.924308	113.0474	ConFracC
3511.651	3511.733	3511.692	19.20678	18.84927	ConFracC
3527.419	3527.482	3527.45	16.24445	347.4742	ConFracC
3527.67	3527.704	3527.687	5.27656	95.0324	ConFracC
3529.158	3529.191	3529.175	6.109942	126.6216	ConFracC
3534.484	3534.561	3534.522	17.05123	36.90308	RFracC
3534.503	3534.585	3534.544	18.10767	40.32297	RFracC
3545.095	3545.136	3545.116	8.67638	137.1268	ConFracC
3555.144	3555.184	3555.164	12.37303	319.9394	ConFracC
3555.037	3555.078	3555.058	15.128	276.9339	ConFracC
3557.765	3557.82	3557.792	18.90249	229.159	ConFracC
3565.385	3565.441	3565.413	18.10289	215.6393	ConFracC
3567.251	3567.287	3567.269	13.70524	228.3638	ConFracC
3567.817	3567.824	3567.82	3.031488	231.5191	ConFracC
3567.847	3567.866	3567.856	2.082015	149.2879	ConFracC
3573.733	3573.774	3573.754	14.47776	222.0767	ConFracC
3573.515	3573.536	3573.525	9.822256	279.9561	ConFracC
3580.399	3580.421	3580.41	1.707118	104.9207	ConFracC
3585.92	3585.968	3585.944	9.02145	48.86298	ConFracC
3591.732	3591.756	3591.744	11.07913	264.5861	ConFracC
3592.519	3592.56	3592.539	8.72744	13.60587	ConFracC
3593.866	3593.895	3593.881	9.271422	204.9465	ConFracC
3594.008	3594.027	3594.017	1.209717	31.93298	ConFracC
3595.377	3595.408	3595.393	11.07621	217.1126	ConFracC
3604.402	3604.433	3604.417	12.57011	231.428	ConFracC
3605.573	3605.604	3605.588	4.04087	78.77101	ConFracC
3605.656	3605.687	3605.672	10.35274	200.764	ConFracC
3615.764	3615.795	3615.779	6.565154	355.6938	ConFracC
3641.337	3641.395	3641.366	12.03296	32.68606	ConFracC
3669.788	3669.846	3669.817	19.39544	223.5621	ConFracC
3669.745	3669.803	3669.774	19.62461	227.5514	ConFracC
3669.965	3670.006	3669.985	15.02705	226.6771	ConFracC
3672.814	3672.829	3672.821	5.306635	305.8528	ConFracC
3757.794	3757.852	3757.823	18.84826	223.8842	ConFracC
3770.607	3770.641	3770.624	5.893166	40.12036	ConFracC
3771.361	3771.396	3771.379	13.17034	237.8255	ConFracC
3838.809	3838.863	3838.836	14.6688	1.758011	ConFracD
3840.239	3840.293	3840.266	17.54826	240.9797	ConFracD
3850.05	3850.079	3850.064	8.231789	357.6497	ConFracD
3873.679	3873.723	3873.701	8.486413	100.9858	ConFracD
3875.072	3875.129	3875.101	11.68226	105.4646	ConFracD

3879.508	3879.61	3879.559	23.04458	91.77526	ConFracD
3883.172	3883.201	3883.186	5.538144	159.1316	ConFracD
3903.691	3903.725	3903.708	12.59978	314.9913	ConFracD
3903.62	3903.654	3903.637	12.4756	318.6778	ConFracD
3903.651	3903.695	3903.673	15.16598	317.3113	ConFracD
3905.896	3905.94	3905.918	9.481239	160.7593	ConFracD
3927.309	3927.353	3927.331	9.234252	75.79255	ConFracD
4105.41	4105.454	4105.432	10.26598	158.1097	RFracC
4105.41	4105.454	4105.432	10.26598	158.1097	RFracC
4148.177	4148.221	4148.199	13.12415	230.295	ConFracC
4158.563	4158.674	4158.618	26.81364	130.1102	ConFracC
4166.489	4166.52	4166.505	10.38075	295.2579	RFracC
4185.143	4185.174	4185.159	7.402809	53.57116	ConFracC
4184.884	4184.983	4184.934	26.69913	236.3959	ConFracC
4185.884	4185.92	4185.902	8.991888	168.9522	ConFracC
4186.712	4186.748	4186.73	8.13345	106.6702	ConFracC
4188.565	4188.601	4188.583	8.435559	142.6517	ConFracC
4190.391	4190.449	4190.42	16.49719	225.3619	ConFracC
4191.081	4191.175	4191.128	26.11162	257.8885	ConFracC
4192.547	4192.585	4192.566	9.257028	54.12883	ConFracC
4194.853	4194.918	4194.886	17.77041	204.1577	ConFracC
4195.048	4195.113	4195.081	17.69281	201.6708	ConFracC
4200.957	4200.997	4200.977	9.501353	102.3924	ConFracC
4201.356	4201.397	4201.377	10.55134	175.5803	ConFracC
4201.833	4201.939	4201.886	28.56818	246.9215	ConFracC
4201.964	4202.017	4201.99	15.57218	325.6588	ConFracC
4202.034	4202.109	4202.071	21.5686	279.1171	ConFracC
4202.308	4202.355	4202.331	14.65932	263.7	ConFracC
4202.461	4202.509	4202.485	11.95448	54.54577	ConFracC
4200.1	4200.148	4200.124	11.48853	86.77192	ConFracC
4201.265	4201.287	4201.276	6.91042	330.5649	ConFracC
4201.708	4201.732	4201.72	8.194347	271.7044	ConFracC
4203.532	4203.556	4203.544	5.764544	172.5319	ConFracC
4203.822	4203.845	4203.833	6.779125	208.142	ConFracC
4204.296	4204.351	4204.324	16.56535	261.1742	ConFracC
4205.351	4205.455	4205.403	28.32841	261.2587	ConFracC
4204.853	4204.886	4204.869	10.92872	277.3097	ConFracC
4204.651	4204.766	4204.708	30.74735	281.3523	ConFracC
4204.572	4204.603	4204.587	10.25677	277.4337	ConFracC
4205.636	4205.667	4205.651	9.069035	350.3904	ConFracC
4206.787	4206.88	4206.834	25.92887	269.6467	ConFracC
4207.373	4207.439	4207.406	19.51808	275.668	ConFracC
4207.727	4207.793	4207.76	18.88565	234.1696	ConFracC
4209.491	4209.523	4209.507	10.6598	281.4146	ConFracC
4209.31	4209.332	4209.321	7.888751	264.0209	ConFracC
4209.663	4209.71	4209.686	11.10785	132.9336	ConFracC
4211.613	4211.659	4211.636	14.59276	278.0696	ConFracC
4212.309	4212.435	4212.372	33.35034	265.8235	ConFracC
4213.44	4213.46	4213.45	6.714271	324.0895	ConFracC
4234.953	4234.973	4234.963	7.167663	288.3527	ConFracC
4239.005	4239.025	4239.015	3.79575	104.4041	RFracC
4242.067	4242.097	4242.082	10.03944	302.0243	ConFracC

4242.402	4242.435	4242.418	9.203565	206.492	ConFracC
4245.469	4245.521	4245.495	14.81675	206.0741	ConFracC
4247.588	4247.641	4247.614	15.89605	290.7997	ConFracC
4248.369	4248.421	4248.395	15.1361	216.5782	RFracC
4263.282	4263.305	4263.293	6.07458	175.0256	RFracC
4264.891	4264.896	4264.893	0.475362	246.9936	RFracC
4276.204	4276.27	4276.237	19.07073	240.9029	RFracC
4286.713	4286.716	4286.715	0.807858	236.6849	ConFracC
4288.847	4288.862	4288.855	2.908996	115.1208	ConFracC
4290.211	4290.221	4290.216	3.444436	320.4604	ConFracC
4290.266	4290.276	4290.271	3.587231	314.8144	ConFracC
4290.479	4290.505	4290.492	8.58311	257.7316	RFracC
4292.47	4292.496	4292.483	7.469562	189.065	RFracC
4293.651	4293.677	4293.664	6.177805	37.6938	RFracC
4293.792	4293.832	4293.812	10.48458	17.66292	RFracC
4293.73	4293.771	4293.75	9.876876	61.44538	RFracC
4298.834	4298.935	4298.884	24.98962	104.8037	ConFracC
4300.678	4300.697	4300.688	5.806024	206.4497	ConFracC
4300.269	4300.288	4300.279	6.438953	256.2468	ConFracC
4301.703	4301.708	4301.705	2.118431	308.163	ConFracC
4309.219	4309.224	4309.221	1.553265	321.9638	RFracC
4310.731	4310.737	4310.734	1.940487	309.5806	ConFracC
4310.756	4310.773	4310.764	5.859913	255.7494	ConFracC
4314.747	4314.809	4314.778	18.09127	262.241	RFracC
4318.592	4318.683	4318.637	24.99815	289.9934	ConFracC
4319.295	4319.296	4319.296	1.349299	266.9229	ConFracC
4320.582	4320.597	4320.589	3.083173	54.68956	ConFracC
4320.622	4320.664	4320.643	10.28676	65.74076	RFracC
4322.497	4322.531	4322.514	9.454916	172.6026	ConFracC
4322.762	4322.83	4322.796	17.25716	110.6467	ConFracC
4323.178	4323.2	4323.189	5.099109	113.9393	ConFracC
4330.246	4330.268	4330.257	5.176775	115.4267	ConFracC
4338.624	4338.646	4338.635	5.027465	97.67768	ConFracC
4343.011	4343.033	4343.022	6.846129	205.858	ConFracC
4343.071	4343.094	4343.083	5.877012	161.5987	ConFracC
4344.296	4344.367	4344.332	19.98347	296.575	ConFracC
4348.767	4348.782	4348.775	3.585131	144.2363	RFracC
4351.116	4351.132	4351.124	3.453096	100.9875	ConFracC
4350.901	4350.935	4350.918	8.243798	117.8972	ConFracC
4359.011	4359.045	4359.028	10.40988	256.178	ConFracC
4362.795	4362.808	4362.802	4.320869	212.1589	ConFracC
4365.988	4365.999	4365.993	4.335385	254.4716	ConFracC
4366.611	4366.659	4366.635	14.091	283.9969	ConFracC
4369.048	4369.096	4369.072	11.99381	106.223	ConFracC
4368.638	4368.659	4368.649	6.881053	287.9148	RFracC
4369.882	4369.899	4369.89	4.293534	164.7553	RFracC
4378.213	4378.265	4378.239	14.01809	352.6431	ConFracC
4378.32	4378.347	4378.333	7.012834	140.2995	ConFracC
4385.337	4385.379	4385.358	10.87545	6.665892	ConFracC
4388.625	4388.66	4388.643	9.780957	175.2143	ConFracC
4392.94	4392.974	4392.957	8.447952	34.45352	RFracC
4394.288	4394.323	4394.305	8.788136	126.2439	RFracC

4394.272	4394.288	4394.28	3.189938	109.876	RFracC
4396.655	4396.705	4396.68	14.58373	232.7101	RFracC
4410.036	4410.068	4410.052	8.211706	122.0384	RFracC
4420.695	4420.764	4420.73	18.15268	144.4821	ConFracC
4424.729	4424.756	4424.743	8.79863	267.1012	ConFracC
4438.726	4438.751	4438.739	7.577568	179.0744	RFracC
4453.58	4453.605	4453.592	6.91643	154.7763	ConFracC
4477.467	4477.492	4477.48	8.114992	221.3842	ConFracC
4500.293	4500.318	4500.306	8.149257	263.5699	ConFracC
4509.842	4509.867	4509.855	8.249865	267.1758	RFracC
4511.216	4511.224	4511.22	1.123863	133.0676	RFracC
4513.042	4513.06	4513.051	3.98949	358.1951	ConFracC
4513.179	4513.187	4513.183	0.979233	126.0922	ConFracC
4513.276	4513.284	4513.28	0.722299	25.39655	ConFracC
4536.951	4536.989	4536.97	12.16395	250.0896	ConFracC
4538.717	4538.755	4538.736	10.00722	138.9281	RFracC
4538.403	4538.417	4538.41	2.430164	103.2098	RFracC
4548.182	4548.216	4548.199	8.472965	133.1078	ConFracC
4553.102	4553.128	4553.115	6.356415	127.0752	ConFracC
4553.936	4553.981	4553.959	10.90944	84.27125	ConFracC
4555.591	4555.641	4555.616	12.1847	37.65934	ConFracC
4569.164	4569.177	4569.17	3.116657	328.321	ConFracC
4591.295	4591.312	4591.303	4.659828	145.1335	ConFracC
4591.831	4591.846	4591.838	2.960207	108.3405	RFracC
4591.698	4591.713	4591.705	3.617038	134.9411	RFracC
3314.305	3314.322	3314.313	7.269906	235.2166	ConFracC
2941.272	2941.375	2941.324	28.02896	282.2564	RFracC
2882.26	2882.277	2882.268	6.102941	284.999	RFracC
2882.9	2883.093	2882.996	44.90676	259.6764	RFracC
2887.742	2887.79	2887.766	12.63554	352.3753	ConFracC
2887.756	2887.815	2887.785	15.46763	348.6451	ConFracC
2888.059	2888.117	2888.088	15.46806	348.6322	ConFracC
2887.984	2888.042	2888.013	15.46786	348.639	ConFracC
2888.172	2888.231	2888.202	15.35079	352.463	ConFracC
2889.667	2889.725	2889.696	17.34979	283.8255	RFracC
2889.729	2889.787	2889.758	17.20187	290.6984	RFracC
2890.507	2890.565	2890.536	14.52922	116.0619	RFracC
2890.591	2890.649	2890.62	14.85571	129.4708	RFracC
2898.278	2898.347	2898.312	18.37315	338.0722	RFracC
2898.135	2898.203	2898.169	18.4544	335.5786	RFracC
2903.49	2903.52	2903.505	8.280706	163.3041	RFracC
2905.082	2905.113	2905.097	9.836953	281.2561	RFracC
2909.975	2910.005	2909.99	10.04973	221.8542	RFracC
2909.89	2909.92	2909.905	9.812189	210.4356	RFracC
2912.691	2912.721	2912.706	7.838586	149.9229	RFracC
2912.942	2912.972	2912.957	10.0505	220.8672	RFracC
2916.698	2916.723	2916.71	8.811364	232.4706	RFracC
2926.565	2926.644	2926.604	19.82436	117.9762	ConFracC
2934.218	2934.305	2934.262	21.54036	112.4325	ConFracC
2948.123	2948.166	2948.145	10.77534	124.1242	RFracC
2955.935	2955.988	2955.961	12.51166	41.52991	RFracC
2955.795	2955.882	2955.838	24.96079	235.1984	ConFracC

70

2955.822	2955.909	2955.866	24.96266	237.5025	ConFracC
2972.261	2972.329	2972.295	16.86238	97.85419	ConFracC
2975.073	2975.142	2975.108	18.38639	147.5375	ConFracC
2979.79	2979.815	2979.803	4.883426	80.92762	RFracC
3012.407	3012.466	3012.436	14.85685	119.713	RFracC
3012.125	3012.163	3012.144	8.919205	105.9705	RFracC
3023.636	3023.648	3023.642	1.122422	27.71471	RFracC
3024.638	3024.65	3024.644	3.294231	300.1624	RFracC
3024.691	3024.703	3024.697	2.672072	313.7396	RFracC
3025.282	3025.294	3025.288	1.832017	337.2459	RFracC
3035.939	3035.951	3035.945	4.139463	281.9808	RFracC
3036.181	3036.193	3036.187	4.141716	281.9436	RFracC
3084.405	3084.503	3084.454	24.05229	108.0378	ConFracC
3084.441	3084.518	3084.48	19.51176	118.4142	ConFracC
3084.551	3084.646	3084.599	23.73573	115.961	ConFracC
3084.615	3084.709	3084.662	24.07391	124.9448	ConFracC
3084.677	3084.771	3084.724	24.57651	137.5677	ConFracC
3084.749	3084.844	3084.796	24.67795	140.0624	ConFracC
3084.585	3084.68	3084.632	24.17319	127.4889	ConFracC
3089.09	3089.161	3089.125	19.34124	147.8944	ConFracC
3099.207	3099.279	3099.243	18.21043	117.43	ConFracC
3099.14	3099.211	3099.176	17.68791	101.5641	ConFracC
3105.236	3105.256	3105.246	6.827504	272.9741	ConFracC
3106.553	3106.653	3106.603	25.90377	140.9243	ConFracC
3147.61	3147.622	3147.616	3.350948	155.2163	ConFracC
3156.481	3156.503	3156.492	3.885743	18.80738	ConFracC
3184.606	3184.672	3184.639	18.32834	294.1173	ConFracC
3197.912	3197.958	3197.935	12.64493	298.1575	ConFracC
3262.75	3262.777	3262.764	8.377373	272.6904	RFracC
3273.927	3273.968	3273.948	9.379685	88.36595	RFracC
3288.617	3288.667	3288.642	16.16542	242.7529	RFracC
3300.766	3300.792	3300.779	4.81155	11.2847	ConFracC
3306.592	3306.618	3306.605	8.641227	272.818	ConFracC
3307.02	3307.046	3307.033	7.816755	289.6575	ConFracC
3309.454	3309.491	3309.473	9.244685	123.1783	ConFracC
3309.79	3309.826	3309.808	9.780314	134.4519	ConFracC
3309.664	3309.7	3309.682	8.781384	112.5667	ConFracC
3312.447	3312.483	3312.465	8.722111	328.9098	ConFracC
3315.27	3315.306	3315.288	10.52787	290.2976	ConFracC
3315.506	3315.542	3315.524	10.36028	293.7415	ConFracC
3315.323	3315.374	3315.349	13.59324	307.5913	ConFracC
3316.011	3316.05	3316.031	8.319063	79.16333	ConFracC
3318.483	3318.531	3318.507	13.30907	300.9121	ConFracC
3318.607	3318.671	3318.639	18.55768	282.3802	ConFracC
3318.695	3318.759	3318.727	16.71919	321.4101	ConFracC
3324.307	3324.357	3324.332	11.15533	20.75811	ConFracC
3331.318	3331.368	3331.343	14.25724	299.0785	ConFracC
3353.62	3353.652	3353.636	5.772718	61.39018	ConFracC
3369.855	3369.912	3369.883	17.08929	294.3928	ConFracC
3372.436	3372.462	3372.449	8.45779	179.9683	ConFracC
3373.72	3373.747	3373.734	9.949583	265.9564	ConFracC
3373.625	3373.652	3373.638	10.33688	223.4529	ConFracC

3375.159	3375.186	3375.173	4.218713	65.9835	ConFracC
3377.077	3377.139	3377.108	17.09054	318.4331	ConFracC
3377.773	3377.817	3377.795	14.18981	275.8028	ConFracC
3380.397	3380.44	3380.419	8.676064	59.63046	ConFracC
3383.418	3383.461	3383.439	9.117756	24.77167	ConFracC
3383.35	3383.393	3383.372	9.105438	24.8764	ConFracC
3383.387	3383.43	3383.408	9.339984	16.89186	ConFracC
3386.359	3386.378	3386.369	8.30493	260.2264	ConFracC
3387.362	3387.381	3387.371	5.429276	315.7254	ConFracC
3388.197	3388.238	3388.217	9.978066	346.6035	ConFracC
3388.565	3388.644	3388.605	23.85956	265.4582	ConFracC
3390.653	3390.713	3390.683	19.33751	228.65	ConFracC
3392.141	3392.175	3392.158	9.525589	165.8694	ConFracC
3394.033	3394.109	3394.071	17.7143	28.35622	ConFracC
3394.37	3394.425	3394.398	12.57553	18.54086	ConFracC
3396.853	3396.881	3396.867	4.756496	54.88199	ConFracC
3398.018	3398.061	3398.04	9.641211	8.573071	ConFracC
3399.599	3399.642	3399.62	14.32119	206.6384	ConFracC
3400.486	3400.529	3400.508	14.47042	274.165	ConFracC
3402.543	3402.586	3402.565	10.36694	350.0034	ConFracC
3402.642	3402.685	3402.663	11.84507	323.056	ConFracC
3403.127	3403.17	3403.148	8.572324	66.5525	ConFracC
3404.213	3404.265	3404.239	11.59336	24.67444	ConFracC
3407.846	3407.899	3407.873	12.00927	12.34869	ConFracC
3407.669	3407.722	3407.696	13.94959	333.1164	ConFracC
3409.132	3409.161	3409.147	5.273843	20.39375	ConFracC
3409.232	3409.261	3409.246	4.660136	60.48121	ConFracC
3412.841	3412.86	3412.851	2.444724	17.23527	ConFracC
3412.976	3412.996	3412.986	2.210247	94.40247	ConFracC
3413.004	3413.023	3413.013	2.138691	88.51199	ConFracC
3414.912	3414.931	3414.922	4.284365	153.9317	ConFracC
3415.003	3415.023	3415.013	4.86565	163.1427	ConFracC
3415.699	3415.718	3415.708	7.158406	289.3418	ConFracC
3418.018	3418.038	3418.028	2.017506	80.72476	ConFracC
3421.96	3421.998	3421.979	8.12906	12.49089	ConFracC
3423.888	3423.927	3423.907	12.228	298.5719	ConFracC
3424.412	3424.451	3424.432	13.27108	278.3459	ConFracC
3424.816	3424.869	3424.843	11.01873	83.11823	ConFracC
3424.724	3424.755	3424.739	5.267411	81.94889	ConFracC
3425.16	3425.191	3425.175	6.255999	122.1853	ConFracC
3431.491	3431.522	3431.507	10.34546	193.6101	ConFracC
3435.382	3435.414	3435.398	6.060977	121.7476	ConFracC
3436.912	3436.943	3436.927	6.487663	134.1944	ConFracC
3440.628	3440.659	3440.643	6.980718	356.6025	ConFracC
3441.564	3441.595	3441.58	10.97558	207.2077	ConFracC
3442.831	3442.871	3442.851	14.61796	267.3494	ConFracC
3443.958	3443.999	3443.979	13.06111	304.267	ConFracC
3447.732	3447.844	3447.788	24.98137	61.32453	ConFracC
3449.831	3449.86	3449.845	4.622198	37.98033	ConFracC
3450.833	3450.861	3450.847	4.45284	51.78162	ConFracC
3451.108	3451.137	3451.123	4.456672	57.88879	ConFracC
3451.646	3451.675	3451.661	4.398198	79.20211	ConFracC

3451.946	3451.996	3451.971	10.13853	82.64978	ConFracC
3456.609	3456.659	3456.634	11.27203	16.11661	ConFracC
3457.562	3457.586	3457.574	10.13702	271.6087	RFracC
3460.802	3460.874	3460.838	22.17162	286.5143	ConFracC
3463.402	3463.445	3463.424	8.150238	65.99273	ConFracC
3463.483	3463.526	3463.505	8.606345	39.6464	ConFracC
3466.129	3466.156	3466.143	3.79715	45.63374	ConFracC
3470.141	3470.172	3470.157	8.336356	338.5484	ConFracC
3470.654	3470.686	3470.67	12.00385	274.4914	ConFracC
3471.961	3471.993	3471.977	12.21387	266.0996	ConFracC
3475.41	3475.441	3475.425	4.970062	87.80961	ConFracC
3480.53	3480.561	3480.546	7.949998	338.9803	ConFracC
3493.469	3493.517	3493.493	9.423537	95.96975	ConFracC
3494.417	3494.465	3494.441	10.18289	21.94628	ConFracC
3501.387	3501.416	3501.401	7.840486	172.9462	ConFracC
3504.53	3504.592	3504.561	12.76612	71.11573	ConFracC
3509.677	3509.74	3509.708	14.21849	21.10074	ConFracC
3512.57	3512.608	3512.589	14.00376	283.4448	ConFracC
3520.68	3520.718	3520.699	8.069753	10.90736	ConFracC
3608.982	3609.052	3609.017	14.56024	53.22757	ConFracC
3608.24	3608.292	3608.266	9.632466	55.38071	ConFracC
3607.924	3607.976	3607.95	9.406178	82.67404	ConFracC
3610.738	3610.789	3610.764	9.389338	77.36146	ConFracC
3618.222	3618.273	3618.247	18.28334	278.873	ConFracC
3621.409	3621.446	3621.427	7.969801	2.817199	ConFracC
3627.709	3627.746	3627.727	14.65639	243.9699	ConFracC
3638.602	3638.658	3638.63	10.59541	95.29503	ConFracC
3642.41	3642.466	3642.438	19.58101	238.538	ConFracC
3651.668	3651.853	3651.76	38.54665	33.43885	ConFracC
3651.811	3651.886	3651.848	16.22992	39.94475	ConFracC
3653.555	3653.621	3653.588	14.55611	22.36246	RFracC
3658.753	3658.78	3658.766	10.06844	305.4304	ConFracC
3658.353	3658.419	3658.386	13.77633	37.40313	ConFracC
3658.33	3658.395	3658.362	13.84639	35.84181	ConFracC
3658.289	3658.355	3658.322	15.1097	13.59903	ConFracC
3658.235	3658.3	3658.267	14.47917	23.70196	ConFracC
3659.081	3659.122	3659.101	6.863661	57.54274	ConFracC
3665.751	3665.793	3665.772	7.184299	113.9995	ConFracC
3669.328	3669.37	3669.349	6.78767	60.21765	ConFracC
3671.597	3671.639	3671.618	14.71728	299.5122	ConFracC
3671.645	3671.687	3671.666	14.71728	299.5122	ConFracC
3679.744	3679.862	3679.803	33.07622	214.5093	ConFracC
3723.59	3723.637	3723.613	9.369697	128.694	RFracC
3757.633	3757.689	3757.661	17.93905	220.0912	ConFracC
3761.502	3761.558	3761.53	17.5534	355.4279	ConFracC
3762.854	3762.91	3762.882	13.73538	32.00806	ConFracC
3772.149	3772.191	3772.17	9.383217	11.18301	ConFracC
3785.69	3785.732	3785.711	7.603013	66.17936	ConFracC
3785.989	3786.031	3786.01	9.336468	24.3361	ConFracC
3785.818	3785.86	3785.839	7.365358	84.85845	ConFracC
3785.885	3785.927	3785.906	7.489847	74.69615	ConFracC
3786.139	3786.181	3786.16	7.915497	57.60994	ConFracC

3806.266	3806.355	3806.31	21.50342	39.10829	ConFracC
3806.356	3806.455	3806.405	23.00697	52.14903	ConFracC
3809.35	3809.406	3809.378	11.92484	68.16945	ConFracC
3810.648	3810.704	3810.676	12.63642	43.9165	ConFracC
3810.8	3810.856	3810.828	12.92945	38.17047	ConFracC
3810.878	3810.934	3810.906	12.86854	39.58523	ConFracC
3810.916	3810.972	3810.944	12.86854	39.58523	ConFracC
3810.966	3811.022	3810.994	12.86854	39.58523	ConFracC
3812.696	3812.786	3812.741	22.23861	180.2221	ConFracC
3813.345	3813.396	3813.371	17.44924	260.6856	ConFracC
3819.051	3819.102	3819.077	16.63212	319.2798	ConFracC
3821.328	3821.408	3821.368	18.07709	62.09184	ConFracC
3821.603	3821.645	3821.624	7.651763	88.93873	ConFracC
3822.343	3822.413	3822.378	17.9119	26.16248	ConFracC
3824.434	3824.499	3824.467	14.77741	52.11721	ConFracC
3835.877	3835.942	3835.909	18.67714	206.1615	RFracC
3839.021	3839.039	3839.03	6.444295	329.251	RFracC
3839.981	3840.018	3839.999	13.97607	273.7264	ConFracC
3842.787	3842.862	3842.825	16.81531	65.17735	ConFracC
3845.449	3845.481	3845.465	12.06995	308.6903	ConFracC
3845.406	3845.439	3845.422	12.05633	308.5868	ConFracC
3845.684	3845.717	3845.701	12.60949	290.9366	ConFracC
3853.486	3853.519	3853.502	9.816466	214.5417	ConFracC
3857.897	3857.929	3857.913	5.282516	86.25399	ConFracC
3862.049	3862.114	3862.082	21.16571	301.5533	ConFracC
3866.022	3866.088	3866.055	14.30461	75.99306	ConFracC
3869.934	3869.981	3869.957	10.38505	45.01026	ConFracC
3869.644	3869.691	3869.667	9.682509	63.56473	ConFracC
3870.804	3870.85	3870.827	13.78603	348.9317	ConFracC
3871.909	3871.955	3871.932	10.81356	38.89199	ConFracC
3871.792	3871.839	3871.816	13.36679	357.0255	ConFracC
3871.037	3871.083	3871.06	11.05802	33.38673	ConFracC
3875.923	3875.969	3875.946	9.745155	58.5082	ConFracC
3875.386	3875.432	3875.409	9.786578	56.89528	ConFracC
3878.173	3878.22	3878.197	11.48695	30.67158	ConFracC
3879.233	3879.38	3879.306	33.39084	50.74778	ConFracC
3879.414	3879.475	3879.444	13.04215	90.10043	ConFracC
3880.771	3880.808	3880.789	6.811205	88.56583	ConFracC
3881.488	3881.54	3881.514	10.70028	80.21091	ConFracC
3890.99	3891.041	3891.015	17.05236	267.3575	RFracC
3890.811	3890.863	3890.837	17.06009	267.2992	RFracC
3890.628	3890.68	3890.654	17.45195	285.4347	RFracC
3891.741	3891.792	3891.766	10.76252	85.16861	RFracC
3891.508	3891.559	3891.533	10.50395	114.48	RFracC
3890.224	3890.276	3890.25	17.43615	280.7709	RFracC
3890.289	3890.34	3890.314	17.3771	278.036	RFracC
3890.372	3890.423	3890.397	17.40771	280.0552	RFracC
3893.464	3893.501	3893.482	7.580923	58.96091	ConFracC
3893.107	3893.144	3893.126	7.578122	60.18191	ConFracC
3892.993	3893.03	3893.012	7.046348	78.89303	ConFracC
3899.859	3899.915	3899.887	12.19121	81.98849	ConFracC
3909.783	3909.825	3909.804	9.783694	42.87658	ConFracC

3909.723	3909.765	3909.744	9.843901	41.49157	ConFracC
3909.533	3909.575	3909.554	8.727014	68.53556	ConFracC
3912.946	3912.988	3912.967	14.83352	284.1529	ConFracC
3916.789	3916.831	3916.81	8.42437	83.1385	ConFracC
3918.352	3918.408	3918.38	11.94162	101.8858	ConFracC
3941.359	3941.41	3941.385	11.68456	81.39092	ConFracC
3942.638	3942.689	3942.663	10.79333	133.9961	ConFracC
3944.605	3944.657	3944.631	13.90651	223.0301	ConFracC
3959.354	3959.405	3959.38	16.90966	286.2612	ConFracC
3960.756	3960.807	3960.782	16.79855	279.7288	ConFracC
3965.768	3965.819	3965.794	11.02813	90.97926	RFracC
4030.696	4030.771	4030.733	17.44588	97.32182	RFracC
4077.161	4077.203	4077.182	10.2784	34.74734	ConFracC
4084.659	4084.796	4084.727	31.46944	68.85484	ConFracC
4087.304	4087.369	4087.337	16.09394	49.47981	RFracC
4089.583	4089.653	4089.618	17.10647	56.75131	RFracC
4098.219	4098.256	4098.237	8.638208	47.26877	ConFracC
4127.839	4127.895	4127.867	17.50914	298.7445	RFracC
4127.492	4127.52	4127.506	6.109904	167.1261	RFracC
4137.754	4138.01	4137.882	52.32204	230.2421	ConFracC
4138.686	4139.079	4138.882	60.36137	131.7411	ConFracC
4136.725	4137.161	4136.943	65.11273	208.5241	ConFracC
4146.801	4146.848	4146.825	11.86043	174.7932	ConFracC
4147.666	4147.718	4147.692	13.66942	190.7075	ConFracC
4147.391	4147.442	4147.416	13.6665	190.739	ConFracC
4147.928	4147.979	4147.953	13.36359	181.7366	ConFracC
4153.719	4153.771	4153.745	13.88643	197.8776	ConFracC
4156.913	4156.988	4156.951	18.87363	160.3797	ConFracC
4160.533	4160.608	4160.57	18.15628	103.3791	ConFracC
4175.583	4175.629	4175.606	13.3987	346.0966	ConFracC
4176.593	4176.639	4176.616	12.69145	11.60465	ConFracC
4177.002	4177.048	4177.025	11.68082	155.603	ConFracC
4178.879	4178.926	4178.902	13.70434	235.3391	ConFracC
4189.823	4189.869	4189.846	13.2338	213.6212	ConFracC
4191.803	4191.849	4191.826	13.90846	236.8533	ConFracC
4193.359	4193.439	4193.399	22.40086	232.211	ConFracC
4193.248	4193.328	4193.288	22.43126	233.3996	ConFracC
4196.733	4196.814	4196.774	22.80143	255.6821	ConFracC
4197.434	4197.515	4197.475	22.89443	301.0985	ConFracC
4197.757	4197.837	4197.797	22.65917	317.5045	ConFracC
4198.463	4198.543	4198.503	19.65392	90.33915	ConFracC
4198.653	4198.734	4198.693	22.89286	299.9694	ConFracC
4198.868	4198.948	4198.908	21.40073	6.981616	ConFracC
4200.831	4200.877	4200.854	11.10666	89.50336	ConFracC
4209.806	4209.853	4209.829	11.40729	55.26719	ConFracC
4211.165	4211.211	4211.188	14.57675	273.6899	ConFracC
4211.078	4211.124	4211.101	14.57048	272.5949	ConFracC
4211.369	4211.459	4211.414	25.43404	273.1565	ConFracC
4213.005	4213.085	4213.045	19.55853	123.0762	ConFracC
4223.307	4223.359	4223.333	15.56354	253.2395	RFracC
4223.269	4223.301	4223.285	10.02822	235.5491	RFracC
4223.206	4223.238	4223.222	9.943884	232.2721	RFracC

4223.953	4223.985	4223.969	10.49463	261.1273	RFracC
4230.498	4230.597	4230.548	25.37314	24.1621	RFracC
4236.782	4236.824	4236.803	12.28467	226.0136	RFracC
4248.728	4248.798	4248.763	19.65612	212.8366	ConFracC
4251.093	4251.164	4251.128	20.50645	263.3572	ConFracC
4275.388	4275.459	4275.424	17.60449	118.3737	RFracC
4281.687	4281.729	4281.708	12.3892	222.2508	RFracC
4282.333	4282.375	4282.354	10.78303	23.98044	RFracC
4282.494	4282.594	4282.544	26.52752	211.0823	ConFracC
4291.462	4291.538	4291.5	19.7833	6.340434	RFracC
4313.64	4313.716	4313.678	19.20392	33.82478	RFracC
4314.589	4314.665	4314.627	21.33712	272.9072	RFracC
4315.919	4315.994	4315.957	20.65961	322.0706	RFracC
4316.155	4316.23	4316.193	18.95439	65.43073	ConFracC
4315.642	4315.703	4315.672	17.6754	275.1299	ConFracC
4320.183	4320.258	4320.22	21.2021	235.2617	RFracC
4327.778	4327.853	4327.815	19.29386	28.57103	RFracC
4328.083	4328.159	4328.121	18.91635	61.44708	RFracC
4336.329	4336.404	4336.367	20.79476	211.2307	RFracC
4346.805	4346.851	4346.828	13.61704	301.5851	RFracC
4349.727	4349.773	4349.75	11.61978	90.88589	RFracC
4350.7	4350.746	4350.723	11.60715	77.09184	RFracC
4353.822	4353.868	4353.845	11.57443	74.33957	RFracC
4353.427	4353.463	4353.445	9.424438	135.2257	ConFracC
4354.079	4354.116	4354.098	8.983275	78.41855	ConFracC
4360.93	4361.01	4360.97	22.06658	204.7454	ConFracC
4362.433	4362.499	4362.466	18.87498	250.1442	ConFracC
4365.461	4365.527	4365.494	18.74154	230.282	ConFracC
4367.142	4367.208	4367.175	18.87985	266.8971	ConFracC
4377.674	4377.73	4377.702	14.45774	17.52341	ConFracC
4380.396	4380.432	4380.414	10.80479	195.6436	RFracC
4387.567	4387.618	4387.592	15.34521	254.6465	ConFracC
4389.494	4389.516	4389.505	5.083188	104.5374	RFracC
4393.528	4393.551	4393.54	6.36867	171.2796	RFracC
4395.41	4395.451	4395.43	10.26797	86.81078	RFracC
4394.889	4394.965	4394.927	19.24062	114.9135	ConFracC
4399.059	4399.134	4399.097	19.18296	25.22947	ConFracC
4400.401	4400.529	4400.465	30.75472	48.15115	ConFracC
4400.256	4400.356	4400.306	24.54494	66.28566	ConFracC
4402.716	4402.781	4402.748	18.98121	243.6445	RFracC
4402.675	4402.726	4402.7	15.25343	248.2155	RFracC
4402.658	4402.709	4402.683	14.92545	200.8135	RFracC
4403.168	4403.22	4403.194	15.18216	221.6878	RFracC
4406.365	4406.46	4406.412	25.16693	171.2369	ConFracC
4406.252	4406.351	4406.301	26.08251	162.4931	ConFracC
4412.727	4412.797	4412.762	17.71694	78.65693	ConFracC
4412.647	4412.698	4412.673	12.94067	95.43556	ConFracC
4419.358	4419.409	4419.384	14.12915	159.59	ConFracC
4423.723	4423.774	4423.748	13.01447	7.889063	ConFracC
4428.104	4428.156	4428.13	15.38904	221.5122	ConFracC
4433.211	4433.262	4433.237	15.41093	262.7119	RFracC
4438.901	4438.952	4438.926	12.31086	77.21182	RFracC

4441.1	4441.151	4441.126	15.17559	282.5319	RFracC
4452.833	4452.885	4452.859	12.53921	50.55031	RFracC
4516.343	4516.394	4516.369	12.44529	73.37229	RFracC
4517.666	4517.76	4517.713	23.21237	37.07061	RFracC
4534.129	4534.181	4534.155	12.46392	39.48627	RFracC
4534.833	4534.885	4534.859	12.5873	100.1782	RFracC
4539.427	4539.479	4539.453	13.69049	142.8816	RFracC
4542.251	4542.298	4542.275	12.15102	131.6635	RFracC
4542.611	4542.657	4542.634	11.18432	54.19694	RFracC
4550.098	4550.144	4550.121	11.48781	106.1444	RFracC
4600.389	4600.517	4600.453	30.18974	74.8103	RFracC
4601.888	4601.958	4601.923	18.32081	126.1019	RFracC
4601.752	4601.823	4601.788	18.21334	122.2393	RFracC
4602.188	4602.258	4602.223	18.04219	115.7872	RFracC
4601.241	4601.311	4601.276	17.76159	103.9328	RFracC
4601.564	4601.635	4601.6	17.94331	111.8385	RFracC
4622.26	4622.45	4622.355	43.15361	305.4797	RFracC
4628.336	4628.526	4628.431	40.96096	12.36274	RFracC
4637.603	4637.683	4637.643	21.58572	307.3802	RFracC
4639.349	4639.429	4639.389	23.18362	212.8738	RFracC
4639.53	4639.61	4639.57	23.04962	203.6682	RFracC
4640.639	4640.68	4640.66	13.50232	214.1212	ConFracC
4642.854	4642.895	4642.874	12.09857	297.6955	ConFracC
4664.175	4664.217	4664.196	9.914344	107.5293	ConFracC
4666.571	4666.613	4666.592	10.8175	133.5191	ConFracC
4683.824	4683.866	4683.845	10.28185	353.6795	ConFracC
4698.075	4698.116	4698.096	9.396317	35.27985	ConFracC

77